ABSTRACT

Annexin A2 (AnxA2) belongs to a family of Ca^{2+}-dependent phospholipid binding proteins. AnxA2 is abundantly expressed in the cytosol of many different cell types and is translocated to the outer surface of the plasma membrane in response to elevated concentrations of intracellular Ca^{2+}. It is known that the binding of Ca^{2+} to the C-terminal Ca^{2+}-binding domains is essential for the recruitment of AnxA2 to the inner leaflet of the plasma membrane. However, the mechanism by which AnxA2 is translocated from the inner leaflet of the plasma membrane to the outer leaflet remains unknown. Since, AnxA2 does not possess a signal sequence that is essential for the classical ER-Golgi secretion; we believe that the protein follows a non-classical pathway of protein secretion. Here, we show that Ca^{2+}- induced translocation of AnxA2 to the cell surface is a multi-step pathway that involves association of AnxA2 with specific domains of the plasma membrane called lipid rafts and its recruitment to the intracellular membranes of the endosomal pathway followed by extracellular secretion by association with the secretory vesicles called exosomes. In our studies, we also investigated the role of AnxA2 in inducing neovascular responses. We have shown that angiogenic insults like hypoxia upregulate the expression of AnxA2. AnxA2-induced angiogenic responses were identified to be regulated by the N-terminus which is important for the binding of several proteolytic components including, tissue plasminogen activator (tPA), plasminogen, procathepsin B and tenascin C. Targeting the N-terminus of AnxA2 with a competitive hexapeptide that prevents the binding of proteolytic components inhibited the AnxA2-mediated neovascular responses. In summary, our data

suggests that AnxA2 is transported to the cell surface following an unconventional pathway of protein secretion and extracellular AnxA2 is an active proteolytic receptor that can have potential roles in pathological conditions associated with excessive extracellular proteolytic events.

MECHANISMS OF CELL SURFACE TRAFFICKING AND POTENTIAL FUNCTIONS OF EXTRACELLULAR ANNEXIN A2

DISSERTATION
Presented to the Graduate Council of the
Graduate School of Biomedical Sciences
University of North Texas Health Science Center at Fort Worth

In Partial Fulfillment of the Requirements

For the Degree of

DOCTOR OF PHILOSOPHY

By

Mallika Valapala, M.S.

UNT Health Science Center

Fort Worth, Texas

October, 2010

ACKNOWLEDGEMENTS

I am heartfully thankful to my mentor, Dr. Jamboor K Vishwanatha, who has been a consistent source of encouragement, guidance and support and providing me the opportunity not only to science but to help me grow as a person. I am thankful to Mrs. Lavanya Vishwanatha for her kindness, support and for making me feel like home away from home. I thank the members of my advisory committee Dr. Robert Wordinger, Dr. Dan Dimitrijevich, Dr. Raghu Krishnamoorthy, Dr. Rajendra Sharma, Dr. Ignacy Gryczynski and Dr, Neeraj Agarwal for playing a pivotal role in my graduate career. I greatly appreciate their time in the committee meetings and their encouragement, support and guidance throughout my graduate studies. I am thankful to Dr. Alkananda Basu for giving me the opportunity to come to the US and be a part of the Department of Molecular Biology and Immunology. I also would like to extend my thanks to the administrative staff who have been very helpful and supportive throughout my time here.

I am especially thankful to my friend Dr. Subhamoy Dasgupta for being such an inspiration. I would like to express my profound appreciation to have him as a friend and for playing such an instrumental role in my graduate career. This work would not have been possible without his support and I cherish his friendship forever. I am eternally thankful to all my friends, Dr. Sheetal Bodhankar, Dr. Navin Rauniyar, Dr. Priya Muthu, Dr. Shashank Bharill, Sanjay Thamake, Smrithi Rajendiran, Marilyne Kpetemey, Prachi Dongre, Amol Rajmane, Pabak Sarkar, Erika Kafka, Sreejetha Dasgupta, Sangram Raut and many more who have been always there whenever I needed them. Their unconditional support through the thick and thin of

my time here has been a true blessing. I would like to thank all my roommates, Sowmya, Bharati, Kirti Salwe, Kirti Jain, Priya Muthu, Prachi Dongre, Amee Mehta, Nittya Suwanassom, Deepti Patki and Amrutha oak who have been a part of my life during my time here.

I would like to extend my sincere thanks to my past and current lab mates, Dr. Arthur Brandon, Dr, Praveen Kumar Shetty, Dr. Anindita Mukherjee, Dr. Amalendu Ranjan, Dr. Jwalitha Shankardas, Dr. Subhamoy Dasgupta, Dr. Amber Ondrichek, Sanjay Thamake, Smrithi Rajendiran, Marilyne Kpetmey, Erika Kafka, who have created such a wonderful and nourishing work environment. The personal and professional discussions we have had in the evenings over a cup of coffee have been very memorable.

On the personal note, I like to thank my parents, Suresh and Sudha Valapala for being a source of unconditional love and support. I am what I am today because of them and I can never thank them enough for believing in me. A special thanks to my uncle, Suresh Gangarapu for being a pillar of strength and supporting me through every walk of life. I thank my bother, Sai Krishna Valapala for being there always for me. I like to thank each and every member of my family back home for their love and support. I would also like to extend my thanks to my parents-in law, sister and bother in-law for their encouragement. I can never express how infinitely grateful I am for sharing my life with my husband, Venkatesh Gogineni. I can't thank him enough for being with me through the best and the difficult times and for always reminding me of my potential. I would like to dedicate this work to my husband for being a wonderful man and a true inspiration.

TABLE OF CONTENTS

CHAPTER II- CELL SURFACE TRANSLOCATION OF ANNEXIN A2 IS CRITICAL FOR GLUTAMATE-INDUCED EXTRACELLULAR PROTEOLYSIS IN RETINAL GANGLION CELLS

CHAPTER III- LIPID RAFT ENDOCYTOSIS AND EXOSOMAL TRANSPORT FACILITATE EXTRACELLULAR TRAFFICKING OF ANNEXIN A2

CHAPTER IV- A COMPETITIVE HEXAPEPTIDE INHIBITOR OF ANNEXIN A2 PREVENTS HYPOXIA-INDUCED ANGIOGENIC EVENTS

CHAPTER I

INTRODUCTION

A. Annexins: A multigene family of Ca^{2+} and phospholipid binding proteins

Annexins belong to a family of multigene Ca^{2+} and phospholipid binding proteins with markedly conserved structural homology among species and divergent roles in many biological processes (1). The annexin family comprises of >500 different gene products and 400 sequenced proteins which are widely conserved across most phyla and species (2). In vertebrates 12 annexins have been classified under the annexin A family and named as annexin A1-A13 (AnxA1-A13) leaving AnxA12 unassigned in the original nomenclature (2). The annexin family of proteins is known to be encoded by 1-20 annexin genes in most eukaryotic species (1). Although the annexin genes have duplicated extensively during the course of the evolution, these family of proteins have remained highly conserved across several eukaryotic species (3). Genes encoding for human annexins (AnxA1-A12) are dispersed throughout the genome and range in size from 15 kb (AnxA9) to 96 kb (AnxA10) (1, 3).

B. Molecular structure of annexins

Their unique architecture allows them to bind to the cellular membranes in a reversible manner in response to several stimuli (4). Structurally all annexins are characterized by a bipartite structure with a variable amino terminal domain and a conserved carboxyl terminal

domain (5). The amino terminus is the site for extensive post translational modifications and interactions with other proteins whereas the C-terminus imparts on all annexins their Ca^{2+} and phospholipid-binding activity (5). All annexins except AnxA6 possess four repeats of approximately 70 amino acids in their carboxyl terminus. Each of these repeats possess a α-helical domain that comprises a Ca^{2+}-binding site (6). These sites impart on annexins the ability to interact with the membranes in a regulated manner in response to changes in intracellular Ca^{2+} concentrations with varying affinities (7). On binding to Ca^{2+}, the α-helical domain undergoes a conformational change and forms a compact, slightly curved disc that possesses a hydrophobic convex surface that harbors the Ca^{2+} and membrane binding sites and a concave surface that points away from the membrane and is available for interaction with other proteins (8). However the exact molecular events that contribute to these changes in the structure of annexins is not clear

.

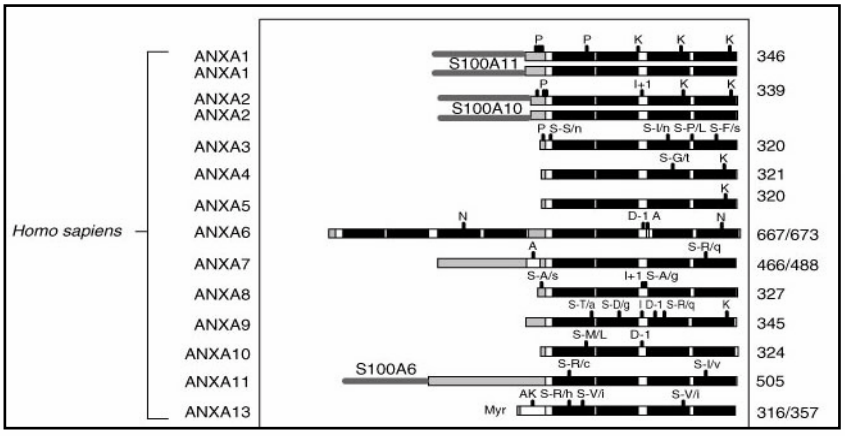

Figure 1. Domain structure of the annexin family of proteins: The bipartite structure of the 12 human annexins showing the four conserved Ca^{2+}-binding repeats (black). The variable N-terminal domain (shaded) differing in length and sequence among the members of the annexin family. Interaction of AnxA1, AnxA2 and AnxA11 with the S100 family of proteins (S100A11, S100A10 and S100A6 respectively). P, known phosphorylation sites; K, KGD synapomorphy (a conserved, inherited characteristic of proteins); I, codon insertions (+x

denotes the number of codons inserted); S-A/b, nonsynonymous coding polymorphisms (SNPs) with the amino acid in the major variant (A) and that in the minor variant (b); N, putative nucleotide-binding sites; D, codon deletions (-x denotes the number of codons deleted); A, alternatively spliced exons; Myr, myristoylation. The total length of each protein is indicated on the right. Stephen E. Moss et al. Genome Biology. 2004

The N-terminal domain of annexins has gained considerable attention over the past decade as it is a site that is diverse in sequence and length among the members of the annexin family. On binding to the membrane, the N-terminus folds into a structurally separate unit on the concave side of the membrane and opposite to the membrane-binding assembly (9). It is a site for regulatory interactions with other protein ligands and also regulates the AnxA2 membrane assembly in response to different intracellular stimuli (10). In most members of the AnxA2 family, the N-terminus regulates the functions of AnxA2 binding to the EF-hand superfamily of Ca^{2+}-binding proteins (5, 6). AnxA1 and AnxA2 also interact with the S100 family members like S100A11 and S100A10 respectively which are characterized by two consecutive EF hand domains (11). High resolution crystal structures have shown that the extreme N-terminal regions of annexins, specifically AnxA2 adapts an amphipathic α-helix that forms a binding pocket formed by both subunits of the S100 dimer (12). This interaction facilitates the formation of a highly symmetrical and stable molecular entity comprising of two central S100 dimers connecting two annexin monomers (12). Such a molecular structure is assumed to provide stability to the annexin membrane complexes by bridging two membrane bound core domains by a S100 dimer (13). In addition to contributing to the stability of annexin membrane complexes, N-terminus is also a site for several protein-protein interactions and post- translational modifications (5). Several post translational modifications have been reported for the annexin family including miristoylation of AnxA13

and serine/threonine as well as tyrosine phosphorylation of several annexins including annexins A1, A2, A4, A6 and A7 (5, 6). In the unphosphorylated state the N-terminal phosphorylation residues are often buried within the core domain and crystallographic studies have shown that considerable reorientation in required for the phosphorylation residues to be accessible to the serine/threonine or tyrosine kinases (9). Whether these structural changes occur after the binding of annexins to the membranes or whether they are necessary prerequisites for annexin binding to the membrane is an area of intense debate.

C. Annexin family of membrane-bound proteins with diverse functions

C1. Annexins as membrane scaffolding proteins

One of the unique characteristics of the annexin family of proteins is their ability to bind to the acidic phospholipids in a Ca^{2+}-dependent manner (10). It has been reported that many members of the annexin family can bind to the cellular membranes either as single molecules or as protein complexes with ligands attached to the N-terminus (6). Atomic microscopy images of AnxA1 and AnxA2 have revealed that these proteins bind to the phospholipid bilayers rich in phosphatidyl serine/phosphatidyl choline mixtures and form monolayer protein clusters that are amorphous and mobile across the bilayers (14). Furthermore, binding of annexins to the negatively charged phospholipids is accompanied by a segregation of membrane lipids and recruitment of actin assembly within the annexin clusters underneath the plasma membrane (15). Indeed, it has been reported that AnxA2 preferentially binds to phosphatidylinositol-4,5 bisphosphate (PtdIns(4,5)P2) and this binding leads to the formation and stabilization of actin assembly sites at cellular membranes (15). Although the binding of AnxA2 to the peripheral regions of the membrane has been established, several questions remain to be answered. It still needs to be established whether AnxA2 binding is essential for the segregation and formation of

negatively charged phospholipid clusters or whether AnxA2 preferentially localizes to the (PtdIns(4,5)P2) rich regions of the membrane.

In addition to binding as peripheral membrane proteins to the plasma membrane, annexin family of proteins (AnxA1, A2 , A4 , A6 and A7) can aggregate the vesicular and plasma membrane in a Ca^{2+}-dependent manner (6). This activity of aggregation of two membranes is called bivalent membrane activity and it has proposed that this process is a result of the interactions between the core domains of annexins on both the membranes (5). In the case of AnxA2 and AnxA7, which form a heteromeric complex with the S100 family of proteins S100A10 and S100A11 respectively, the S100 proteins of the heteromeric complex acts as a bridge to bring together the two core domains (12, 13). In addition, it has been shown that phosphorylation of AnxA2 at its N-terminal domains inhibits the membrane bridging activity of the heterotetramer. Although phosphorylation of AnxA2 at the N-terminus is known to inhibit its ability to bring two membranes together, the monovalent ability of AnxA2 to bind to single membranes is not influenced (16).

C2. Annexins in membrane organization and traffic

In addition to its role in membrane stabilization, AnxA2 has also been identified as a F-actin- binding protein localized to the actin rich regions of the membrane (17). By binding to the actin cytoskeleton, AnxA2 functions in propelling the endocytic vesicles form the plasma membrane to the cell interior (18). The binding of AnxA2 to the actin-polymerizing platforms has been shown to occur in a Ca^{2+}-dependent manner requiring a carboxyl terminal sequence located in the third repeat of AnxA2 (19) . This C-terminal sequence is remarkably conserved among the annexin family of actin-binding proteins except AnxA4 which does not bind F-actin (19).

Despite its ability to bundle actin filaments AnxA2 has not been found to be associated with the cytoplasmic actin bundles (15, 17). The protein however, was found to be localized to the membrane associated dynamic actin structures facilitating in phagocytosis, endocytosis and cell migration (20). This suggests that the actin-binding activity of AnxA2 is restricted to the assembly of actin structures at the cellular membranes. Substantial evidence indicates that binding of AnxA2 to the cellular membranes is essential for its recruitment to the actin–assembly platforms (15, 17). Structural studies have indicated that most actin-assembly structures underneath the plasma membrane share raft-like characteristics (21). Whether AnxA2 is preferentially localized to the raft regions of the membrane or whether it laterally diffuses to the membrane raft structures when there is an active actin–polymerization process is still uncertain (4). Biochemical studies have also indicated that AnxA2 preferentially binds to the negatively charged membrane microdomains with similar affinity to that of many pleckstrin-homology domain proteins and with unusually high specificity (22). Taken together, these results suggest that AnxA2 has a role in the organization of raft-like membrane microdomains at sites of actin-assembly and this organization is important not only for cellular signaling but also for the organization of membrane structure (23).

C3. Annexin membrane interactions

The mechanisms by which AnxA2-mediated membrane scaffold functions are regulated have remained an area of intense investigation. Since AnxA2 belongs to a class of Ca^{2+}-dependent phospholipid-binding proteins, it has been speculated that intracellular Ca^{2+} is a major activator of the domain-organizing ability of AnxA2 (5). Although the biochemical properties of annexins indicate that they are freely soluble proteins distributed in the cytosol of resting cells

under physiological Ca^{2+} concentrations it has been shown that they localize to the membranes in response to elevated levels of intracellular Ca^{2+} (7). Annexin family of proteins have been found to localize to cellular membranes in response to intracellular stimuli that induce intracellular Ca^{2+} mobilization although the concentrations of free Ca^{2+} required for the membrane translocation differ between different annexins (24). Thus the recruitment of annexins to their target membranes is dependent upon the mode of Ca^{2+} mobilization, the location of the rise in intracellular Ca^{2+} concentration and the signaling events that induce a rise in the levels of intracellular Ca^{2+} (24, 25). These events could enable the cells to respond to divergent stimuli that culminate in the increase in intracellular Ca^{2+} concentrations by undergoing a range of highly dynamic membrane reorganizations supported by AnxA2-induced membrane scaffolds (7). Although a majority of the annexin family of proteins interact with cellular membranes in a Ca^{2+}-dependent manner, there are many exceptions to this expected pattern. It has been shown that many other factors such as heat stress and changes in cellular pH also influence the membrane-binding ability of annexins (10). Furthermore, the presence of the C- terminal Ca^{2+}-binding sites is essential for the binding of annexins to cellular membranes in a Ca^{2+}-dependent manner and some annexins such as AnxA9 and AnxA10 are not affected by intracellular Ca^{2+} concentrations as they do not possess the C-terminal Ca^{2+}-binding sites (6, 26, 27).

C4. Binding of annexins to endosomal membranes

Several annexins including AnxA1, A2 and A6 possess unique endosomal targeting sequences at their N-terminus that is necessary for their interaction with the endosomal membranes (28). In contrast to the typical Ca^{2+}-dependent membrane binding, some members of

the annexin family particularly AnxA2 has been shown to bind to the endosomal membranes in the presence of Ca^{2+} chelator agents (29). This Ca^{2+}-independent binding of AnxA2 does not require the binding of the p11 to the N-terminus and is also independent of the Ca^{2+}-binding sites in the C-terminus of AnxA2 (28). However, the binding of AnxA2 to the endosomal membranes is dependent on the phosphorylation of certain tyrosine residues in the N-terminus of AnxA2 (30). The atypical or Ca^{2+}-independent membrane binding of AnxA2 was also demonstrated to happen at regions of the endosomal membranes which are rich in cholesterol and sphingolipids (31). Many recent studies have underscored the importance of the unique and variable N-terminus in the localization of individual annexin molecules to their target membranes (32). Moreover members of the annexin family including AnxA1 and AnxA2 are found to localize to the membranes of the endosomes and facilitate in the internalization of the cargo in a Ca^{2+}-dependent manner (30, 33). In response to stimulation by growth factors like epidermal growth factor (EGF), the EGF receptors are known to phosphorylate annexins and this phosphorylation converts a Ca^{2+}-independently associated AnxA2 into a form that requires Ca^{2+} for its binding (34). The mechanisms involved in this atypical and Ca^{2+}-independent organelle membrane association of annexins still remains to be elucidated. Moreover the presence of C-terminal type II Ca^{2+}-binding sites is critical for the binding of several annexins including AnxA2 to the cellular membranes and annexins expressing inactivated Ca^{2+} repeats lose their ability to bind to cellular membranes even under elevated concentrations of intracellular Ca^{2+} (5).

D. Extracellular annexin activities

Despite being characterized as soluble cytosolic proteins that do not possess a signal sequence which could direct them across the classical secretory pathway, many members of the annexin family have been found to be present on the extracellular surface of many

cells (4). Extracellular binding sites have been identified for many members of the annexin family and extracellular annexins have been proposed to possess divergent biological functions (4). Among the members of the annexin family, AnxA1 has the longest history of reported extracellular activity. Extracellular AnxA1 has been identified as a negative regulator of leukocyte extravasation and consequently inhibits the degree of inflammation (35). AnxA1 has also been identified as a selective surface marker of the vascular endothelium and is expressed in several solid tumors (36). These studies on AnxA1 have lead to the identification of extracellular functions of the other members of the annexin family.

E. Potential biological roles of extracellular AnxA2

E1. Plasminogen activation

AnxA2, like AnxA1 are unique members of the annexin family exhibiting divergent intracellular and extracellular functions (6). The presence of AnxA2 in the extracellular surface was first identified in the vascular endothelium with proposed functions in the regulation of cell surface fibrinolysis (37). Although the presence of AnxA2 on the extracellular surface seemed to be restricted to the vascular endothelium where it was originally identified as a receptor for plasminogen activation, its extracellular functions have been identified later in many cell types (38). AnxA2 acts as a profibrinolytic receptor by binding to tissue plasminogen activator (tPA) and plasminogen facilitating in the generation of plasmin (39). Kinetic studies have shown that when soluble AnxA2 was added to tPA and plasminogen *in vitro*, the rate of plasmin generation increased by ~60 fold (39). Additional support for the role of AnxA2 as a profibrinolytic receptor comes from the observation that AnxA2 knockout mice show a complete reduction in the generation of extracellular

plasmin on the surface of endothelial cells and show an incomplete reduction of injury-induced arterial thrombi (40) Furthermore, overexpression of AnxA2 on the surface of leukemic cells derived from acute promyelocytic leukemia (APL) patients has been attributed to dysregulated fibrinolytic activity and correlates with the clinical manifestations of bleeding (41). In addition, emerging evidence indicates that expression of AnxA2 on the surface of monocytes and macrophages contribute to the ability of the cells to degrade the extracellular matrix (ECM) and migrate to sites of inflammation (42). Binding studies have shown that the presence of lysine residues in plasminogen is essential for its binding to AnxA2 and it was abrogated by 90-95% in the presence of a lysine analog €-amino caproic acid (€- ACA) and also by the treatment of AnxA2 with carboxypeptidase B indicating that the binding occurs by a C-terminal lysine-dependent mechanism (43). In contrast the binding of tPA to AnxA2 is €-ACA resistant and occurs via a high affinity binding site on tPA and binding to

AnxA2 also confers protection on tPA from its physiological inhibitor, plasminogen activator inhibitor -1 (PAI-1) (44, 45).

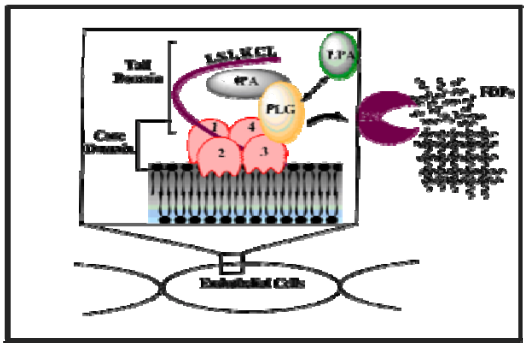

Figure 2. Binding of AnxA2 to the cell surface of endothelial cells. The core domain of AnxA2 (pink) and tail domain (red) bind to both plasminogen and tPA respectively, thereby increasing the catalytic efficiency of plasmin generation. The plasmin acts on the components of the ECM like fibrin and degrades it to fibrin degradation products (FDPs). AnxA2 has also been suggested to bind to lipo protein A (LPA) at the site of plasminogen binding.

E2. Tenascin C (TN-C)-mediated signal transduction

It has been emphasized by several reports that the large tenascin C (TN-C) splice variant is important for several biological functions that include active cell migration and tissue remodeling (46). AnxA2 has been identified as a candidate receptor for the alternately spliced segment of TN-C (47). The high affinity interaction of AnxA2 and TN-C induces migration, loss of focal adhesion and an induction of mitogenic response in endothelial cells (48). Additionally TN-C splice variants and AnxA2 are overexpressed in tumor tissues and their expression is correlated with the increase in the migratory and invasive potential of cancer cells, pointing to a possible interaction between the two proteins in advanced stages of tumor progression (46). Conversely in prostate cancer AnxA2 has been localized to the cytosol and underneath the plasma membrane and its expression is reduced or lost in advanced stages (49). This implies that dysregulation of AnxA2 cell surface expression is a common event in many cell types.

E3. Exocytosis

In secretory cells, the secretory granules are transported to the cell periphery and upon appropriate stimulus they fuse with the plasma membrane to release their contents into the extracellular milieu (50). AnxA2 has been shown to be involved in the Ca^{2+}-dependent exocytosis of the secretory granules in adrenal chromaffin cells (50). AnxA2 forms huge dense complexes with the secretory vesicles and the plasma membrane, increases the density of the fusion complexes thereby allowing the formation of multiple pores during membrane fusion (51). The presence of multiple fusion points would result in the destabilization of the membrane causing membrane disruption and the release of membrane fragments. AnxA2 has been localized to the cytoplasmic domain of the chromaffin granules and facilitates as a fusogen to bring

together the two opposing membranes in a Ca^{2+}-dependent manner (52). However, the functional implication of AnxA2 in exocytosis has remained a controversial because inhibition of both the cytosolic AnxA2 and the inhibition of AnxA2 binding to p11 by specific inhibitors did not influence the secretion in permeabilized chromaffin cells (6, 51).

F. Cell surface translocation of AnxA2: An ultimate puzzle

As summarized above, AnxA2 is involved in a wide variety of biological processes on the cell surface. All these functions seem befitting to a class of abundant Ca^{2+}-binding proteins that are involved in several structural and scaffolding properties of the membranes. Although these proteins have been implicated to bind to the intracellular faces of both organellar and plasma membranes in a Ca^{2+}-dependent manner, the mechanism by which it translocates to the extracellular face of the plasma membrane remains to be elucidated (10). Since AnxA2 does not possess a classical signal sequence that could direct to the membrane, it is speculated that AnxA2 follows a non-classical and ER-Golgi independent pathway of secretion (38). Furthermore, the high degree of conservation of the Ca^{2+}-binding sites in the C-terminus of AnxA2 indicates that Ca^{2+} signaling has essential roles in AnxA2 biology, in particular in the regulation of both its intracellular and extracellular functions (6). This proposal aims at understanding the molecular mechanisms involved in the cell translocation of AnxA2 and the role of Ca^{2+} signaling in regulating the extracellular activities of AnxA2. Furthermore, this proposal also addresses the role of an extracellular AnxA2-mediated plasmin-generating complex in regulating the angiogenic responses.

G. Rationale for the central hypothesis

AnxA2 acts as a peripheral membrane-binding protein on the cell surface and is a high affinity co-receptor for tPA and plasminogen. Extracellular AnxA2 also serves as a cell surface receptor for many ECM modulating proteins like tenascin C and procathepsin B, and its interaction with the components of the plasminogen system, tPA and plasminogen, is well characterized (5, 53). The plasmin-plasminogen system comprises a proteolytic cascade comprising the two plasminogen activators, tissue plasminogen activator (tPA) and urokinase plasminogen activator (uPA), that culminate in the conversion of the inactive zymogen substrate plasminogen to active plasmin (54). Plasmin, a potent trypsin-like endopeptidase, cleaves the components of the extracellular matrix (ECM) like laminin and contributes to the loss of cell-laminin interactions which leads to the detachment induced apoptosis or anoikis of neurons (55) .The generation of plasmin is a highly regulated process mediated by several cell surface receptors which act as binding sites for both the substrate plasminogen and its activator, tPA (44). AnxA2 is identified as a common receptor with distinct domains for the binding of tPA and its substrate plasminogen (56). AnxA2-mediated co-assembly of tPA and plasminogen accelerates the catalytic efficiency of tPA-mediated plasmin generation by 60-fold (57). Although the generation of cell surface plasmin has been implicated in the neuronal cell death on excitotoxicity, the mechanisms that govern the cell surface translocation of a plasmin–generating AnxA2 proteolytic complex is yet to be elucidated. Detailed analysis of the molecular structure of AnxA2 reveals that the remarkable sequence conservation of Ca^{2+}-binding endonexin repeats suggests the importance of AnxA2 in regulating Ca^{2+}-mediated signaling events in the cell (58). The Ca^{2+}-binding sites of AnxA2 are important for its binding to the intracytoplasmic leaflet of the plasma membrane in response to intracellular Ca^{2+} signaling (4, 6). The conservation of the

Ca^{2+}-binding sites among several members of the annexin family have raised speculations regarding the role of Ca^{2+} in the cell surface translocation of AnxA2. However, it is possible that the hyper-variable N-terminus may impart of annexins their characteristic membrane-binding ability. The Ca2+-binding residues in the conserved domain of AnxA2 comprise of 4 repeats of a 70 amino acid sequence called annexin repeats and they confer the ability of AnxA2 to interact reversibly with the cellular membranes in a regulated manner (4). The N-terminal 30 amino acids of AnxA2 form the regulatory domain and contain the binding site for the light chain p11/S100A10 (5). The N-terminus also possesses three potential phosphorylation sites. Tyrosine 23 which is a substrate for phosphorylation by Src kinase (6, 59), serine 25 which has been reported to be phosphorylated by protein kinase C in vitro and in vivo (60) and serine 11 which can only be phosphorylated in vitro (61). Further studies are needed to examine the importance the C-terminal Ca^{2+} binding sites and also the hyper-variable N-terminus in the cell surface translocation of AnxA2 to the cell surface. Based on this information, we believe that the cell surface translocation of AnxA2 occurs in a Ca^{2+}-dependent manner and this process is influenced by the phosphorylation of certain key residues in the hyper-variable N-terminus.

H. Hypothesis and specific aims

Although annexins have been identified as a family of soluble cytosolic proteins, several members of the family have been proposed to function in extracellular molecular processes (1). One such member is AnxA2 which has been identified as both a soluble and membrane-bound protein. AnxA2 lacks a membrane targeting signal sequence and the mechanism by which AnxA2 translocates to the extracellular surface is not known(38). Cell surface AnxA2 has been identified as an endothelial and leukocyte cell surface receptor for the binding of two major

proteins of the fibrinolytic cascade, plasminogen and tissue plasminogen activator (tPA)(43). Abundant expression of cell surface AnxA2 on cancer cells and monocytes has been found to contribute to the invasive potential across the extracellular matrix (ECM) by the generation of plasmin (62). Cell surface AnxA2 also acts as a pro-angiogenic factor by increasing the generation of plasmin, facilitating the degradation of ECM and the release of matrix-bound proangiogenic factors such as vascular endothelial growth factor (VEGF) and fibroblast growth factor (FGF) (43).

Although extracellular AnxA2 has been implicated in several diverse biological processes on the cell surface, the mechanism of its translocation the cell surface remains to be elucidated (5, 63). Several *in vitro* and *in silico* studies have shown that AnxA2 does not possess a classical membrane-targeting signal sequence and therefore cannot go through the conventional endoplasmic reticulum signaling pathway (63). Although several non classical pathways for extracellular secretion of AnxA2 have been proposed (64, 65), the signaling events in the process still remain elusive. Biochemical analyses have indicated that annexins are soluble cytosolic proteins that are freely distributed in the cytosol in resting concentrations of intracellular Ca^{2+} and their affinity for the phospholipid bilayer is enhanced on elevation of intracellular Ca^{2+} levels (7). A majority of the proposed functions of cell surface AnxA2 could be linked to the disturbances in Ca^{2+} homeostasis(6). Furthermore, the most common characteristic feature of different members of the AnxA2 family is that they bind to the phospholipids in a Ca^{2+}-dependent manner (6). These results have provided the most compelling evidence that Ca^{2+} signaling is a key component of AnxA2 dynamics to the membrane. The objective of this proposal is to understand the mechanism by which disturbances in Ca^{2+} homeostasis results in the mobilization of AnxA2 to the membrane. Furthermore, this proposal also addresses the

functional significance of cell surface AnxA2-mediated plasmin generation in the angiogenic responses and the effects of inhibition of the fibrinolytic activity on angiogenic responses. ***We hypothesize that the cell surface translocation of AnxA2 involves several Ca^{2+}-induced signaling events which happen in localized regions of the plasma membrane and the export of AnxA2 to the cell surface forms an active proteolytic, plasmin-generating center.***

The proposed hypothesis will be addressed in the following specific aims

1. To determine the mechanisms involved in Ca^{2+}-dependent cell surface translocation of AnxA2

2. To determine the involvement of cell surface AnxA2 in plasmin-induced angiogenic responses

3. To study the plasma membrane dynamics involved in the extracellular secretion of AnxA2.

Specific Aim 1: To determine the mechanisms involved in Ca^{2+}-dependent cell surface translocation of AnxA2.

Rationale: AnxA2 acts as a peripheral membrane-binding protein on the cell surface and is a high affinity co-receptor for tPA and plasminogen. Extracellular AnxA2 also serves as a cell surface receptor for many ECM modulating proteins like TN-C and procathepsin B, and its interaction with the components of the plasminogen system, tPA and plasminogen, is well characterized (5, 53). The plasmin-plasminogen system comprises a proteolytic cascade comprising the two plasminogen activators, tissue plasminogen activator (tPA) and urokinase plasminogen activator (uPA), that culminate in the conversion of the inactive zymogen substrate plasminogen to active plasmin (54). Plasmin, a potent trypsin-like endopeptidase, cleaves the components of the extracellular matrix (ECM) like laminin and contributes to the loss of cell-laminin interactions which leads to the detachment induced apoptosis or anoikis of neurons

(55). The generation of plasmin is a highly regulated process mediated by several cell surface receptors which act as binding sites for both the substrate plasminogen and its activator, tPA (43)(44). AnxA2 is identified as a common receptor with distinct domains for the binding of tPA and its substrate plasminogen (39). AnxA2-mediated co-assembly of tPA and plasminogen accelerates the catalytic efficiency of tPA-mediated plasmin generation by 60-fold (43). Although the generation of cell surface plasmin has been implicated in the neuronal cell death, the mechanisms that govern the cell surface translocation of a plasmin–generating AnxA2 proteolytic complex is yet to be elucidated. Detailed analysis of the molecular structure of

AnxA2 reveals that the remarkable sequence conservation of Ca^{2+}-binding endonexin repeats suggests the importance of AnxA2 in regulating Ca^{2+}-mediated signaling events in the cell (58). The Ca^{2+}-binding sites of AnxA2 are important for its binding to the intracytoplasmic leaflet of the plasma membrane in response to intracellular Ca^{2+} signaling (5, 6). The conservation of the Ca^{2+}-binding sites among several members of the annexin family have raised speculations regarding the role of Ca^{2+} in the cell surface translocation of AnxA2. However, it is possible that the hyper-variable N-terminus may impart on annexins their characteristic membrane-binding ability. The Ca^{2+}-binding residues in the conserved domain of AnxA2 comprise of 4 repeats of a 70 amino acid sequence called annexin repeats and they confer the ability of AnxA2 to interact reversibly with the cellular membranes in a regulated manner (5). The N-terminal 30 amino acids of AnxA2 form the regulatory domain and contain the binding site for the light chain p11/S100A10 (5). The N-terminus also possesses three potential phosphorylation sites. Tyrosine 23 which is a substrate for phosphorylation by Src kinase (6, 59), serine 25 which has been reported to be phosphorylated by protein kinase C *in vitro* and *in vivo* (60) and serine 11 which

can only be phosphorylated *in vitro* (61). Further studies are needed to examine the importance the C-terminal Ca^{2+} binding sites and also the hyper-variable N-terminus in the cell surface translocation of AnxA2 to the cell surface. Based on this information, we hypothesize that the cell surface translocation of AnxA2 occurs in a Ca^{2+}-dependent manner and this process is influenced by the phosphorylation of certain key residues in the hyper-variable N-terminus.

Figure 3. Potential sites of p11 binding and phosphorylation on the N-terminus of Anx A2. P11 binding sites at isoleucine 5 and leucine 6 are shown in orange. Phosphorylation of serine 11 and serine 25 by protein kinase C are depicted in blue and phosphorylation at tyrosine 23 by pp60SRC kinase is shown in red.

Specific Aim 2 To study the dynamics involved in the translocation of AnxA2 to the cell surface across the submembrane compartments

Rationale: AnxA2 is a soluble secretory protein lacking a signal sequence that could direct it across the classical secretory pathway (5, 38) . Although several alternate pathways have been proposed for their extracellular localization of AnxA2 none of them clearly explain the mechanisms involved in the cell surface translocation of AnxA2 (63). Another challenging problem presented by AnxA2 is its preference for negatively charged glycerophospholipids. Since these negatively charged phospholipids form the ubiquitous components of most biological membranes an explanation for the preferential localization of AnxA2 to acidic phospholipids on the target membranes is not explained (14). In this proposal we are interested in understanding

the role of the preferential membrane association in contributing to extracellular activities of AnxA2. It has also been observed that AnxA2 directly binds to phosphatidylinositol (4,5)-bisphosphate [PtdIns(4,5)P_2] rich regions of the plasma membrane. Since PtdIns(4,5)P_2 clusters with the lipid raft markers, the targeting of AnxA2 to specific lipid raft domains could influence the extracellular functions of AnxA2 (4). Lipid rafts are dynamic and transient nanoscale structures rich in cholesterol and sphingolipids. Although they are transient and heterogeneous structures, they fuse to form larger and more stable platforms for signaling events through protein-protein and protein-lipid interactions (66). Lipid rafts are liquid-ordered domains containing saturated fatty acids that are more rigid than the non-raft regions of the plasma membrane (66). Although a vast majority of membrane proteins are localized to the liquid disordered regions of the plasma membrane, some proteins are preferentially localized to the ordered raft domains (67). The association of proteins into the lipid rafts occurs by three different modes, proteins targeted to the outer leaflet of the plasma membrane via the glycosyl- phosphatidylinositol (GPI) anchors, proteins targeted to the inner leaflet via acylation, plamitoylation or by direct interaction with cholesterol, proteins with hydrophobic transmembrane domains that are specifically targeted to the raft regions (68). Recent studies have indicated that approximately half of intracellular AnxA2 is associated with the PtdIns(4,5)P_2 rich regions of the plasma membrane where it may be involved in the organization of the raft domains (23). Furthermore, studies have also indicated that this pool of AnxA2 is released upon sequestration of cholesterol (23, 65). Hence, it is speculated that interaction of AnxA2 with the rafts may be regulated by intracellular Ca^{2+} or phosphorylation or a combination of both.

Here, we propose that AnxA2 is first recruited to the inner leaflet of the plasma

membrane by specific interaction with PtdIns(4,5)P_2. The interaction of AnxA2 with PtdIns(4,5)P_2 represents the entry point in the unconventional secretion of AnxA2. Since PtdIns(4,5)P_2 is strongly enriched in lipid microdomains enriched in cholesterol, we hypothesize that clustering within the specialized membrane domains or rafts is essential for the recruitment of AnxA2 to the outer leaflet of the plasma membrane.

Potential intracellular pathways for unconventional protein secretion

Four potential mechanisms have been proposed to mediate the unconventional secretion of soluble secretory proteins that do not possess a leader sequence. They include both the vesicular and nonvesicluar pathways of protein secretion (65).

1. Direct translocation from the cytosol to the extracellular space across the plasma membrane

2. Lysosome-mediated extracellular secretion

3. Exosome-mediated delivery via multivesicular bodies (MVBS) and

4. Extracellular secretion by plasma membrane blebbing and vesicle shedding

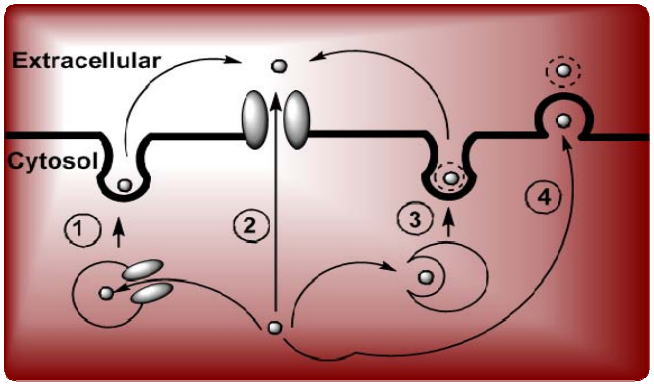

Figure 4. Vesicular and nonvesicular pathways involved in the secretion of unconventional proteins

Exosome-mediated unconventional mechanism of AnxA2 transport to the extracellular milieu

Exosomes are initially described as structures released from the cells during reticulocyte maturation (69). Exosomes are composed of multivesicular bodies (MVBs) and are released upon fusion of MVBs with the plasma membrane (70). Substantial evidence indicates the existence of lipid rafts in the secreted exosomes including the presence of high levels of cholesterol to phospholipid ratio, several GPI-anchored proteins like CD55,CD58 and CD9 and the presence of the he heterotrimeric G protein α -subunit ($G_{\alpha 2}$) (69). The presence of the raft markers in these structures indicates that lipid rafts may participate in the molecular segregation of exosomes (71). It has been recently demonstrated that several heat shock proteins translocate from the lipid rafts into the exosomes through their interaction with raft-associated proteins like flotilin-1 (72). Hence lipid rafts domains present on the endosomal membranes serve as sorting platforms for the localization of proteins within the MVBs that are later secreted into the extracellular space. Studies have proposed that the exosomal secretion of proteins to the extracellular surface is one of the non-classical mechanisms of secretion of proteins that do not possess a signal sequence (73) . Recent evidence also indicates that AnxA2 is present in the exosomes secreted from some cancer cells, neuronal cells and dendritic cells and is involved in several functions associated with cell-cell communication (74).

Based on these findings, we hypothesize that AnxA2 binds to the negatively charged phospholipids and laterally mobilizes to the lipid rafts in a Ca^{2+}-dependent manner. The raft-associated AnxA2 is later localized to the exosomal raft components and is destined for extracellular secretion. Upon fusion of the multivesicular bodies on contact with the plasma

membrane, exosomal AnxA2 is released and binds to specific sites on the plasma membrane.

Specific Aim 3: To determine the involvement of cell surface AnxA2 in plasmin-induced angiogenic responses

Rationale: Vascular occlusion in the retinal capillaries results in the generation of acute hypoxic conditions in the retinal capillaries which later progresses to chronic hypoxia (75). In response to chronic hypoxia, endothelial cells upregulate the expression of $VEGF_{165}$ mediated by hypoxia inducible factor 1α (HIF-1α) (76). The sequence of events including changes in the basement membrane, endothelial cell migration, proliferation and vessel formation cause the new vessels to extend from the retina to other avascular ocular regions (77). Proteolysis of the ECM is an important prerequisite for the endothelial cells to migrate, proliferate and form a new blood vessel and this process requires an array of extracellular proteolytic events (78). The extracellular proteolytic system comprises of the members of the blood fibrinolytic cascade involving the plasminogen activators, tissue plasminogen activator (tPA) and urokinase plasminogen activator (uPA), their physiological inhibitor, plasminogen activator inhibitor-1 (PAI-1) and the cell surface receptors for plasmin generation, like AnxA2 (79). Plasmin, which is a central component of this system, is a broad spectrum trypsin-like serine protease degrades several components of the ECM (laminin and fibrin), is capable of activating inactive pro-matrix metalloproteinases (MMPs) and also increases the bio-availability of $VEGF_{165}$ (80). On the surface of endothelial cells, AnxA2 is expressed as a peripheral membrane protein and acts as a pro-fibrinolytic co-receptor for tPA and plasminogen (81). tPA binds to the amino terminus of AnxA2 and this binding is inhibited by a hexapeptide analog overlapping the regions 7-12 (LCKLSL) (4).The binding of plasminogen however requires the carboxy terminal lysine residues and can be inhibited by €-aminocaproic acid or carboxypeptidase (82). Kinetic studies

have shown that AnxA2 enhances the catalytic efficiency of plasmin generation by about 60-fold and mediates the localized generation of plasmin (52). Studies in AnxA2-null mice have provided functional insights into the role of AnxA2 in neovascularization (83). In neonatal retina, neovascular response to oxygen is severely impaired in the absence of AnxA2. Abundant expression of AnxA2 is observed in the inner limiting membrane (ILM) penetrating retinal neovessels (83). Taken together these results indicate that AnxA2 is important in the maintenance of the homeostasis of the ECM and disregulated activity of AnxA2 can have potential implications on neovascularization.

REFERENCES

1. Moss, S. E., and Morgan, R. O. (2004) *Genome Biol.* **5**, 219

2. Morgan, R. O., and Fernandez, M. P. (1997) *Cell Mol. Life Sci.* **53**, 508-515

3. Barton, G. J., Newman, R. H., Freemont, P. S., and Crumpton, M. J. (1991) *Eur. J. Biochem.* **198**, 749-760

4. Rescher, U., and Gerke, V. (2004) *J. Cell. Sci.* **117**, 2631-2639

5. Gerke, V., and Moss, S. E. (2002) *Physiol. Rev.* **82**, 331-371

6. Gerke, V., Creutz, C. E., and Moss, S. E. (2005) *Nat. Rev. Mol. Cell Biol.* **6**, 449-461

7. Burgoyne, R. D., and Geisow, M. J. (1989) *Cell Calcium* **10**, 1-10

8. Rosengarth, A., and Luecke, H. (2003) *J. Mol. Biol.* **326**, 1317-1325

9. Swairjo, M. A., and Seaton, B. A. (1994) *Annu. Rev. Biophys. Biomol. Struct.* **23**, 193-213

10. Raynal P, and Pollard HB. (1994) *Biochim. Biophys. Acta* **1197(1)**, 63-93

11. Heizmann, C. W. (2002) *Methods Mol. Biol.* **172**, 69-80

12. Rety, S., Sopkova, J., Renouard, M., Osterloh, D., Gerke, V., Tabaries, S., Russo-Marie, F., and Lewit-Bentley, A. (1999) *Nat. Struct. Biol.* **6**, 89-95

13. Lewit-Bentley, A., Rety, S., Sopkova-de Oliveira Santos, J., and Gerke, V. (2000) *Cell Biol.*

Int. **24**, 799-802

14. Lambert, O., Cavusoglu, N., Gallay, J., Vincent, M., Rigaud, J. L., Henry, J. P., and Ayala-Sanmartin, J. (2004) *J. Biol. Chem.* **279**, 10872-10882

15. Hayes, M. J., Shao, D. M., Grieve, A., Levine, T., Bailly, M., and Moss, S. E. (2009) *Biochim. Biophys. Acta* **1793**, 1086-1095

16. Hubaishy, I., Jones, P. G., Bjorge, J., Bellagamba, C., Fitzpatrick, S., Fujita, D. J., and Waisman, D. M. (1995) *Biochemistry* **34**, 14527-14534

17. Hayes, M. J., Shao, D., Bailly, M., and Moss, S. E. (2006) *EMBO J.* **25**, 1816-1826

18. Morel, E., Parton, R. G., and Gruenberg, J. (2009) *Dev. Cell.* **16**, 445-457

19. Rescher, U., Ludwig, C., Konietzko, V., Kharitonenkov, A., and Gerke, V. (2008) *J. Cell. Sci.* **121**, 2177-2185

20. Merrifield, C. J., Rescher, U., Almers, W., Proust, J., Gerke, V., Sechi, A. S., and Moss, S. E. (2001) *Curr. Biol.* **11**, 1136-1141

21. Babiychuk, E. B., and Draeger, A. (2000) *J. Cell Biol.* **150**, 1113-1124

22. Hayes, M. J., Merrifield, C. J., Shao, D., Ayala-Sanmartin, J., Schorey, C. D., Levine, T. P., Proust, J., Curran, J., Bailly, M., and Moss, S. E. (2004) *J. Biol. Chem.* **279**, 14157-14164

23. Rescher, U., Ruhe, D., Ludwig, C., Zobiack, N., and Gerke, V. (2004) *J. Cell. Sci.* **117**, 3473-3480

24. Barwise, J. L., and Walker, J. H. (1996) *J. Cell. Sci.* **109 (Pt 1)**, 247-255

25. Blanchard, S., Barwise, J. L., Gerke, V., Goodall, A., Vaughan, P. F., and Walker, J. H. (1996) *J. Neurochem.* **67**, 805-813

26. Goebeler, V., Ruhe, D., Gerke, V., and Rescher, U. (2003) *FEBS Lett.* **546**, 359-364

27. Morgan, R. O., Jenkins, N. A., Gilbert, D. J., Copeland, N. G., Balsara, B. R., Testa, J. R., and Fernandez, M. P. (1999) *Genomics* **60**, 40-49

28. Emans, N., Gorvel, J. P., Walter, C., Gerke, V., Kellner, R., Griffiths, G., and Gruenberg, J. (1993) *J. Cell Biol.* **120**, 1357-1369

29. Jost, M., Zeuschner, D., Seemann, J., Weber, K., and Gerke, V. (1997) *J. Cell. Sci.* **110 (Pt 2)**, 221-228

30. Morel, E., and Gruenberg, J. (2009) *J. Biol. Chem.* **284**, 1604-1611

31. Zeuschner, D., Stoorvogel, W., and Gerke, V. (2001) *Eur. J. Cell Biol.* **80**, 499-507

32. Ayala-Sanmartin, J., Gouache, P., and Henry, J. P. (2000) *Biochemistry* **39**, 15190-15198

33. Rescher, U., Zobiack, N., and Gerke, V. (2000) *J. Cell. Sci.* **113 (Pt 22)**, 3931-3938

34. Futter, C. E., Felder, S., Schlessinger, J., Ullrich, A., and Hopkins, C. R. (1993) *J. Cell Biol.* **120**, 77-83

35. Perretti, M., and Gavins, F. N. (2003) *News Physiol. Sci.* **18**, 60-64

36. Perretti, M., and Flower, R. J. (2004) *J. Leukoc. Biol.* **76**, 25-29

37. Hajjar, K. A., and Acharya, S. S. (2000) *Ann. N. Y. Acad. Sci.* **902**, 265-271

38. Siever, D. A., and Erickson, H. P. (1997) *Int. J. Biochem. Cell Biol.* **29**, 1219-1223

39. Cesarman GM, Guevara CA, and Hajjar KA. (1994) *J. Biol. Chem.* **269(3)**, 21198-203

40. Ling Q, Jacovina AT, Deora A, Febbraio M, Simantov R, Silverstein RL, Hempstead B, Mark WH, and Hajjar KA. (2004) *J. Clin. Invest.* **113(1)**, 38-48

41. Menell JS, Cesarman GM, Jacovina AT, McLaughlin MA, Lev EA, and Hajjar KA. (1999) *N. Engl. J. Med.* **340(13)**, 994-1004

42. Brownstein, C., Deora, A. B., Jacovina, A. T., Weintraub, R., Gertler, M., Khan, K. M., Falcone, D. J., and Hajjar, K. A. (2004) *Blood* **103**, 317-324

43. Kim J, and Hajjar KA. (2002) *Front. Biosci.* **1(7)**, 341-8

44. Longstaff, C. (2002) *Front. Biosci.* **7**, d244-55

45. Herren, T., Swaisgood, C., and Plow, E. F. (2003) *Front. Biosci.* **8**, d1-8

46. Esposito, I., Penzel, R., Chaib-Harrireche, M. *et al.* (2006) *J. Pathol.* **208**, 673-685

47. Chung, C. Y., and Erickson, H. P. (1994) *J. Cell Biol.* **126**, 539-548

48. Chung, C. Y., Murphy-Ullrich, J. E., and Erickson, H. P. (1996) *Mol. Biol. Cell* **7**, 883-892

49. Yee, D. S., Narula, N., Ramzy, I., Boker, J., Ahlering, T. E., Skarecky, D. W., and Ornstein, D. K. (2007) *Arch. Pathol. Lab. Med.* **131**, 902-908

50. Chasserot-Golaz, S., Vitale, N., Umbrecht-Jenck, E., Knight, D., Gerke, V., and Bader, M. F. (2005) *Mol. Biol. Cell* **16**, 1108-1119

51. Faure, A. V., Migne, C., Devilliers, G., and Ayala-Sanmartin, J. (2002) *Exp. Cell Res.* **276**, 79-89

52. Kobayashi, R., Nakayama, R., Ohta, A., Sakai, F., Sakuragi, S., and Tashima, Y. (1990) *Biochem. J.* **266**, 505-511

53. Mai, J., Finley, R. L.,Jr, Waisman, D. M., and Sloane, B. F. (2000) *J. Biol. Chem.* **275**, 12806-12812

54. Plow, E. F., Herren, T., Redlitz, A., Miles, L. A., and Hoover-Plow, J. L. (1995) *FASEB J.* **9**, 939-945

55. Syrovets, T., and Simmet, T. (2004) *Cell Mol. Life Sci.* **61**, 873-885

56. Cesarman, G. M., Guevara, C. A., and Hajjar, K. A. (1994) *J. Biol. Chem.* **269**, 21198-21203

57. Kim, J., and Hajjar, K. A. (2002) *Front. Biosci.* **7**, d341-8

58. Hajjar, K. A., Guevara, C. A., Lev, E., Dowling, K., and Chacko, J. (1996) *J. Biol. Chem.* **271**, 21652-21659

59. Glenney, J. R.,Jr. (1985) *FEBS Lett.* **192**, 79-82

60. Gould, K. L., Woodgett, J. R., Isacke, C. M., and Hunter, T. (1986) *Mol. Cell. Biol.* **6**, 2738-2744

61. Regnouf, F., Sagot, I., Delouche, B., Devilliers, G., Cartaud, J., Henry, J. P., and Pradel, L. A. (1995) *J. Biol. Chem.* **270**, 27143-27150

62. Hajjar KA, and Acharya SS. (2000) *Ann N Y Acad Sci. 2000 may;902:265-71.* **902**, 265-71

63. Danielsen, E. M., van Deurs, B., and Hansen, G. H. (2003) *Biochemistry* **42**, 14670-14676

64. Nickel, W. (2003) *Eur. J. Biochem.* **270**, 2109-2119

65. Zhang, N. N., Liu, X., Sun, J., Wu, Y., and Li, Q. W. (2009) *Yi Chuan* **31**, 29-35

66. Lajoie, P., Goetz, J. G., Dennis, J. W., and Nabi, I. R. (2009) *J. Cell Biol.* **185**, 381-385

67. Simons, K., and Ikonen, E. (1997) *Nature* **387**, 569-572

68. Mishra, S., and Joshi, P. G. (2007) *J. Neurochem.* **103 Suppl 1**, 135-142

69. Denzer, K., Kleijmeer, M. J., Heijnen, H. F., Stoorvogel, W., and Geuze, H. J. (2000) *J. Cell. Sci.* **113 Pt 19**, 3365-3374

70. Johnstone, R. M. (2006) *Blood Cells Mol. Dis.* **36**, 315-321

71. de Gassart, A., Geminard, C., Fevrier, B., Raposo, G., and Vidal, M. (2003) *Blood* **102**, 4336-4344

72. Zhan, R., Leng, X., Liu, X., Wang, X., Gong, J., Yan, L., Wang, L., Wang, Y., Wang, X., and Qian, L. J. (2009) *Biochem. Biophys. Res. Commun.*

73. Simons, M., and Raposo, G. (2009) *Curr. Opin. Cell Biol.*

74. Staubach, S., Razawi, H., and Hanisch, F. G. (2009) *Proteomics* **9**, 2820-2835

75. Tchedre, K. T., and Yorio, T. (2008) *Invest. Ophthalmol. Vis. Sci.* **49**, 2577-2588

76. Vorwerk, C. K., Naskar, R., and Dreyer, E. B. (1999) *Klin. Monatsbl. Augenheilkd.* **214**, 2-11

77. Liu, J., and Vishwanatha, J. K. (2007) *Mol. Cell. Biochem.* **303**, 211-220

78. Chintala, S. K., Zhang, X., Austin, J. S., and Fini, M. E. (2002) *J. Biol. Chem.* **277**, 47461-47468

79. Jacovina, A. T., Zhong, F., Khazanova, E., Lev, E., Deora, A. B., and Hajjar, K. A. (2001) *J. Biol. Chem.* **276**, 49350-49358

80. Jindal, H. K., and Vishwanatha, J. K. (1990) *J. Biol. Chem.* **265**, 6540-6543

81. Zhang, X., Chaudhry, A., and Chintala, S. K. (2003) *Mol. Vis.* **9**, 238-248

82. Deora, A. B., Kreitzer, G., Jacovina, A. T., and Hajjar, K. A. (2004) *J. Biol. Chem.* **279**, 43411-43418

83. Choi, D. W. (1992) *J. Neurobiol.* **23**, 1261-1276

CHAPTER II

CELL SURFACE TRANSLOCATION OF ANNEXIN A2 IS CRITICAL FOR GLUTAMATE-INDUCED EXTRACELLULAR PROTEOLYSIS IN RETINAL GANGLION CELLS

ABSTRACT

Glutamate-induced elevation in intracellular Ca^{2+} has been implicated in the loss of retinal ganglion cells (RGCs) in glaucoma. RGCs respond to increased glutamate levels by activating an extracellular proteolytic cascade involving the components of the plasmin-plasminogen system. Annexin A2 (AnxA2) is a Ca^{2+}-dependent phospholipid binding protein and serves as an extracellular proteolytic center by recruiting tissue plasminogen activator and plasminogen, and mediating localized generation of plasmin. Here we characterize the expression of AnxA2 in the rat RGCs. Ratiometric Ca^{2+} imaging and time lapse confocal microscopy demonstrated glutamate-induced Ca^{2+} influx. We showed that glutamate translocated both endogenous and AnxA2-GFP to the cell surface in a process dependent on the activity of the NMDA receptor. Glutamate-induced translocation of AnxA2 is dependent on the phosphorylation of tyrosine 23 at the N-terminus and mutation of tyrosine 23 to a non-phosphomimetic variant inhibits the translocation process. The cell surface translocated AnxA2 forms an active plasmin-generating complex and this activity can be neutralized by anti-AnxA2 antibody or blocked by a hexapeptide directed against the N-terminus. These results suggest an

involvement of AnxA2 in potentiating neuronal cell death processes in the retina.

INTRODUCTION

Progressive and irreversible loss of retinal ganglion cells (RGCs) is a characteristic feature of glaucoma, a neurodegenerative disease of the eye (1). Although elevated intraocular pressure (IOP) has been attributed to be a major factor contributing to the loss of RGCs (2), the molecular mechanisms underlying the RGC death are poorly understood. Excessive accumulation of excitatory amino acids such as glutamate has been implicated in the pathogenesis of glaucoma (3). Glutamate-induced intracellular increase in Ca^{2+} levels leads to the hyper-activation of several normal Ca^{2+}-mediated physiological processes including the activation of intracellular kinases, phosphatases, phospholipases and proteases which contribute to the degeneration of the neurons (4). Despite these observations, other publications have questioned the role of glutamate in the pathogenesis of glaucoma (5, 6). Our study provides insight into one of the mechanisms that might contribute to glutamate-induced glaucomatous changes in the retina.

Recent evidence suggests that the components of the plasmin-plasminogen system are involved in glaucomatous damage of RGCs after ischemic and excitotoxic injury (7). The plasmin-plasminogen system comprises a proteolytic cascade comprising the two plasminogen activators, tissue plasminogen activator (tPA) and urokinase plasminogen activator (uPA), that culminate in the conversion of the inactive zymogen substrate plasminogen to active plasmin (8). Plasmin, a potent trypsin-like endopeptidase, cleaves the components of the extracellular matrix (ECM) like laminin in the nerve fiber layer and contributes to the loss of ganglion cell-laminin

interactions which leads to the detachment induced apoptosis or anoikis of RGCs (7, 9). Furthermore, tPA-knockout mice are resistant to N-Methyl-D-Aspartate (NMDA) excitotoxin-induced retinal damage (10). Although the role of tPA in the excitotoxic and ischemic damage in the central nervous system (CNS) is well elucidated, its role in the retina is still unclear.

The culminating step in the plasmin-plasminogen proteolytic cascade is the generation of cell surface plasmin (8). This is a highly regulated process mediated by several cell surface receptors which act as binding sites for both the substrate plasminogen and its activator, tPA (11). Annexin A2 (AnxA2) is identified as a common receptor with distinct domains for the binding of tPA and its substrate plasminogen (12). AnxA2-mediated co-assembly of tPA and plasminogen accelerates the catalytic efficiency of tPA-mediated plasmin generation by 60-fold (12). The mechanisms that regulate the plasmin generating activity of AnxA2 could have potential contributions in the pathogenesis of retinal diseases where the plasmin-plasminogen system is implicated.

AnxA2 is a member of the family of Ca^{2+}-dependent anionic phospholipid (aPL)-binding proteins involved in mediating several intracellular actions of Ca^{2+} (13). The aPL and Ca^{2+} binding properties of AnxA2 are imparted by the conserved carboxyl-terminal core domain whereas the variable N-terminus is the site for post-translational modifications and interactions with other proteins (14). The Ca^{2+}-binding residues in the conserved domain of AnxA2 comprise of 4 repeats of a 70 amino acid sequence called annexin repeats and they confer the ability of AnxA2 to interact reversibly with the cellular membranes in a regulated manner (15). The N-terminal 30 amino acids of AnxA2 comprise the regulatory domain and contain the binding site for the light chain p11/S100A10 (16). The N-terminus also possesses phosphorylation sites on

tyrosine 23 which is a substrate for phosphorylation by Src kinase (13, 17), serine 25 which has been reported to be phosphorylated by protein kinase C *in vitro* and *in vivo* (18) and serine 11 which can only be phosphorylated *in vitro* (19). The biological role of tyrosine-phosphorylated AnxA2 is still debatable. Tyrosine-phosphorylation has been shown to act both as a targeting (20) and inhibitory signal (21) for the binding of AnxA2 heterotetramer, a complex of two AnxA2 heavy (p36) and light chains (p11/S100A100) to the plasma membrane. Studies have also indicated that AnxA2 is initially targeted to the phospholipid component of the plasma membrane and this binding mediates the phosphorylation of tyrosine 23 by Src-kinase (22). Serine 25 has been shown to be phosphorylated by protein kinase C both *in vitro* and *in vivo* and this phosphorylation inhibits the ability of AnxA2 to aggregate lipid vesicles and promotes nuclear entry of AnxA2 (19, 23, 24)

Most members of the annexin family, including AnxA2 are recruited to cellular membranes in response to several stimuli which induce intracellular Ca^{2+} mobilization (15, 25). Interaction of AnxA2 at the N-terminus with p11/S100A10 or by phosphorylation has been proposed to play a regulatory role in the Ca^{2+}-dependent association to the cell membranes (20, 26). Here we used a glutamate-induced Ca^{2+} influx model in RGC-5 cells to examine the Ca^{2+}-induced translocation of AnxA2 and its N-terminal phosphorylation mutants to the outer surface of the plasma membrane. Our data indicates that glutamate induces the cell surface translocation of AnxA2 and phosphorylation of tyrosine 23 at the N-terminus of AnxA2 is an essential prerequisite for the translocation process. We also show that glutamate-induced cell surface translocation of AnxA2 is associated with a concomitant increase in the cell surface generation of plasmin which can be inhibited by an antibody or a peptide directed against the N-terminus of AnxA2. Taken together, the data shown here suggest that glutamate induces the cell surface

translocation of the plasmin-generating receptor AnxA2 which can potentiate tPA-mediated RGC loss even under conditions where there is no upregulation in the secreted levels of tPA.

MATERIALS AND METHODS

Cell culture and glutamate treatment

The transformed rat RGC line, RGC-5 which has been previously characterized to express several RGC specific markers (27) was a kind gift from Dr. Neeraj Agarwal (University of North Texas Health Science Center, Fort Worth, TX). The cells were cultured in low-glucose Dulbecco's modified Eagle's medium (DMEM) (Gibco) supplemented with 10% fetal bovine serum (FBS) (Gibco), 100 U/mL penicillin, and 100 μg/mL streptomycin (Gibco) in a humidified atmosphere of 95% air and 5% CO2 at 37°C. Differentiation of RGC-5 cells was achieved by supplementing the conditioned medium derived from human non-pigmented ciliary epithelial cells (HNPEs) according to methods previously published (28).

Plasmid constructs and transient transfection

For the construction of a plasmid expressing AnxA2-GFP fusion protein (AnxA2-GFP), full length AnxA2 was cloned into pEGFP-N1 vector (Clontech). We used site-directed mutagenesis kits (Clontech) to generate both single and double phosphorylation and non-phosphorylation mutants of AnxA2 at tyrosine 23 and serine 25. The protein products of the mutants will be subsequently mentioned as AnxA2Y23E-GFP, AnxA2Y23F-GFP,AnxA2S25E-GFP, AnxA2S5A-GFP, AnxA2S11A-GFP, AnxA2S11E-GFP,AnxA2Y23ES25E-GFP, AnxA2Y23FS25E, AnxA2Y23ES25A and AnxA2Y23FS25A. Transient transfection was performed according to the previously published protocols (29).

Elution of cell surface AnxA2

Ca^{2+}-binding proteins on the cell surface were eluted by a previously described procedure (30). Briefly, confluent RGC-5 cells were washed with ice cold PBS and incubated in the presence of versene (Gibco) for 20 mins at 37°C. The versene eluates were centrifuged and concentrated using NANOSEP omega 10K filters (Pall Corporation) and subjected to SDS-PAGE and western immunoblot analysis. The versene eluates were checked for lack of cytosolic proteins by immunoblotting with anti-3-phosphoglycerate kinase (PGK) (31).

Cell-surface biotinylation

RGC-5 cells treated with glutamate are washed three times with ice cold PBS and were biotinylated with 0.5 mg/ml of sulfo-NHS biotin (Pierce) for 30 mins at room temperature according to the previously published protocols (32). After a series of washes, the cells were lysed in the presence of Triton-X-100 lysis buffer and the surface labeled proteins were purified by incubation with avidin-conjugated Sepharose (Sigma) overnight at 4°C. After another series of washes, Laemmlli sample buffer was added to release the surface proteins and they were separated by SDS-PAGE (4-12%), transferred onto nitrocellulose membranes and immunoblotted with anti-AnxA2 antibody (Transduction Laboratories) to detect endogenous AnxA2 or anti-GFP antibody (Cell signaling Technology) to detect AnxA2-GFP fusion protein.

Total internal reflection (TIRF) microscopy

For TIRF microscopy (33), cells were grown on 22 mm glass coverslips (VWR International), fixed in 2% ice cold paraformaldehyde in PBS for 10 min at 4°C. The cells were processed for AnxA2 immunostaining with a mouse monoclonal anti-AnxA2 antibody (Transduction Laboratories, 1:500 dilution) and observed under the Olympus IX71 microscope

equipped with a commercial TIRF attachment using Olympus 60x NA=1.45 PlanApo oil objective and Hamamatsu C4742-95 high-resolution digital camera utilizing a progressive scan interline transfer CCD chip with no mechanical shutter and Peltier cooling. Images were acquired with identical image acquisition parameters to monitor differences in the fluorescence intensity between treated and untreated cells.

Live-cell imaging of glutamate-induced intracellular Ca^{2+} dynamics

RGC-5 cells were grown on sterile glass coverslips and loaded with 3 μM of a Ca^{2+} indicator dye, Fluo-3 (Molecular Probes) in Ca^{2+}-free HEPES-buffered saline solution for 30 mins at 37°C. Ca^{2+}-dependent fluorescence responses of Fluo-3 were monitored real time by live-cell confocal imaging under the Zeiss LSM 410 microscope using Zeiss 40x, NA=1.2 C-Apochromat water immersion objective. After the addition of 500 μM glutamate, cells were imaged at an interval of every 10 secs using the LSM 4 software (Carl Zeiss) at 488 nm excitation and 526 nm emission wavelengths. To assess the extent of photobleaching of Fluo-3, the loaded cells were exposed to laser illumination continuously for 5 mins.

Intracellular Ca^{2+} ($[Ca^{2+}]_i$) measurement

Glutamate-induced Ca^{2+} mobilization in RGC-5 cells was measured using a ratiometirc Ca^{2+} imaging technique with Fura-2 AM Ca^{2+}-indicator dye at 340 nm and 380 nm excitation wavelength and 510 nm emission wavelength according to the previously published protocols (34) . The imaging was performed using a Diaphot microscope (Nikon) and metafluor software (Universal Imaging). The nanomolar concentrations of $[Ca^{2+}]_i$ was calculated using the Grynkiewicz equation (35).

Immunoprecipitation and immunoblotting

RGC-5 cells were transiently transfected with wild-type pAnxA2-GFP plasmid. The cells

were treated with glutamate for 4 hrs and subjected to versene cell surface elution and whole cell lysis (Triton-X-100 lysis buffer + 10% glycerol). The eluates and the lysates were incubated at 4°C for 12 hrs with 2 μg anti-GFP antibody (Cell Signaling Technology) immobilized on agarose beads (Sigma). Beads were washed in Triton-X-100 lysis buffer in the presence of 10% glycerol and resuspended in Laemmli sample buffer. The immunoprecipitates were analyzed by SDS-PAGE and subjected to immunoblotting with anti-phosphotyrosine (Cell Signaling Technology) and anti-phosphoserine (Sigma) antibodies.

Plasmin generation assay

A fluorogenic plasmin generation assay was performed on RGC-5 cells treated with 500 μM of glutamate for 4 hrs in the presence of anti-AnxA2 N-terminal antibody (Santa Cruz Biotechnology Inc., 20 μg/ml) or pre-immune rabbit IgG (Santa Cruz Biotechnology Inc., 20 μg/ml) for 3 hrs in complete medium. The assay was performed according to the previously published protocols (20, 36). Initial rates of plasmin generation were obtained every 4 mins by measuring the relative fluorescence units (RFU) at 400 nm excitation and 505 nm emission in a spectrophotometer (Synergy HT-Biotek). The data are represented as a fold change in plasmin generation by normalizing the RFU/min^2 of the untreated controls to the treated samples**.**

We also performed, a chromogenic plasmin generation assay in the presence of competitive peptide inhibitors for the binding of tPA to AnxA2. The assay was performed according to previously published protocols (32, 37) RGC-5 cells grown on 12-well plates were treated with 500 μM glutamate for 4 hrs. After a few washes with PBS, the cells were treated with 10 nM recombinant tPA (Molecular Innovations) in the presence of either an experimental

peptide (LCKLSL) or a control peptide (LGKLGL) or in the absence of both for 1 hr at 37°C. The reaction was initiated by the addition of 100 nM Glu-plasminogen (American Diagnostica). The reaction was monitored by taking 100 µl aliquots of the reaction mixture every 4 mins in a 96-well plate and adding 100 µl of 1 mM of chromogenic plasmin substrate, S-255 (Diapharma), dissolved in HBSS. The rates of plasmin generation were monitored by measuring the change in absorbance at 405 nm (Synergy HT-BioTek)

Image analysis

Fluoresence intensity quantification was performed by selecting individual cells using the NIH ImageJ program. For comparison purposes all images were acquired with identical image acquisition parameters and subjected to background correction by subtracting the mean fluorescence intensity of the area void of cells from that of individual cells. Mean values of fluorescence intensity ± S.E are given.

Statistical analysis

Results were expressed as mean and statistical analysis was performed using GraphPad Prism 4.02 software. One sample t-test was performed and $p<0.05$ was considered significant.

RESULTS

AnxA2 is bound to the extracellular surface of RGC-5 cells in a Ca^{2+}-dependent manner

One of the most important characteristic features of AnxA2 is its ability to interact with the plasma membrane in a Ca^{2+}-dependent manner. Substantial evidence indicates that elevation in the intracellular Ca^{2+} concentrations is a major stimulus for the translocation of AnxA2 to the plasma membrane (15). We studied the Ca^{2+}-dependent membrane association of AnxA2 in RGC-5 cells by treatment with mild concentrations of a Ca^{2+} ionophore, A23187 (5 μM). Since AnxA2 is a Ca^{2+}-dependent phospholipid binding protein, it has been grouped under the category of EDTA extractable proteins (EEPs) (38). In order to elute cell surface AnxA2, we used versene, an EDTA and PBS buffer as stated previously (30). We also analyzed the cell surface levels of AnxA2 after Ca^{2+} ionophore treatment by conjugating all cell surface proteins with a water soluble and cell-impermeable amine reactive biotin and immobilized with streptavidin. Western immunoblot analysis of versene eluates and cell surface biotinylated extracts revealed that treatment with A23187 increased the cell surface levels of AnxA2 by 73 ± 2.5% (mean ± S.E.; n=3) compared to the DMSO controls (Fig.1 A).

Glutamate induces mobilization of intracellular Ca^{2+} in RGC-5 cells

We also studied glutamate-induced intracellular Ca^{2+} mobilization by live cell confocal microscopy. In RGC-5 cells preloaded with 3 μM of Fluo-3 changes in fluorescence intensity were observed starting from 80 secs after addition of glutamate. The baseline levels were

reached at ~500 secs (Fig. 1B). To better understand glutamate-induced Ca^{2+} dynamics in RGC-5 cells, we performed live-cell ratiometric Ca^{2+} imaging using Fura-2 dual excitation Ca^{2+} indicator dye. Glutamate at a concentration of 500 μM resulted in a peak increase in the intracellular $[Ca^{2+}]_i$ to 767.96 ± 11.23 nM compared to the basal level of 120.41 ± 5.301 nM in a total of 15 cells counted. Elevation of $[Ca^{2+}]_i$ was biphasic with a transient peak due to the release of intracellular reserves of Ca^{2+} followed by a plateau (Fig. 1C). Both these studies revealed that glutamate at a concentration of 500 μM leads to a mobilization of intracellular Ca^{2+} from intracellular Ca^{2+} reserves.

Glutamate-induced intracellular Ca^{2+} mobilization stimulates the translocation of both endogenous and AnxA2-GFP to the cell surface in RGC-5 cells

We studied the effect of glutamate exposure on the translocation of AnxA2 to the plasma membrane. In RGC-5 cells, glutamate at a concentration of 500 μM increased the cell surface levels of endogenous AnxA2 in a time-dependent manner starting from 10 mins following the addition of glutamate. The surface levels of AnxA2, 4 hrs after treatment with glutamate remained elevated by 71 ± 3.2% (mean ± S.E.; n=3) compared to the levels at 0 mins after treatment with glutamate (Fig. 2A, left upper panel). The intracellular expression levels of AnxA2 however remained invariant (Fig. 2A). Coomassie stained bands were used as a control for loading for the versene eluates and immunoblotting with PGK was used as a loading control for cell lysates. Western immunoblot analysis of the cell surface biotinylated proteins revealed a similar increase at 4 hrs 82 ± 1.8% (mean ± S.E.; n=3) in the levels of cell surface AnxA2 after glutamate treatment compared to the levels of AnxA2 at 0 hrs (Fig. 2A). The membranes were reprobed for Na, K-ATPase to confirm equal loading in each lane.

Figure 1

A

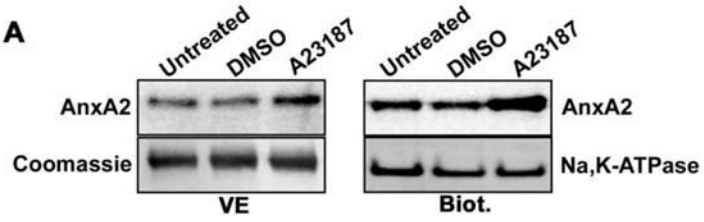

B

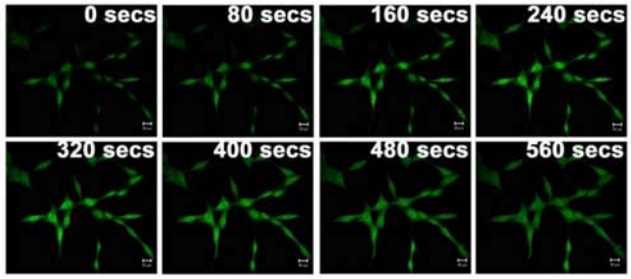

C

Baseline $[Ca^{2+}]_i$ nM	Peak $[Ca^{2+}]_i$ nM	Cells n
120.41±5.301	767.96±11.23	15

Figure 1. AnxA2 translocates to the cell surface in response to increased concentrations of intracellular Ca^{2+}, and glutamate mobilizes intracellular Ca^{2+} in RGC-5 cells

A. A representative western immunoblot of versene cell surface eluates from RGC-5 cells treated with the Ca^{2+} ionophore A23187. Following a 4 hr treatment with A23187, the RGC-5 monolayers were incubated with versene for 20 min at 37°C. The cell surface eluates were concentrated and immunoblotted for AnxA2 using a mouse monoclonal anti-AnxA2 antibody (upper panel). To normalize for loading, an SDS-PAGE was performed with identical concentrations of protein as in the upper panel and the gel was stained with Coomassie blue (lower panel). A ~50kD Coomassie stained band whose levels seemed invariant with the treatment conditions was used to account for differences in protein loading. For cell surface biotinylation, RGC-5 cells treated with A23187 were incubated for 30 mins in a cell-impermeable sulfo-NHS-Biotin reagent. After cell lysis, the biotinylated proteins were precipitated with streptavidin-conjugated agarose beads and eluted with Laemmlli buffer. The extracts were immunoblotted with anti-AnxA2 antibody. As a loading control the blot was probed with anti-Na,K-ATPase antibody. **B.** RGC-5 cells preloaded with 3 μM Fluo-3 for 30 mins were imaged under the Zeiss LSM confocal microscope for 700 secs after treatment with 500 μM glutamate at a rate of one image taken every 10 secs. The wavelengths were set to 488 nm excitation and 526 nm emission and the images were taken at identical image acquisition parameters under a 20X objective. A significant increase in Fluo-3 intensity was observed starting from 80 secs and remained elevated until about 500 secs before dropping to baseline levels. **C.** Glutamate-induced Ca^{2+} transients were measured using the live cell Fura-2 ratiometric Ca^{2+} imaging. RGC-5 cells pre-incubated with Fura-2 for 30 min were placed on a microscope stage and treated with 500 μM glutamate. The traces represent the effect of

glutamate on intracellular free Ca^{2+} concentrations and the horizontal axis represents the time during which the treatments were made. The baseline levels of $[Ca^{2+}]_i$ were measured to be 120.41 ± 5.3 nM and the peak levels were 767.96 ± 11.23 nM in 15 individual cells. (VE, versene eluate; Biot., biotinylated extract).

To visualize the cell surface-associated AnxA2 exclusively, RGC-5 cells treated with glutamate for 4 hrs were immunostained with anti-AnxA2 antibody and examined by TIRF microscopy. As TIRF microscopy selectively excites the fluorophores present at the plasma membrane, cell surface-associated AnxA2 was observed as punctuate spots on the membrane. On quantification of the number of cell surface-associated spots, we also observed that there was a significant difference in the expression levels of cell surface AnxA2 in glutamate treated cells compared to the untreated controls (Fig. 2B). These results suggest that glutamate-treated RGC-5 cells exhibit increased levels of cell surface-associated AnxA2.

To further confirm glutamate-induced cell surface translocation of AnxA2, we used a plasmid vector containing AnxA2 fused with GFP at its carboxyl terminus. RGC-5 cells on transient transfection with AnxA2-GFP plasmid construct expressed AnxA2-GFP fusion protein of ~62kD on western immunoblotting with anti-GFP antibody. The fusion protein was not observed in cells transfected with the empty vector (data not shown). Further, we examined the cell surface translocation of AnxA2-GFP fusion protein on treatment with glutamate. Western immunoblotting of the versene eluates (Fig. 2C, left upper panel) and cell surface biotinylated extracts (Fig. 2C, right lower panel) demonstrated an increase in the expression levels of AnxA2-GFP fusion protein in glutamate (250 μM and 500 μM) treated RGC-5 cells. These results suggest that glutamate-mediated elevation in the intracellular levels of Ca^{2+} mobilizes AnxA2-GFP fusion protein to the plasma membrane in a Ca^{2+}-dependent manner. Coomassie staining (Fig. 2C, left lower panel) and immunoblotting with anti-Na,K-ATPase antibody were used as loading controls for versene elution and cell surface biotinylation (Fig. 2C, right lower panel) respectively.

Figure 2

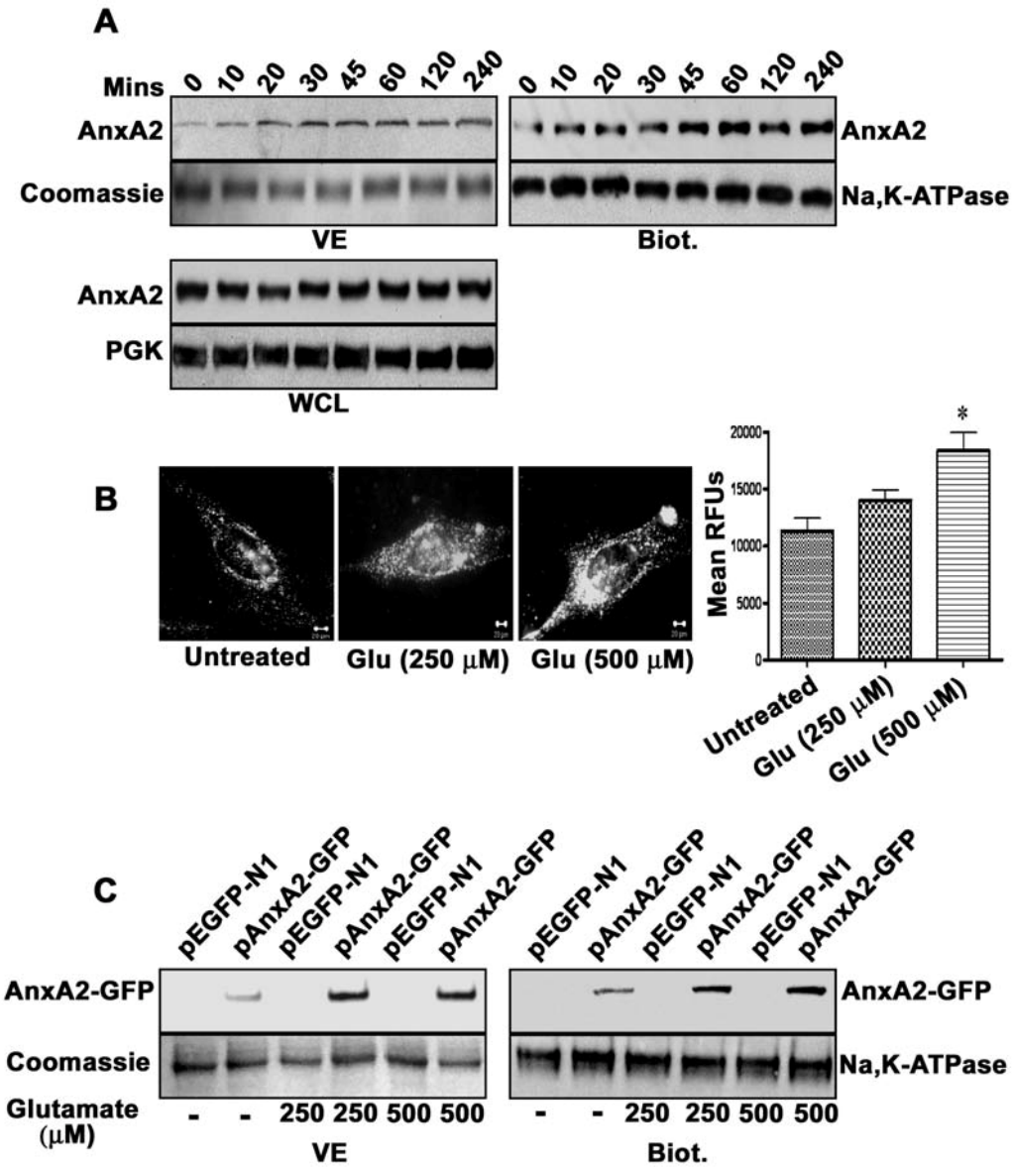
A
Mins
0 10 20 30 45 60 120 240
AnxA2
Coomassie
VE
Biot.
AnxA2
Na,K-ATPase
AnxA2
PGK
WCL
B
Untreated
Glu (250 μM)
Glu (500 μM)
Mean RFUs
20000
15000
10000
5000
0
*
Untreated
Glu (250 μM)
Glu (500 μM)
C
pEGFP-N1
pAnxA2-GFP
AnxA2-GFP
Coomassie
Glutamate (μM)
- - 250 250 500 500
VE
Biot.
AnxA2-GFP
Na,K-ATPase

Figure 2. **Glutamate induces cell surface translocation of endogenous and AnxA2-GFP in RGC-5 cells.**

A. Western immunoblot analysis of versene eluates (left panel) and cell surface biotinylated extracts (right panel) from RGC-5 cells treated with 500 μM glutamate for the indicated time periods. After collecting the versene eluates, the whole cell lysates were immunoblotted with anti-AnxA2 antibody to determine the intracellular levels of AnxA2. PGK was used to account for loading differences. Coomassie staining of the versene eluates was used as a control for loading and Na,K-ATPase was used as a loading control for biotinylation. **B.** Representative images of TIRF microscopy performed on control and glutamate (250 μM and 500 μM) treated RGC-5 cells according to the procedures described above. The images were acquired at identical acquisition settings. A significant increase in the cell surface-associated levels of AnxA2 was observed in glutamate treated RGC-5 cells compared to the untreated controls. A graphical representation of mean relative fluorescence units (RFUs) of cell surface AnxA2 immunostaining was plotted after normalizing for the background intensity. **C.** RGC-5 cells were transiently transfected with either pEGFP-N1 empty plasmid vector or AnxA2-GFP plasmid vector and treated with glutamate (250 μM and 500 μM) for 4 hrs. Versene eluates and cell surface biotinylated extracts were collected. Western immunoblotting with anti-GFP antibody revealed a 62kD band representative of AnxA2-GFP fusion protein whose levels were upregulated on treatment with glutamate (500 μM) in both the versene eluates (left upper panel) and cell surface biotinylated extracts (right upper panel). The fusion protein was not detected in the empty vector transfected cells. Coomassie stained bands (left lower panel) and Na,K-ATPase (right lower panel) were used as loading controls for versene eluates and biotinylated extracts respectively. (VE, versene eluate; Biot., biotinylated extract; WCL, whole cell lysate)

Glutamate-induced cell surface translocation of AnxA2 is N-methyl-D-aspartate (NMDA) receptor-mediated

Glutamate-induced excitotoxicity is mediated by the hyper stimulation of the NMDA-type glutamate receptors (39). In the presence of MK-801 (25 μM), a selective antagonist of the NMDA receptor, glutamate-induced elevation in the cell surface levels of annexin A2 was reduced by 65 % compared to the untreated controls (Fig. 3A). NBQX, a non-NMDA receptor antagonist failed to result in a similar effect (Fig. 3B) suggesting that the activity of NMDA receptor is essential for glutamate to exert its effects on AnxA2 translocation.

Phosphorylation of AnxA2 at tyrosine 23 is critical for glutamate-induced AnxA2 cell surface translocation

Since the endogenous and wild-type AnxA2-GFP fused protein responded similarly to glutamate treatment; we next asked whether the phosphorylation status of AnxA2 is important in the translocation process. Since AnxA2 possesses three potential phosphorylation sites, tyrosine 23, serine 25 and serine 11, at its N-terminus, we tested the involvement of these three sites in the translocation process. For this purpose, we constructed single point mutants with a phosphomimetic (AnxA2Y23E-GFP, AnxA2S25E-GFP and AnxA2S11E-GFP) and a non-phosphomimetic variant (AnxA2Y23F-GFP, AnxA2S25A-GFP and AnxA2S11A-GFP) at both tyrosine 23 and serine 25. On transient transfection of RGC-5 cells and glutamate treatment (500 μM for 4 hrs), we studied the extent to which the mutant variants are translocated to the cell surface using versene cell surface elution and cell surface biotinylation. It was observed that the cell surface levels of AnxA2Y23F-GFP were significantly reduced by 81 ± 5% (mean ± S.E.; n=4) and 79 ± 2% (mean ± S.E.; n=3) compared to the wild-type AnxA2-GFP in the versene

Figure 3

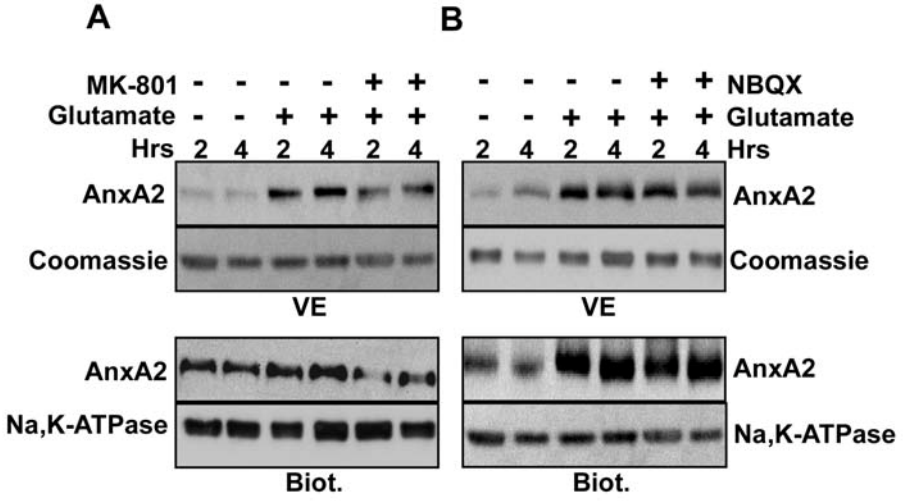
A
B
MK-801 - - - - + +
Glutamate - - + + + +
Hrs 2 4 2 4 2 4
NBQX
AnxA2
Coomassie
VE
Na,K-ATPase
Biot.

Figure 3. Glutamate-induced AnxA2 cell surface translocation is NMDA receptor-mediated

A. Western immunoblot of the versene eluates (left top panel) and cell surface biotinylated extracts (left bottom panel) from RGC-5 cells treated with MK-801 (10 μM), a NMDA receptor antagonist in the presence of glutamate. For comparison, we also checked the cell surface levels of AnxA2 in glutamate untreated and glutamate treated cells in the absence of MK-801 for the indicated time. **B.** The effect of an inhibitor for the non-NMDA receptor, NBQX (25 μM) on glutamate-induced cell surface translocation of AnxA2 was also tested. A western immunoblot for the versene eluates (right top panel) and cell surface biotinylated extracts (right bottom panel) is shown. For versene eluates a Coomassie stained gel and for biotinylated extracts immunoblotting with anti-Na,K-ATPase antibody served as a loading control. (VE, versene eluate; Biot., biotinylated extract)

eluates and cell surface biotinylated extracts respectively (Fig. 4A). All other variants at tyrosine 23 and serine 25 AnxA2Y23E-GFP, AnxA2S25E-GFP and AnxA2S25A-GFP (Fig. 4B, C and D respectively) had similar cell surface distribution as that of wild-type AnxA2-GFP on glutamate treatment. Furthermore the serine 11 phosphorylation mutants, AnxA2S11E-GFP and AnxA2S11A-GFP, did not influence the cell surface translocation of AnxA2 (data not shown). The intracellular levels of AnxA2-GFP did not seem to be affected on glutamate treatment in the cell lysates of all the phosphorylation mutants.

To further investigate whether phosphorylation at tyrosine 23 occurs in conjunction with phosphorylation at serine 25 to facilitate the cell surface translocation of AnxA2, we constructed phospho-mimicking and non-phospho-mimicking double mutants of AnxA2 at tyrosine 23 and serine 25. Both cell surface biotinylation and versene elution revealed that the double non phospho-mimicking mutant AnxA2Y23FS25A-GFP showed the similar distribution as the single non phospho-mimicking mutant AnxA2Y23F-GFP with markedly reduced 90 ± 4.2% (mean ± S.E.; n=3) cell surface distribution and predominant cytosolic distribution compared the wild-type AnxA2-GFP (Fig. 5A). Although AnxA2Y23FS25E-GFP was predominantly distributed in the cytosol its levels on the cell surface were observed to be reduced by 57 ± 3.8% (mean ± S.E.; n=3) compared to wild-type AnxA2-GFP (Fig.5B). The other two mutants AnxA2Y23ES25A-GFP and AnxA2Y23ES25E-GFP were observed to have similar cell surface distribution like that of wild-type AnxA2-GFP with elevated cell surface levels on glutamate treatment and invariant cytosolic levels (Fig. 5 C and D). For all the mutants, Coomassie staining and immunoblotting with anti-Na,K-ATPase was used as a loading control for versene eluates and biotinylated extracts respectively. The purity of the versene eluates was tested in each case by immunoblotting with PGK. Taken together, these results indicate that tyrosine 23 at the

Figure 4

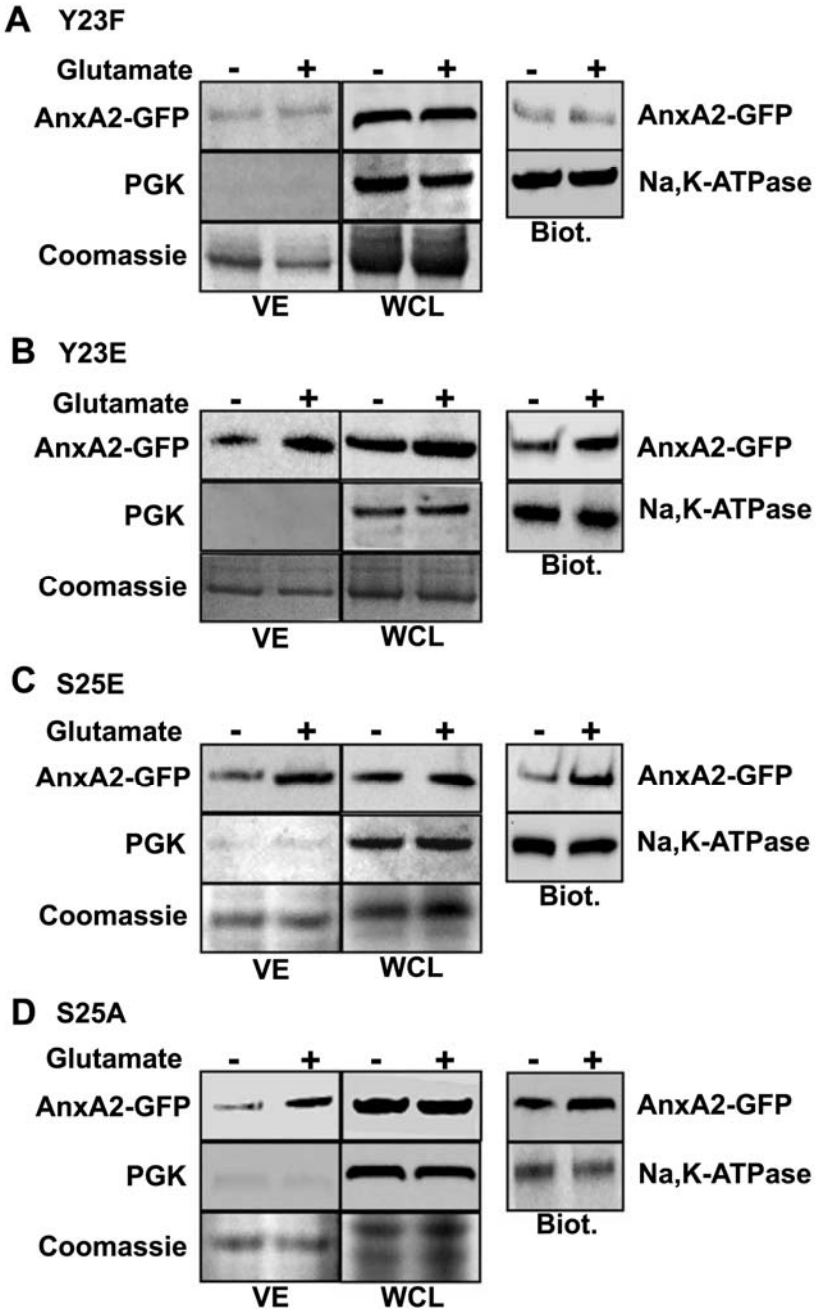
A Y23F
Glutamate - + - + - +
AnxA2-GFP
PGK
Coomassie
VE WCL
AnxA2-GFP
Na,K-ATPase
Biot.
B Y23E
Glutamate - + - + - +
AnxA2-GFP
PGK
Coomassie
VE WCL
AnxA2-GFP
Na,K-ATPase
Biot.
C S25E
Glutamate - + - + - +
AnxA2-GFP
PGK
Coomassie
VE WCL
AnxA2-GFP
Na,K-ATPase
Biot.
D S25A
Glutamate - + - + - +
AnxA2-GFP
PGK
Coomassie
VE WCL
AnxA2-GFP
Na,K-ATPase
Biot.

Figure 4. Cell surface translocation of single phosphorylation mutants at tyrosine 23 and serine 25 on glutamate treatment

A. RGC-5 cells were transfected with a plasmid vector expressing a phosphomimetic mutant at tyrosine 23 (AnxA2Y23F-GFP) and subjected to glutamate treatment for 4 hrs. The versene eluates and cell lysates were collected, SDS-PAGE and western immunoblotting was performed with anti-GFP antibody (left top panel). To determine the purity of the versene eluates, western immunoblotting was performed with PGK (left middle panel). As a control for loading, the gel was stained with Coomassie (left bottom panel). The cell surface AnxA2 was extracted by conjugation with a hydrophilic cell impermeable biotin analog and precipitated with streptavidin. Western immunoblotting of the cell surface biotinylated extracts was performed with anti-GFP antibody (right top panel). As a control for loading the blot was probed with anti-Na,K-ATPase antibody (right bottom panel). **B.** RGC-5 cells were transfected with a plasmid vector expressing the non-phosphomimetic mutant at tyrosine 23 (AnxA2Y23E-GFP) and treated with glutamate for 4 hrs. The versene eluates and cell lysates were collected and subjected to western immunoblotting with anti-GFP antibody (left top panel). Immunoblotting with PGK (left middle panel) and Coomassie staining of the gel (left bottom panel) was performed as described above. The cell surface biotinylated extracts were collected and western immunoblotting was performed with anti-GFP antibody (right top panel), Na.K-ATPase was used to control for loading. **C&D.** RGC-5 cells were transfected with a plasmid vector expressing a phosphomimetic mutant at serine 25 (AnxA2S25E-GFP) and a non-phosphomimetic mutant (AnxA2S25A-GFP), treated with glutamate and subjected with western immunoblotting as described above. (VE, versene eluate; Biot., biotinylated extract; WCL, whole cell lysate)

Figure 5

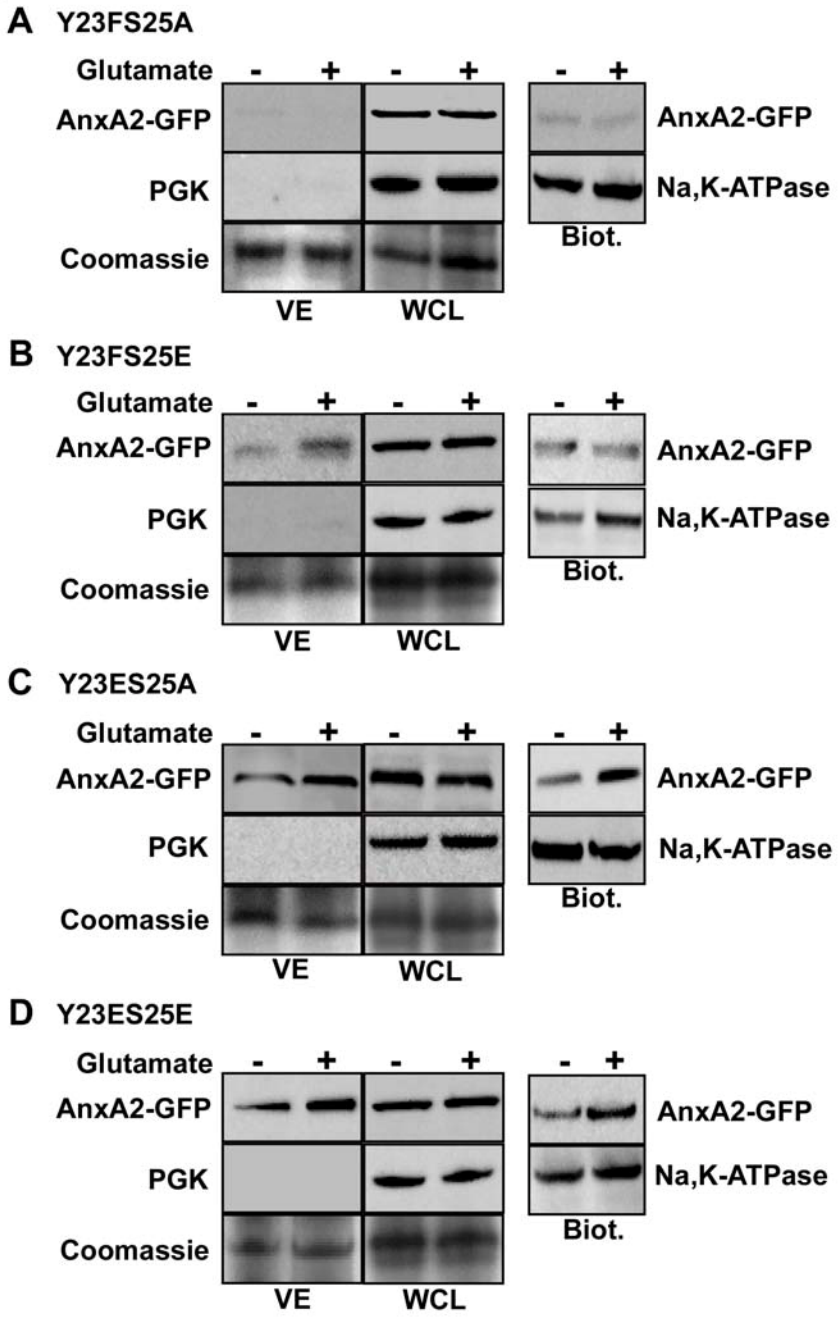
A Y23FS25A
Glutamate - + - + - +
AnxA2-GFP
PGK
Coomassie
VE WCL
AnxA2-GFP
Na,K-ATPase
Biot.
B Y23FS25E
Glutamate - + - + - +
AnxA2-GFP
PGK
Coomassie
VE WCL
AnxA2-GFP
Na,K-ATPase
Biot.
C Y23ES25A
Glutamate - + - + - +
AnxA2-GFP
PGK
Coomassie
VE WCL
AnxA2-GFP
Na,K-ATPase
Biot.
D Y23ES25E
Glutamate - + - + - +
AnxA2-GFP
PGK
Coomassie
VE WCL
AnxA2-GFP
Na,K-ATPase
Biot.

Figure 5. Distribution of tyrosine 23 and serine 25 double phosphorylation mutants of AnxA2 in response to glutamate treatment.

A-D. RGC-5 cells were transiently transfected with plasmid vectors expressing phosphomimetic and non-phosphomimetic double mutants at tyrosine 23 and serine 25 (AnxA2Y23FS25A-GFP, AnxA2Y23FS25E-GFP, AnxA2Y23ES25A-GFP, AnxA2Y23ES25E-GFP). The cells were treated with 500 μM glutamate for 4 hrs. The versene eluates and cell surface biotinylated extracts were collected as previously mentioned and immunoblotted with anti-GFP antibody. The versene eluates were tested for their purity by immunoblotting with anti-PGK antibody. A Coomassie stained gel was used as a loading control for the versene eluates. The biotinylated extracts were probed with anti-Na,K-ATPase antibody to determine equal loading. Glu, VE, WCL and Biot. signify glutamate, versene eluate, whole cell lysate and biotinylated extracts respectively. All the blots were exposed to identical exposure times. (VE, versene eluate; Biot., biotinylated extract; WCL, whole cell lysate).

.

N-terminus of AnxA2 plays a predominant, but not exclusive role in the cell surface translocation of AnxA2. The involvement of serine 25 however can not be ruled out as the double mutant AnxA2Y23FS25E is still able to translocate to the cell surface even in the presence of a non phospho-mimetic residue at tyrosine 23.

Glutamate-induced cell surface AnxA2 is predominantly phosphorylated at tyrosine 23

To confirm the role of tyrosine 23 phosphorylation on the cell surface translocation of AnxA2, versene eluates and whole cell lysates of RGC-5 cells transfected with AnxA2-GFP fusion construct were immunoprecipitated with anti-GFP antibody. On western immunoblotting with anti-AnxA2 antibody a time-dependent increase in the cell surface levels of AnxA2-GFP fusion protein was observed in the versene eluates (Fig. 6A, left panel) whereas the cytosolic levels of the fusion protein remained invariant (Fig. 6A, right panel). Next, we investigated the phosphorylation status of glutamate-induced cell surface AnxA2. For this purpose, the immunoprecipitates were immunoblotted with anti-phosphotyrosine and anti-phosphoserine antibodies. It was observed that the cell surface-associated AnxA2-GFP fusion protein is tyrosine-phosphorylated and its levels are elevated in a time-dependent manner on treatment with 500 μM glutamate (Fig. 6B, left panel). Tyrosine-phosphorylated AnxA2-GFP fusion protein was also detected in the cell lysates (Fig. 6B, right panel). In contrast, we did not detect any serine-phosphorylated AnxA2-GFP in the versene eluates of glutamate treated and untreated cells (Fig. 6C, left panel) although phosphoserine-AnxA2-GFP was detected in the whole cell lysates (Fig. 6C right panel). From this data, it appears that glutamate-induced mobilization of intracellular Ca^{2+} leads to the translocation of tyrosine-phosphorylated AnxA2 to the cell surface. Although serine-phosphorylated AnxA2 was detected within the cell, it does not seem to have a

Figure 6

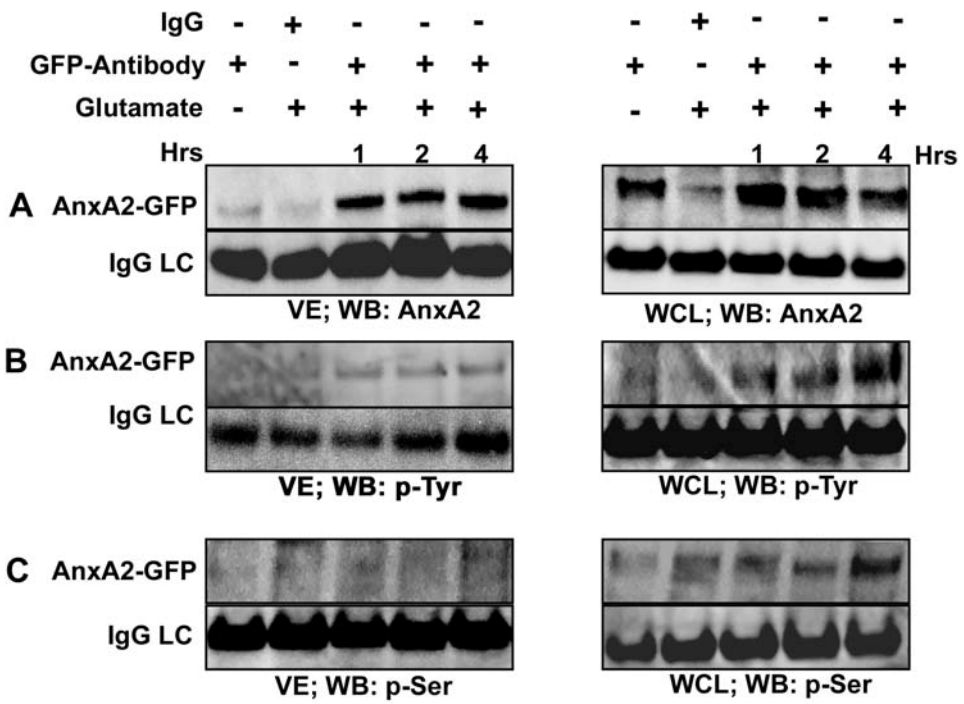
IgG - + - - - - + - - -
GFP-Antibody + - + + + + - + + +
Glutamate - + + + + - + + + +
Hrs 1 2 4 1 2 4 Hrs
A AnxA2-GFP
IgG LC
VE; WB: AnxA2
WCL; WB: AnxA2
B AnxA2-GFP
IgG LC
VE; WB: p-Tyr
WCL; WB: p-Tyr
C AnxA2-GFP
IgG LC
VE; WB: p-Ser
WCL; WB: p-Ser

Figure 6. Glutamate-induced cell surface AnxA2 is tyrosine phosphorylated

A. RGC-5 cells were transfected with a plasmid vector expressing wild-type AnxA2-GFP were treated with 500 μM glutamate for 1, 2 and 4 hrs. The cells were incubated in versene buffer for 20 mins and after collecting the versene eluates, the cells were lysed. The versene eluates and the lysates were immunoprecipitated with anti-GFP antibody. The eluates and lysates were incubated with nonspecific anti-mouse IgG for negative controls. The immunoprecipitates were subjected to SDS-PAGE and analyzed by western immunoblotting with anti-AnxA2 antibody. **B&C.** Immunoprecipitates of the versene eluates and lysates collected as mentioned above were immunoblotted with anti-phosphotyrosine and anti-phosphoserine antibodies respectively. IgG light chain (IgG LC) of the antibody used for immunoprecipitation was used as a control for loading. All the blots were exposed to identical exposure times. (VE, versene eluate; Biot., biotinylated extract; WCL, whole cell lysate)

significant contribution to the cell surface pool of AnxA2. As a control for loading the light chain of the immunoprecipitated antibody (IgGLC) was used.

Since we detected that cell surface-associated AnxA2 is predominantly tyrosine phosphorylated, we tested if inhibition of the phosphorylation event could prevent the cell surface translocation of AnxA2. Treatment with sodium orthovanadate, a tyrosine phosphatase inhibitor augmented the cell surface levels of AnxA2 in both the glutamate treated 72 ± 1.7% (mean ± S.E.; n=4) and untreated cells 65 ± 2.7% (mean ± S.E., n=4) (Fig. 7A, left panel), whereas okadaic acid, a serine/threonine phosphatase inhibitor had no effect on the cell surface levels of AnxA2 (Fig. 7B, left panel). In addition, when we treated the cells with genistein, a general tyrosine kinase inhibitor, we observed that glutamate-induced translocation of AnxA2 was markedly inhibited (Fig. 7C, left panel). On immunoprecipitation of versene eluates and cell surface biotinylated extracts with anti-GFP antibody and immunoblotting with anti-phosphotyrosine antibody, we detected an increase in the tyrosine-phosphorylation in glutamate treated RGC-5 cells in the presence of sodium orthovanadate (Fig. 7A, right panel), while okadaic acid did not significantly influence the phosphorylation status of cell surface AnxA2 (Fig.7B left panel). In contrast, genistein markedly reduced the expression of cell surface-associated tyrosine-phosphorylated AnxA2 in the presence of glutamate (Fig 7C left panel).

Glutamate enhances AnxA2-mediated cell surface plasmin generation

Having demonstrated that glutamate induces the cell surface translocation of AnxA2, we examined if the increased cell surface pool of AnxA2 is associated with a concomitant increase in AnxA2-mediated generation of plasmin. In RGC-5 cells treated with glutamate, we observed a 1.7 ± 0.4 (mean ± S.E.; n=6) fold increase in the cell surface generation of plasmin in glutamate

Figure 7

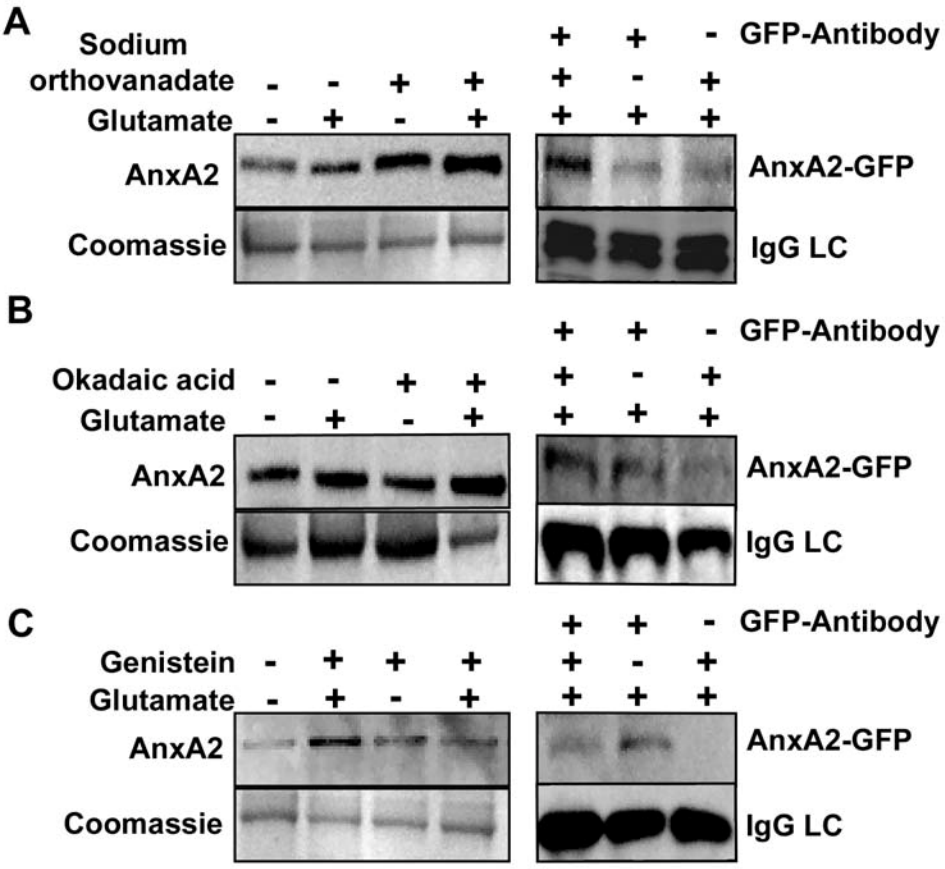
A
Sodium orthovanadate
Glutamate
AnxA2
Coomassie
GFP-Antibody
AnxA2-GFP
IgG LC
B
Okadaic acid
Glutamate
AnxA2
Coomassie
GFP-Antibody
AnxA2-GFP
IgG LC
C
Genistein
Glutamate
AnxA2
Coomassie
GFP-Antibody
AnxA2-GFP
IgG LC

Figure 7. Tyrosine phosphorylation of AnxA2 is critical for its cell surface translocation

A. RGC-5 cells were incubated for 4 hrs with or without glutamate in the presence or absence of a tyrosine phosphatase inhibitor, sodium orthovanadate (1mM). The versene eluates were collected and subjected to SDS-PAGE and western immunoblotting with anti-AnxA2 antibody. A Coomassie stained gel was used as a control for loading (left panel). In addition, RGC-5 cells were transfected with a plasmid expressing wild-type AnxA2-GFP and treated with glutamate and sodium orthovanadate. The versene eluates were subjected to immunoprecipitation with anti-GFP antibody and immunoblotted with anti-phosphotyrosine antibody (right panel). **B.** RGC-5 cells were treated with a serine/threonine phosphatase inhibitor, okadaic acid (100 nM) and glutamate. After collecting the versene eluates, they were subjected to western immunoblotting (left panel) and immunoprecipitation (right panel) as described above. **C.** Cells were treated with a general tyrosine kinase inhibitor genistein (100 μM) for 4 hrs, and glutamate and subjected to procedures described above. For versene eluates Coomassie stained gel and for immunoprecipitation experiments, IgG light chain (IgG LC) from the antibody used for immunoprecipitation were used to normalize for loading. For immunoprecipitation the anti-GFP antibody was omitted and a non-specific antibody was used to serve as negative control.

treated cells compared to the untreated controls (Fig. 8A). Since the N-terminal region of AnxA2 is responsible for its interaction with its binding partners like p11/S100A10 and tPA, we made use of an antibody directed against the N-terminus of AnxA2 to test its involvement in plasmin generation. Both glutamate-induced and baseline levels of plasmin generation were seen to be inhibited by anti-AnxA2 antibody whereas pre-immune IgG did not have any influence.

To further confirm the involvement of the N-terminus of AnxA2 in plasmin generation *in vitro*, we made use of a competitive peptide inhibitor of tPA-binding to AnxA2. Previous reports have identified a hexapeptide LCKLSL from regions 7-12, as the minimum sequence required for the binding of tPA to AnxA2 (40). The competitive peptide was assayed for its ability to inhibit the binding of tPA to AnxA2 both *in vitro* and *in vivo* and it was observed that the LCKLSL peptide resulted in a 40-60% reduction in the binding of tPA to AnxA2. It was also observed that peptides with a replacement of the cysteine residue at position 8 with glycine (LGKLSL), did not possess any inhibitory effects (40).

As shown in the Fig. 8B, the hexapeptide LCKLSL at a concentration of 250 μM resulted in a 1.4 ± 0.2 (mean ± S.E.; n=6) fold reduction in plasmin generation on glutamate treatment compared to the control peptide, LGKLSL. The peptide seemed to have only moderate effects on the baseline levels of plasmin generation in glutamate untreated cells (data not shown). Taken together, these results suggest that glutamate-induced increase in the cell surface levels of AnxA2 directly contribute to a corresponding increase in the AnxA2-mediated cell surface generation of plasmin.

Figure 8

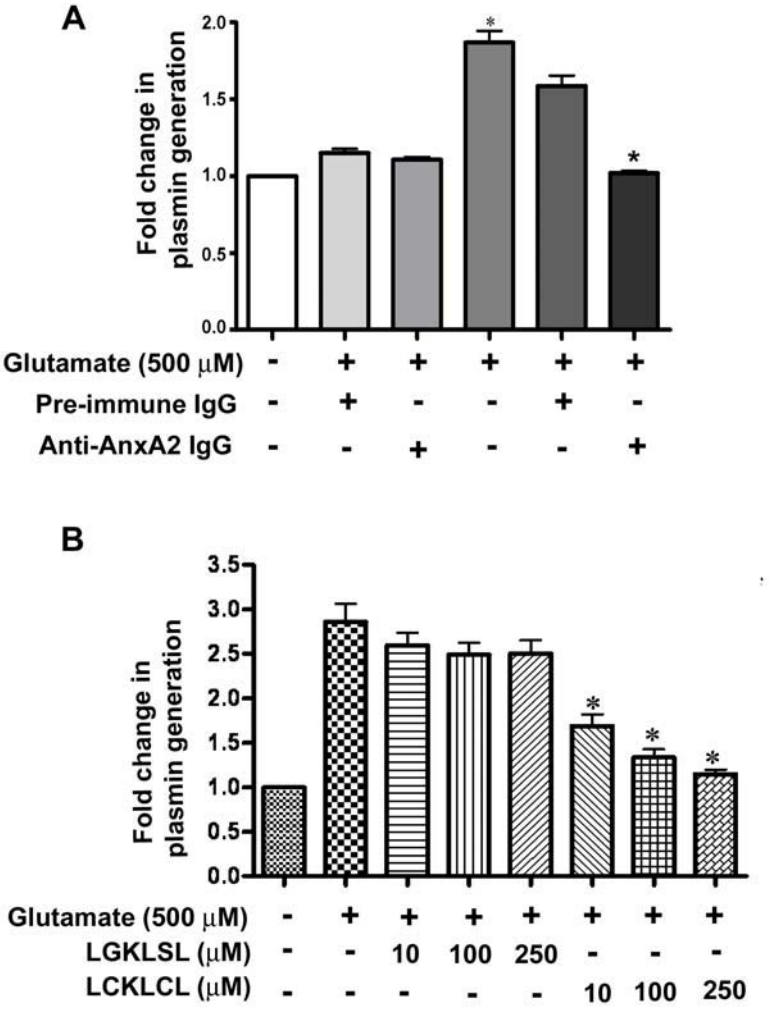
A
Fold change in plasmin generation
2.0
1.5
1.0
0.5
0.0
*
*
Glutamate (500 μM) - + + + + +
Pre-immune IgG - + - - + -
Anti-AnxA2 IgG - - + - - +
B
Fold change in plasmin generation
3.5
3.0
2.5
2.0
1.5
1.0
0.5
0.0
*
*
*
Glutamate (500 μM) - + + + + + + +
LGKLSL (μM) - - 10 100 250 - - -
LCKLCL (μM) - - - - - 10 100 250

Figure 8. Glutamate enhances AnxA2-mediated cell surface plasmin generation.

A. RGC-5 cells untreated and treated with 500 μM glutamate for 4 hrs were incubated in the presence of recombinant plasminogen (100 nM) for 1 hr at 4°C. The cells were treated either with an antibody against the N-terminus of AnxA2 (20 μg/ml) or a pre-immune antibody (20

μg/ml) and subsequently treated with recombinant tPA (10 nM) in the presence of a fluorogenic plasmin substrate. The initial rates of plasmin generation were measured every 4 mins and represented as RFU/min^2. The fold change in plasmin generation was obtained by normalizing different treatment groups with the untreated controls whose value was set to 1.0 (Mean RFU/min^2=320). **B.** RGC-5 cells were cultured in monolayers and treated with 500 μM of glutamate for 4 hrs. The cells were gently washed and treated with recombinant tPA (10 nM) in the presence of either the experimental (LCKLSL) or the control peptide (LGKLSL) at the indicated concentrations for 1 hr at 37°C. After three washes, recombinant plasminogen (100 nM) was added to the reaction mixture and the reaction was monitored by removing aliquots every 4 mins and measuring the amount of plasmin generated by cleavage of a chromogenic substate of plasmin, S-2251. To serve as controls, either tPA or glutamate was omitted from the reaction mixture. The fold change in plasmin generation was obtained by normalizing different treatment groups with the untreated controls whose value was set to 1.0 (Mean absorbance units $(AU)_{405\ nm}$= 3.68).* indicates $p \leq 0.05$.

DISCUSSION

In this study, we provide evidence to show that glutamate-mediated increase in the

intracellular levels of Ca^{2+}results in the cell surface translocation of both endogenous and AnxA2-GFP to the cell surface. We also observed that AnxA2 translocates to the cell surface in the presence of a Ca^{2+} ionophore A23187, suggesting that elevated intracellular Ca^{2+} levels is a key stimulus for the translocation process. Furthermore, we show that the Ca^{2+}-dependent cell surface translocation of AnxA2 requires the phosphorylation of tyrosine 23 at the N-terminus of

AnxA2 and mutation of this residue significantly inhibits the translocation process. The cell surface translocated AnxA2-GFP fusion protein was observed to be tyrosine-phosphorylated on glutamate treatment. We also confirmed the involvement of tyrosine 23 by using a tyrosine phosphatase inhibitor, sodium orthovanadate, and a tyrosine kinase inhibitor, genistein, which augmented and inhibited the translocation process respectively.

Our data on both the single mutants of serine 25 and double mutants at tyrosine 23 and serine 25 suggested that although serine 25 seemed to influence the translocation process, it has minimal contribution compared to tyrosine 23. Further, our observation that serine- phosphorylated AnxA2 was present in the cell lysates and not in the versene eluates suggested that although intracellular AnxA2 is serine-phosphorylated, it could be dephosphorylated during the cell surface translocation process. We also questioned the involvement of serine 11 in the cell surface translocation of AnxA2 and our data on the phosphomimetic and non-phosphomimetic single mutants at serine 11 suggested that this residue does not influence the translocation process. Furthermore, we also demonstrated that the cell surface AnxA2 is an active plasmin- generating complex and this activity can be inhibited by both an antibody and a hexapeptide directed against the N-terminus of AnxA2. These results indicated that the N-terminus of AnxA2 is important not only for

phosphorylation, but also for the binding of tPA and further generation of plasmin.

The proteolytic properties of secreted proteases like tPA and uPA have been implicated in the loss of RGCs on ischemic and excitotoxic injury but the exact molecular mechanisms that contribute to protease-mediated RGC death are still unclear (7). It has been reported that during ischemic and excitotoxic damage, RGCs are vulnerable to elevated levels of extracellular glutamate in the retina caused by disruptions in glutamate homeostasis (41, 42). Elevated intracellular concentrations of Ca^{2+} occurs as a result of hyper-stimulation of glutamate receptors and entry of extracellular Ca^{2+} or the release of Ca^{2+} from the intracellular store-operated Ca^{2+} channels (43). The increased intracellular concentrations of Ca^{2+} leads to the activation of several Ca^{2+}-dependent proteases that contribute to the pathological changes in the retina (44). A variety of ECM modulating proteases have been implicated in the loss of RGCs (45, 46) and development of strategies to prevent these proteolytic processes could offer significant protection to the RGCs.

Previous studies have reported the involvement of secreted proteases tPA and uPA in the ischemia-reperfusion model and the excitotoxin treated models of retinal damage (47, 48). The secreted proteases are known to contribute to RGC loss in mechanisms that are both dependent and independent of plasminogen activation (47, 49). It has been reported that optic nerve crush induces an upregulation of uPA which results in the compromise of the blood retinal barrier (BRB) and extravasation of plasminogen and these studies have also reported that under conditions of optic nerve injury, the secreted levels of tPA are not induced (48). However, studies in the CNS have shown that under conditions of ischemic injury,

extracellular tPA and plasmin can exacerbate ischemic neuronal damage by further damaging the blood brain barrier, activation of the NMDA receptor by cleavage of the NR1 subunit, amplification of intracellular Ca^{2+} signaling and activation of matrix bound metalloproteinases (50, 51). tPA also potentiates neuronal loss and inhibitors of the tPA/plasmin proteolytic cascade have been found to confer protection to the CNS neurons (52). Since retina is commonly viewed as an extension of the CNS, the mechanism of action of tPA could be similar in the two systems. We propose that although secreted levels of tPA are not found to be induced on ischemic injury in the retina, under ischemic conditions when there is a leakage of circulating plasminogen,

extracellular tPA and plasminogen can bind to their cell surface receptors and potentiate the generation of plasmin which could contribute to the loss of RGCs.

Generation of plasmin is a highly orchestrated process involving several cell surface receptors that mediate localized generation of plasmin (53). These receptors also act as docking sites for the binding of circulating plasminogen and tPA and result in not only an increase in the catalytic efficiency of plasmin generation but in the protection of plasmin from being degraded by its physiological inhibitors (54). Hence in order to better understand the role of secreted proteases in retinal damage, it is important to study the cell surface receptors for plasmin generation.

One such cell surface co-receptor for tPA and plasminogen is AnxA2 (55). Extracellular AnxA2 serves as a cell surface receptor for many ECM modulating proteins like tenascin C and procathepsin B, and its interaction with the components of the plasminogen system, tPA and plasminogen, is well characterized (16, 30). Cell surface association of

AnxA2 is a high affinity Ca^{2+}-dependent interaction requiring the binding of Ca^{2+} to the endonexin repeat 2 of AnxA2 (56). The remarkable sequence conservation of the endonexin repeats suggests the importance of AnxA2 in regulating Ca^{2+}-mediated signaling events in the cell (56). Since cell surface AnxA2 is the major fibrinolytic receptor facilitating the enhanced generation of plasmin, regulation of the cell surface translocation of AnxA2 may be an important process in the generation of plasmin and its downstream effects. It is also known that AnxA2 binds to the membrane in a Ca^{2+}-

dependent manner, elevation of intracellular levels of Ca^{2+} has been previously shown to one of

the key stimulus that translocates AnxA2 to the cell surface (25, 57). However, glutamate-induced mobilization of AnxA2 to the extracellular surface of the plasma membrane and its role in the pathogenesis of retinal diseases has not been previously demonstrated. The sequence of events involved in the retinal damage under ischemic and excitotoxic injury and the proposed role of AnxA2 are depicted in fig. 9.

Although, there are initial reports suggesting that AnxA2 is abundantly expressed proteins in the ganglion cell layer of the adult retina, its functions have not been elucidated. The data presented here suggest a role for AnxA2 in potentiating glutamate-induced proteolytic events in the retina. Previous reports have indicated that even modest increase in the cell surface levels of AnxA2 can have profound implications in the pathogenesis of several diseases (58, 59). Dysregulation in the cell surface expression levels of AnxA2 have been shown to manifest as bleeding diseases conferring on the cells the ability to generate increased levels of plasmin (58). Many cancer cells have also been shown to abundantly express cell surface AnxA2 which confers on them the invasive and

metastatic behavior by generation of plasmin or by plasmin- mediated activation of matrix metalloproteinases (60). Therefore AnxA2 can serve as a potential therapeutic target for the neurodegenerative diseases of the eye, like glaucoma.

Figure 9

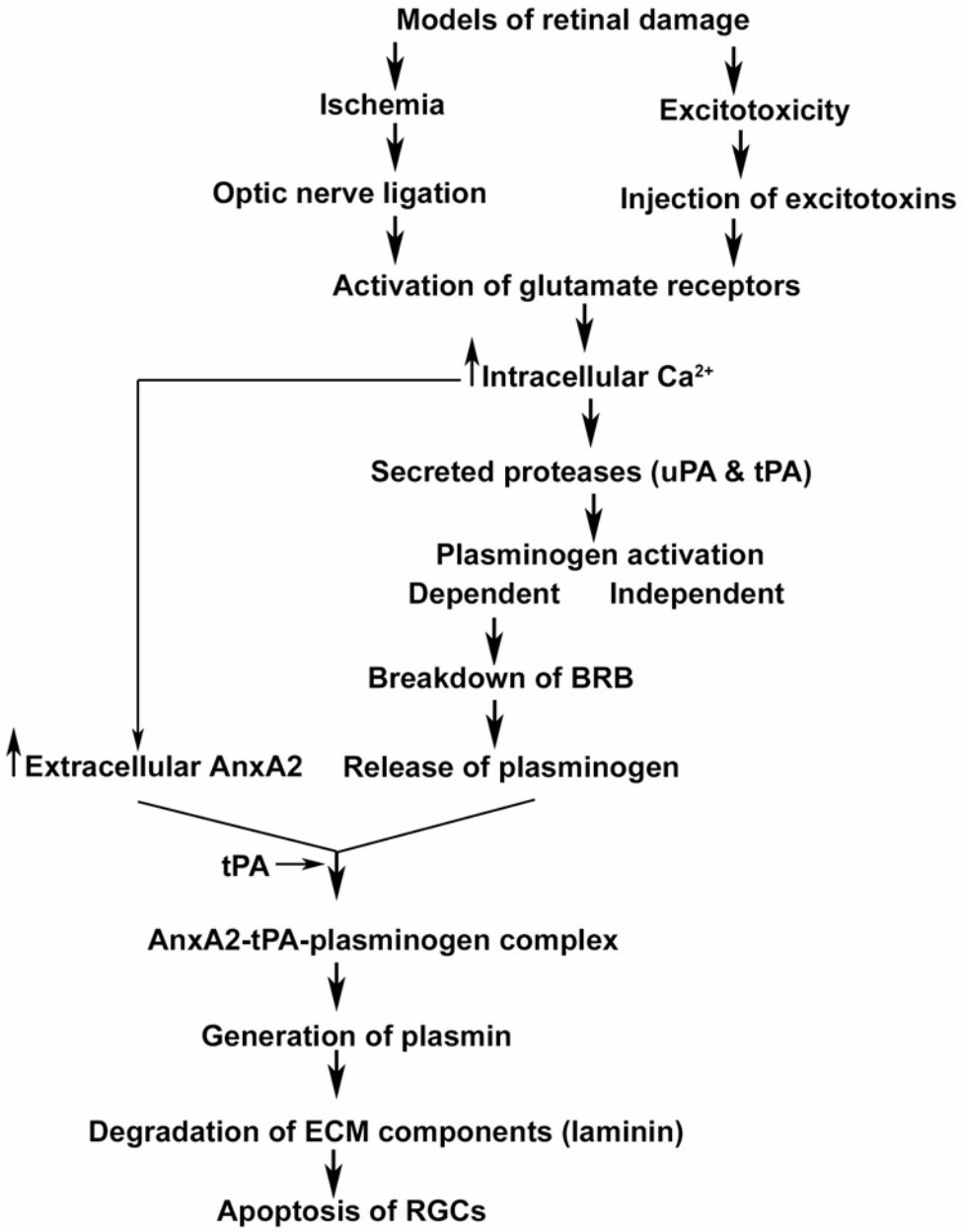
Models of retinal damage
Ischemia
Excitotoxicity
Optic nerve ligation
Injection of excitotoxins
Activation of glutamate receptors
Intracellular Ca^{2+}
Secreted proteases (uPA & tPA)
Plasminogen activation
Dependent
Independent
Breakdown of BRB
Extracellular AnxA2
Release of plasminogen
tPA
AnxA2-tPA-plasminogen complex
Generation of plasmin
Degradation of ECM components (laminin)
Apoptosis of RGCs

Figure 9. Schematic representation of the proteolytic cascade involved in the ischemic and excitotoxic damage of RGCs.

In ischemic and excitotoxic models of retinal damage, previous studies have suggested that excessive accumulation of extracellular glutamate leads to a hyper-stimulation of glutamate receptors which results in the elevated levels of intracellular Ca^{2+}. Previous studies have suggested that elevated levels of intracellular Ca^{2+} leads to the activation of secreted proteases like uPA and tPA. In the present study, we show that AnxA2, an extracellular co-receptor for tPA and plasminogen is mobilized to the cell surface in response to increased intracellular Ca^{2+} levels. It is known that protease-mediated loss of ganglion cells occurs by mechanisms that are both dependent and independent of plasminogen activation. In ischemic retinal damage, plasminogen is released into the retina by the breakdown of the BRB and the proposed role of AnxA2 as an extracellular plasmin-generating complex could be one of the mechanisms of ECM breakdown and subsequent apoptosis of RGCs.

REFERENCES

1. Kuehn, M. H., Fingert, J. H., and Kwon, Y. H. (2005) *Ophthalmol. Clin. North Am.* **18**, 383-95, vi

2. Ji, J., Chang, P., Pennesi, M. E., Yang, Z., Zhang, J., Li, D., Wu, S. M., and Gross, R. L. (2005) *Vision Res.* **45**, 169-179

3. Vorwerk, C. K., Naskar, R., and Dreyer, E. B. (1999) *Klin. Monatsbl. Augenheilkd.* **214**, 2-11

4. Lipton, S. A., and Rosenberg, P. A. (1994) *N. Engl. J. Med.* **330**, 613-622

5. Lotery, A. J. (2005) *Eye* **19**, 369-370

6. Ullian, E. M., Barkis, W. B., Chen, S., Diamond, J. S., and Barres, B. A. (2004) *Mol. Cell. Neurosci.* **26**, 544-557

7. Chintala, S. K. (2006) *Exp. Eye Res.* **82**, 5-12

8. Plow, E. F., Herren, T., Redlitz, A., Miles, L. A., and Hoover-Plow, J. L. (1995) *FASEB J.* **9**, 939-945

9. Syrovets, T., and Simmet, T. (2004) *Cell Mol. Life Sci.* **61**, 873-885

10. Kumada, M., Niwa, M., Wang, X., Matsuno, H., Hara, A., Mori, H., Matsuo, O., Yamamoto, T., and Kozawa, O. (2004) *Toxicol. Appl. Pharmacol.* **200**, 48-53

11. Longstaff, C. (2002) *Front. Biosci.* **7**, d244-55

12. Cesarman, G. M., Guevara, C. A., and Hajjar, K. A. (1994) *J. Biol. Chem.* **269**, 21198-21203

13. Gerke, V., Creutz, C. E., and Moss, S. E. (2005) *Nat. Rev. Mol. Cell Biol.* **6**, 449-461

14. Raynal, P., and Pollard, H. B. (1994) *Biochim. Biophys. Acta* **1197**, 63-93

15. Rescher, U., and Gerke, V. (2004) *J. Cell. Sci.* **117**, 2631-2639

16. Gerke, V., and Moss, S. E. (2002) *Physiol. Rev.* **82**, 331-371

17. Glenney, J. R.,Jr. (1985) *FEBS Lett.* **192**, 79-82

18. Gould, K. L., Woodgett, J. R., Isacke, C. M., and Hunter, T. (1986) *Mol. Cell. Biol.* **6**, 2738-2744

19. Regnouf, F., Sagot, I., Delouche, B., Devilliers, G., Cartaud, J., Henry, J. P., and Pradel, L. A. (1995) *J. Biol. Chem.* **270**, 27143-27150

20. Deora, A. B., Kreitzer, G., Jacovina, A. T., and Hajjar, K. A. (2004) *J. Biol. Chem.* **279**, 43411-43418

21. Hubaishy, I., Jones, P. G., Bjorge, J., Bellagamba, C., Fitzpatrick, S., Fujita, D. J., and Waisman, D. M. (1995) *Biochemistry* **34**, 14527-14534

22. Bellagamba, C., Hubaishy, I., Bjorge, J. D., Fitzpatrick, S. L., Fujita, D. J., and Waisman, D. M. (1997) *J. Biol. Chem.* **272**, 3195-3199

23. Johnstone, S. A., Hubaishy, I., and Waisman, D. M. (1992) *J. Biol. Chem.* **267**, 25976-25981

24. Liu, J., Rothermund, C. A., Ayala-Sanmartin, J., and Vishwanatha, J. K. (2003) *BMC Biochem.* **4**, 10

25. Blanchard, S., Barwise, J. L., Gerke, V., Goodall, A., Vaughan, P. F., and Walker, J. H. (1996) *J. Neurochem.* **67**, 805-813

26. He, K. L., Deora, A. B., Xiong, H., Ling, Q., Weksler, B. B., Niesvizky, R., and Hajjar, K. A. (2008) *J. Biol. Chem.* **283**, 19192-19200

27. Krishnamoorthy, R. R., Agarwal, P., Prasanna, G. *et al.* (2001) *Brain Res. Mol. Brain Res.* **86**, 1-12

28. Tchedre, K. T., and Yorio, T. (2008) *Invest. Ophthalmol. Vis. Sci.* **49**, 2577-2588

29. Liu, J., and Vishwanatha, J. K. (2007) *Mol. Cell. Biochem.* **303**, 211-220

30. Mai, J., Finley, R. L.,Jr, Waisman, D. M., and Sloane, B. F. (2000) *J. Biol. Chem.* **275**, 12806-12812

31. Jindal, H. K., and Vishwanatha, J. K. (1990) *J. Biol. Chem.* **265**, 6540-6543

32. Peterson, E. A., Sutherland, M. R., Nesheim, M. E., and Pryzdial, E. L. (2003) *J. Cell. Sci.* **116**, 2399-2408

33. Burghardt, T. P., Ajtai, K., and Borejdo, J. (2006) *Biochemistry* **45**, 4058-4068

34. Prasanna, G., Krishnamoorthy, R., Clark, A. F., Wordinger, R. J., and Yorio, T. (2002) *Invest. Ophthalmol. Vis. Sci.* **43**, 2704-2713

35. Grynkiewicz, G., Poenie, M., and Tsien, R. Y. (1985) *J. Biol. Chem.* **260**, 3440-3450

36. Jacovina, A. T., Zhong, F., Khazanova, E., Lev, E., Deora, A. B., and Hajjar, K. A. (2001) *J. Biol. Chem.* **276**, 49350-49358

37. Deshet, N., Lupu-Meiri, M., Espinoza, I., Fili, O., Shapira, Y., Lupu, R., Gershengorn, M. C., and Oron, Y. (2008) *J. Cell. Physiol.* **216**, 632-639

38. Kobayashi, R., Nakayama, R., Ohta, A., Sakai, F., Sakuragi, S., and Tashima, Y. (1990) *Biochem. J.* **266**, 505-511

39. Shen, Y., Liu, X. L., and Yang, X. L. (2006) *Mol. Neurobiol.* **34**, 163-179

40. Roda, O., Valero, M. L., Peiro, S., Andreu, D., Real, F. X., and Navarro, P. (2003) *J. Biol. Chem.* **278**, 5702-5709

41. Nishizawa, Y. (2001) *Life Sci.* **69**, 369-381

42. LUCAS, D. R., and NEWHOUSE, J. P. (1957) *AMA Arch. Ophthalmol.* **58**, 193-201

43. Ferreira, I. L., Duarte, C. B., and Carvalho, A. P. (1996) *Eur. J. Pharmacol.* **302**, 153-162

44. Sattler, R., and Tymianski, M. (2000) *J. Mol. Med.* **78**, 3-13

45. Chintala, S. K., Zhang, X., Austin, J. S., and Fini, M. E. (2002) *J. Biol. Chem.* **277**, 47461-47468

46. Agapova, O. A., Kaufman, P. L., Lucarelli, M. J., Gabelt, B. T., and Hernandez, M. R. (2003) *Brain Res.* **967**, 132-143

47. Mali, R. S., Cheng, M., and Chintala, S. K. (2005) *FASEB J.* **19**, 1280-1289

48. Zhang, X., Chaudhry, A., and Chintala, S. K. (2003) *Mol. Vis.* **9**, 238-248

49. Kumada, M., Niwa, M., Hara, A., Matsuno, H., Mori, H., Ueshima, S., Matsuo, O., Yamamoto, T., and Kozawa, O. (2005) *Invest. Ophthalmol. Vis. Sci.* **46**, 1504-1507

50. Tsirka, S. E. (2002) *Biochem. Soc. Trans.* **30**, 222-225

51. Strickland, S., Gualandris, A., Rogove, A. D., and Tsirka, S. E. (1996) *Cold Spring Harb. Symp. Quant. Biol.* **61**, 739-745

52. Tsirka, S. E. (1997) *J. Mol. Med.* **75**, 341-347

53. Miles, L. A., Hawley, S. B., Baik, N., Andronicos, N. M., Castellino, F. J., and Parmer, R. J. (2005) *Front. Biosci.* **10**, 1754-1762

54. Herren, T., Swaisgood, C., and Plow, E. F. (2003) *Front. Biosci.* **8**, d1-8

55. Kim, J., and Hajjar, K. A. (2002) *Front. Biosci.* **7**, d341-8

56. Hajjar, K. A., Guevara, C. A., Lev, E., Dowling, K., and Chacko, J. (1996) *J. Biol. Chem.* **271**, 21652-21659

57. Barwise, J. L., and Walker, J. H. (1996) *J. Cell. Sci.* **109 (Pt 1)**, 247-255

58. Hajjar, K. A., and Acharya, S. S. (2000) *Ann. N. Y. Acad. Sci.* **902**, 265-271

59. Menell, J. S., Cesarman, G. M., Jacovina, A. T., McLaughlin, M. A., Lev, E. A., and Hajjar, K. A. (1999) *N. Engl. J. Med.* **340**, 994-1004

60. Sharma, M. C., and Sharma, M. (2007) *Curr. Pharm. Des.* **13**, 3568-3575

Chapter III

Lipid raft endocytosis and exosomal transport facilitate extracellular trafficking of Annexin A2

ABSTRACT

Annexin A2 (AnxA2), a Ca^{2+}-dependent phospholipid-binding protein is known to associate with the plasma membrane and the endosomal system. Within the plasma membrane, AnxA2 associates in a Ca^{2+}dependent manner with cholesterol-rich lipid raft microdomains. Here, we show that the association of AnxA2 with the lipid rafts is influenced by intracellular levels of Ca^{2+}, cholesterol and by N-terminal phosphorylation at Tyrosine-23. AnxA2 is co-internalized with the lipid raft components and the internalization is blocked in the presence of drugs that disrupt the integrity of the lipid rafts, suggesting the internalization of AnxA2 is through endocytic vesicles that originate from the cell membrane lipid rafts. Lipid raft endocytosis drives the incorporation of AnxA2 first into the detergent-resistant membranes (DRMs) of the endosomes and later into the intralumenal vesicles of the multivesicular body (MVB). AnxA2 present in the MVB intralumenal vesicles is secreted into the extracellular space upon fusion of the MVB with the plasma membrane. Collectively, these results suggest that lipid rafts constitute a route for selective targeting of AnxA2 via secretory vesicles to the cell surface.

INTRODUCTION

AnxA2 is a member of the multigene family of Ca^{2+} and phospholipid-binding proteins, which interact with negatively charged phospholipids in a Ca^{2+}-dependent manner (1). Plasma membrane-associated AnxA2 is implicated in several membrane-related events including fibrinolysis, exocytosis and endocytosis, cell-cell adhesion and membrane-cytoskeletal interactions (2). AnxA2 is a soluble protein predominantly distributed in the cytosol of the cells at resting Ca^{2+} levels and translocated to cellular membranes under elevated concentrations of intracellular Ca^{2+} (3). *In vitro* studies using artificial membranes have shown that AnxA2 preferentially binds to the acidic phospholipids which are enriched in the cytoplasmic leaflet of cellular membranes (4).

The mechanism of cell surface translocation of AnxA2 may occur via a non-classical secretory pathway as AnxA2 lacks a signal sequence that could direct it across the classical ER-Golgi secretory pathway (5). One of the central questions in understanding the Ca^{2+}-dependent plasma membrane dynamics of AnxA2 is how the protein is recruited from the intracytoplasmic leaflet of the plasma membrane to the extracytoplasmic leaflet to be localized to the cell surface.

Membrane association of AnxA2 is largely attributed to the hyper-variable N-terminal domain that precedes the conserved Ca^{2+}-binding core domain (6). Previous reports suggest that AnxA2 preferentially binds to cholesterol and phosphatidylinositol-4,5 bisphosphate (PtdIns(4,5)P2)-rich domains of the membrane called lipid rafts (7). Although AnxA2 influences the raft dynamics and promotes the formation of lipid microdomains, the mechanisms that

influence the raft association and the subsequent functions of lipid raft-associated AnxA2 are not well understood.

Lipid rafts are implicated in diverse cellular processes including cell adhesion, membrane trafficking and signal transduction events (8). The highly fluid raft microdomains serve as platforms for the segregation and sorting of proteins to different cellular compartments (9, 10). The most intriguing observation, however, is the involvement of lipid rafts in sorting of lipid and proteins in the endocytic and secretory pathways (11). Lipid raft endocytosis is characterized as a general mechanism for pathogen entry (12), recycling of extracellular ligands (13) and cell surface trafficking of glycosylphosphatidyl inositol (Gpi)-anchored proteins (14). Recent studies have suggested that lipid raft-associated proteins are trafficked through the endocytic pathway as a result of invagination of the plasma membrane rafts into the endocytic vesicles (15). Proteins that are targeted to the endosomal pathway following internalization from the plasma membrane are progressively shuttled first to the early endosomes and later incorporated into the multivesicular bodies (MVBs) or endosome carrier vesicles (ECVs) to be destined to the late endosomal pathway (16). MVBs are critical intermediates of the endocytic pathway which are formed when the limiting membrane of the early endosomes invaginates into its lumen (17). MVBs contain secreted intralumenal components called exosomes with protein and lipid composition identical to the endosomes reflecting their endosomal origin (18). Exosomes not only possess proteins that are necessary for their biogenesis and maintenance but also contain several plasma membrane and cytosolic proteins (19). Exosomes are also identified to possess distinct membrane domains enriched in cholesterol and GM1 gangliosides and similar in composition to the plasma membrane rafts (20, 21). The presence of raft-like domains in the exosomes suggests that exosomes participate in the sorting of raft-associated proteins. Raft-like domains are found to be present not only in the MVB intralumenal vesicles but also in the late

endosomes and they are thought to originate by the endocytosis of the plasma membrane rafts occurring via clathrin-dependent (22) and independent pathways (15).

In the present study, we questioned whether AnxA2 is trafficked from the plasma membrane lipid rafts to the endosomal pathway and sorted to the intralumenal vesicles of the MVBs to be later released into the extracellular space upon fusion of the MVBs with the plasma membrane. We first sought to determine the molecular mechanisms by which AnxA2 is initially recruited to the plasma membrane lipid rafts. Upon elevation of cytosolic Ca^{2+} levels, AnxA2 is sorted from the plasma membrane rafts first to the endosomal system and later to the exosomal membranes. Within the exosomal membrane, AnxA2 is localized to distinct regions which possess raft-like characteristics and exosomes are also identified to serve as potential intercellular carriers of AnxA2.

The data presented here provide novel insights into the membrane dynamics of AnxA2. We suggest the importance of Tyr-23 phosphorylation in the Ca^{2+}-dependent recruitment of AnxA2 to the plasma membrane rafts. Localization of AnxA2 in the lipid rafts targets AnxA2 for its internalization into the endosomes and its further assortment into the raft-like regions of the exosomal membrane. Upon fusion of the MVBs with the plasma membrane, the MVB intralumenal vesicles called exosomes are secreted into the extracellular space and the released AnxA2 rebinds to the surface of the target cell in a Ca^{2+}-dependent manner.

MATERIALS AND METHODS

Antibodies and reagents

The following antibodies were used: mouse monoclonal anti-AnxA2 (BD Biosciences), mouse monoclonal anti-Na,K-ATPase (a6-FC) (Developmental Studies Hybridoma Bank (DSHB, University of Iowa), rabbit polyclonal anti-PGK (25), rabbit polyclonal anti-GFP (D5.1) (Cell Signaling), mouse monoclonal anti-GFP (Roche Diagnostics), mouse monoclonal anti-phosphotyrosine (P-Tyr-100) (Cell Signaling), mouse monoclonal anti-Caveolin 1 (pY14) (BD Biosciences), mouse monoclonal anti-transferrin receptor (H68.4) (Zymed), mouse monoclonal anti-heat shock cognate protein-70 (SPA-816) (hSC-70) (Stressgen), rabbit polyclonal anti-CD44 antibody (Abcam). Tetraspanin antibodies were purchased from the following sources: rabbit polyclonal anti-CD9 (Abcam), rabbit polyclonal anti-CD63 (Santa Cruz Biotechnology, Inc.), rabbit polyclonal anti-CD81 (H-121) antibodies were purchased from Santa Cruz Biotechnology. Anti-mouse and anti-rabbit IgG (Sigma) and Peroxidase-conjugated goat anti-rabbit and anti-mouse IgG were from Promega.

Reagents were purchased from the following sources: Ca^{2+} ionophore A23187, methyl- β-cyclodextrin (Sigma), Alexa-conjugated cholera toxin subunit B (CTXB) (Invitrogen), sulfo-NHS-Biotin (Pierce), avidin-conjugated Sepharose (Sigma), Fluo-3 AM (Invitrogen), phosphatidyl(N-sulphorhodamine B sulphonyl)ethanolamine (N-Rh-PE) (Avanti Polar Lipids), Brefildin A (Sigma), Triton X-100 (Sigma), CHAPS (Sigma)

Cell culture and ionophore treatment

NIH 3T3 mouse fibroblasts and MBA-MB231 cells were cultured at 5% CO_2 in Dulbecco's Modified Eagle's Medium high glucose and low glucose medium respectively (DMEM; Gibco) supplemented with 10% fetal bovine serum (FBS) and 5% penicillin-streptomycin. A polyclonal population of LNCaP-C1 cells stably expressing GFP and referred was cultured in RPMI 1640 medium (Gibco) supplemented with 10% FBS and 5% penicillin-streptomycin. For ionophore treatment, subconfluent cultures treated with 5 μM of Ca^{2+} ionophore A23187 for the indicated periods of time.

For transfections, cells were cultured in 100 mm dishes to 70% confluence. 20 μg of DNA was incubated with 30 μl of lipofectamine 2000 (Invitrogen) and was later added to 15 ml of Opti-MEM (Gibco) for 6 hr and returned to normal growth medium.

Plasmids and constructs

For the construction of a plasmid expressing full length AnxA2, the cDNA of AnxA2 was cloned into the pEGFP-N1 vector as previously published. The N-terminal phosphomimetic and non-phosphomimetic mutants at Tyr-23 were generated by using Quickchange site-directed mutagenesis kit (Stratagene). In this report, the plasmids are referred to as AnxA2WT-GFP, AnxA2Y23E-GFP and AnxA2Y23F-GFP.

Confocal microscopy

For immunocytochemistry, cells expressing AnxA2Y23E-GFP and AnxA2Y23F-GFP were treated with 5 μM of Ca^{2+} ionophore A23187. The cells were later subjected to monosialoganglioside GM1 labeling with 8 μg/ml of Alexa 555-conjugated cholera toxin B subunit. The cells were washed were fixed with 4% paraformaldehyde and subjected to

immunocytochemistry. The coverslips were mounted on glass slides with Prolong Gold mounting media (Invitrogen). Confocal images were obtained using Zeiss LSM 510 META confocal microscope equipped with a 63X Plan-Apochromat objective and HeNe1, HeNe2, and argon lasers. The weighted colocalization coefficients were calculated using the Zeiss LSM enhanced co-localization software (Zeiss) which is a measure of the sum of the number of co-localizing pixels relative to the sum of the total number of pixel intensities after background correction.

EDTA elution and cell surface biotinylation

Confluent cultures were washed with 0.5 mM EDTA and PBS buffer (Versene, Gibco) for 20 mins at 37^0C. Cell surface proteins were subjected to biotinylation with 0.5 mg/ml of sulfo-NHS biotin (Pierce) and recovered with avidin-conjugated sepharose (Sigma) as previously described with slight modifications (63). Briefly, cells were washed with ice-cold PBS, chilled on ice for 5 min to block endocytosis, and biotinylated with 1 mg EZ-Link Sulfo-NHS-LC-Biotin (Pierce) for 1 h at 4°C. Cells were later washed twice with ice-cold PBS and subsequently incubated on ice with 50 mM glycine/PBS for 15 min to quench the biotinylation reaction. Subsequently, cells were lysed in TNE buffer (25 mM Tris-HCl (pH 7.5), 150 mM NaCl, 5mM EDTA) containing 1% Triton X-100 plus protease and phosphatases inhibitor cocktail (Promega). The post nuclear supernatants were incubated in 60 µl of NeutrAvidin beads (Pierce). After incubation for 1 h at 4°C the supernatant was removed and the beads were washed twice with each buffer A (10 mM Tris–Cl, pH 7.4, 150 mM NaCl, 2 mM EDTA, 0.2% NP-40), boiled in sample buffer and subjected to SDS PAGE Western immunoblot analysis. Alternatively, the post nuclear supernanats were recovered and subjected to Triton X-100 extraction of the DRMs as described

below.

Subcellular fractionation of endosomes

Endosomes were purified using a continuous sucrose flotation gradient as previously described (30). The PNS was loaded on the bottom of a SW40 centrifuge tube and adjusted to 41% sucrose followed by 3 continuous gradients of 35%, 25% and 8% sucrose in the homogenization buffer (250< mM sucrose, 3< mM imidazole, pH 7.4, 1< mM EDTA, 0.03< mM cycloheximide and protease inhibitors). Gradients were centrifuged at 200,000 X g and the interfaces were collected. Late endosomes were collected in the fractions floating at the interface between 25% and 8% sucrose, early endosomes were enriched in the fractions at the 35-25% interface and the heavy biosynthetic membranes were found at the 41-35% interface.

Isolation of DRMs from the late endosomes

Endosomes were first purified by subcellular fractionation as described above and the DRMs were isolated as described previously (29). Briefly, the isolated exosomes were diluted four times, centrifuged and suspended in a lysis buffer (25 mM Tris-HCl pH 7.4, 150 mM NaCl) in the presence of 1% Triton X-100. After incubation for 20 min at 4ºC, the lysate was adjusted to 40% sucrose and overlaid with 30% sucrose followed by centrifugation at 200,000 X g in a Beckman SW40 rotor. Ten fractions were collected from the top, precipitated with TCA and subjected to western immunoblot analysis.

Isolation of exosomes

Fetal bovine serum contains endogenous exosomes, in order to eliminate exosomes from FBS, the culture medium (DMEM, 10% FBS and 5% penicillin-streptomycin) was centrifuged overnight at 120,000 X g. Exosomes were isolated from the culture medium by serial

centrifugation as previously published (64). The culture medium was subjected to serial centrifugations at 800 X g for 10 min to remove the cells and at 12,000 X g for 30 min to remove the cell debris. The exosomes were pelleted from the supernatant by centrifugation at 100,000 X g for 15 hr, washed, resuspended and repelleted in PBS using a SW28 rotor (Beckman).

Extraction of lipid rafts by Triton X-100

Separation of the membrane into Triton-soluble and insoluble components was performed as published (65). Briefly, cells were lysed in buffer A [25 mM 2-(N-morpholino)-ethanesulfonic acid, 150 mM NaCl (pH 6.5)]. The lysate was treated with equal volume of the buffer A mixed with 2% Triton X-100, 2 mM Na_3VO_4, and 2 mM PMSF and incubated on ice for 30 min. The lysates were centrifuged at 14,000 X g for 30 min and the supernatant was collected and referred to as TS fraction. The insoluble pellets were resuspended with buffer B [1% Triton X-100, 10 mM Tris-Cl (PH 7.6), 500 mM NaCl, 2 mM Na_3VO_4, 60 mM β-octylglucoside, and 1 mM PMSF] for 30 min on ice and centrifuged at 14,00 X g for 20 min. The supernatant was collected and referred to as TI fraction.

Sucrose gradient fractionation

Cells: Lipid raft fractions were isolated according to the previously published protocols with few modifications (66). Briefly cells were grown to near confluence, transfected and treated in four 100 mm dishes. The cells were lysed in 500 mM Na_2CO_3, pH 11 with a cocktail of protease and phosphatase inhibitors, the lysate was homogenized with 20 strokes in a pre-chilled Dounce homogenizer followed by homogenization with a polytron homogenizer three times for 10 sec with intervals of 10-15 sec followed by sonication three times for 20 sec with an interval of 60 sec. 2 ml of the homogenized sample was mixed with 2 ml of 90% sucrose in MBS (25 mM 2-(N-Morpholino) ethanesulfonic acid, 150 mM NaCl, pH 6.0). A discontinuous sucrose gradient

was generated by overlaying with 4 ml of 35 % sucrose in 1X MBS and 250 mM Na_2CO_3 followed by overlaying with 4 ml of 5% sucrose in 1X MBS and 250 mM Na_2CO_3. The gradient was centrifuged at 40,000 X g in a SW40Ti rotor (Beckman). Twelve 1 ml fractions were collected from the top of the tube and the fractions were subjected to trichloroacetic acid (TCA) precipitation followed by SDS PAGE and western immunoblotting.

Exosomes: Exosomes collected by serial centrifugation were subjected to further purification as described previously (20). The exosomal pellet was resuspended in 5 ml of 2.6 M sucrose, 20 mM Tris- HCl, pH 7.2 and a linear sucrose gradient of (2.0–0.25 M sucrose, 20 mM Tris-HCl, pH 7.2) was layered on the top of the exosome suspension in a SW41 tube for 16 hr at 270,000 X g (Beckman) and the pellets were subjected to SDS PAGE and western immunoblotting.

Lipid rafts were isolated from the exosomes as described (21). Freshly isolated vesicles (2 mg) from the culture medium and suspended in 1.5 ml of buffer A (50 mM Tris·HCl, pH 7.2/150 mM NaCl, pH 7.2) in combination with 1% Triton X-100 or 1% CHAPS with protease and phosphatase inhibitors. The suspension was mixed in 1.5 ml of 95% sucrose, overlaid with 3 ml of 35% sucrose and 3 ml of 5% sucrose and centrifuged at 150,000 X g for 16 hr at 4 ºC. 1 ml fractions from the top were collected and subjected to SDS PAGE and immunoblot analysis.

Fluorescent lipid N-Rh-PE labeling of the multivesicular bodies (MVBs) and intracellular Ca^{2+} labeling with Fluo-3 AM

MVBs were labeled with N-Rh-PE as described previously (67). Briefly the ethanolic solution of the fluorescent lipid (<1% v/v) was injected by a Hamilton syringe into the medium and after vigorous vortexing, the cells were incubated in the medium for 60 min at 4°C. The cells were later washed with PBS to remove any unbound lipids and loaded with 15 µM of Fluo-3 AM

(Molecular Probes) for 30 min at 37 ºC. After subjecting the cells to ionophore treatment, cells were washed with PBS and immediately mounted on glass coverslips and visualized under the Zeiss LSM 510 confocal microscope using a 40X objective and the filter settings are described.

Immunofluorescence analysis of exosomal protein transfer

Exosomes were freshly harvested from the culture medium MDA-MB231 cells, suspended in 1X PBS and quantified for protein concentration by BCA assay (Pierce). LNCaP-C1 cells were cultured on coverslips and incubated with 30 µg of exosomes collected from MDA-MB231 cells for 12 hr at 37°C. The cells were fixed and stained with anti-AnxA2 antibody (1:1000). LNCaP-C1 cells were incubated in 0.5 mM EDTA for 1 hr to chelate off MDA-MB231 derived cell surface AnxA2.

Quantification of released exosomes

Quantification of secreted exosomes was performed by measuring the activity of acetylcholine esterase (ACH) as previously described (68) . Briefly, 50 µl of the pelted exosomes was suspended in 100 µl of PBS. 37.5 µl of this PBS-diluted fraction was incubated in the presence of 1.25 mM acetylthiocholine and 0.1 mM 5,'5'-dithio-bis(2-nitrobenzoic acid) and the reaction mixture was brought to a final volume of 300 µl in a 96-well plate. The incubation was carried out at 37°C and the change in absorbance at 412 nm was monitored every 5 min. The data presented represents the enzymatic activity 20 min after incubation.

Flow cytometry

Exosomes (10 µg of protein) were bound to 5 µg aldehyde surface latex beads (Invitrogen) for 1 hr at room temperature. Bound exosomes were spun down and incubated in FACS permeabilization buffer. The unoccupied sites were saturated with vesicle free fetal calf serum

and the exosomes were incubated with primary antibodies or control isotype for 1 hr at room temperature. The exosomes were spun down and incubated with FITC-conjugated secondary antibodies for 30 min at room temperature. The staining was analyzed on the FITC-channel by flow cytometry.

RESULTS

Depletion of cellular cholesterol inhibits the Ca^{2+}-dependent cell surface translocation of AnxA2

Because raft microdomains are involved in the sorting of proteins across the plasma membrane (14, 23), we examined whether depletion of membrane rafts would prevent the extracellular trafficking of AnxA2. Methyl-β-cyclodextrin (MβCD) extracts cholesterol and induces variable amounts of cholesterol in the biological membranes, thereby disrupting the integrity of the lipid rafts. The effective concentration of MβCD required to deplete cholesterol from the cellular membranes of NIH 3T3 cells was determined from a previous study (24). Pretreatment of NIH 3T3 cells with MβCD solubilized a significant fraction of AnxA2 from the cell surface of ionophore-stimulated cells (Fig.1A). The mean pixel intensity of AnxA2 normalized with Na,K-ATPase was plotted to show the effect of MβCD on the cell surface levels of AnxA2. As shown in Figure 1A, MβCD pretreated cells showed ~30% increase in ionophore-induced cell surface levels of AnxA2 compared to ~80% increase in ionophore stimulated cells untreated with MβCD after 6 hr of ionophore treatment.

Previous studies have indicated that AnxA2 is effectively released from the cholesterol-containing liposomes by treatment with filipin, a cholesterol-sequestering drug that inhibits lipid-raft dependent endocytosis (25). We studied the effect of filipin on the lipid raft localization and extracellular trafficking of AnxA2 in the presence of the ionophore. First, we tested the

efficiency of filipin in influencing the internalization of Alexa 594-conjugated cholera toxin B and transferrin which are endocytosed by lipid raft and clathrin-mediated endocytosis respectively (data not shown).

NIH 3T3 cells were incubated with filipin before treatment with the ionophore for the indicated periods of time. Extracellular AnxA2 was recovered by cell surface biotinylation and the cells were later processed for detergent-resistant membrane (DRM) isolation. Western immunoblot analysis of the cell surface and pooled DRM fractions indicate that ionophore treatment induces not only the cell surface expression of AnxA2 but also results in an increased association of AnxA2 with the DRM fractions (Fig. 1B). In addition, ionophore- induced extracellular and DRM association of AnxA2 was inhibited in cell pretreated with filipin. These

results show that Ca^{2+}-dependent association of AnxA2 with the cell surface and the DRMs is largely dependent on the cellular levels of cholesterol.

Phosphorylation of AnxA2 at Tyr-23 is essential for the cell surface translocation of AnxA2 on ionophore stimulation

Increase in the intracellular levels of Ca^{2+} is known to precede the activation of pp60-C-Src, a tyrosine kinase that phosphorylates AnxA2 at Tyr-23 (26). We investigated the involvement of Tyr-23 phosphorylation in cell surface trafficking of AnxA2 on ionophore treatment. EDTA eluates from cells transfected with AnxA2Y23E-GFP and stimulated with ionophore were immunoblotted with GFP antibody to reveal a marked increase in the cell surface levels AnxA2Y23E-GFP on ionophore treatment compared to the vehicle control (Fig. 1D, left panel). However, in cells transfected with AnxA2Y23F-GFP, both

basal and ionophore- stimulated cell surface levels of AnxA2 were markedly reduced (Fig. 1C, right panel). Also, ionophore treatment did not result in any significant changes in the intracellular levels of AnxA2 in cells transfected with either of the constructs. PGK and Coomassie staining of the gel were used as loading controls for whole cell lysates and EDTA eluates respectively (Fig. 1C).

Immunoprecipitation of EDTA eluates collected from cells expressing AnxA2WT-GFP with Anti-GFP and Anti-AnxA2 antibodies revealed a marked increase in the cell surface levels of tyrosine-phosphorylated AnxA2-GFP on ionophore treatment (Fig. 1D, upper and lower panels respectively). The role of tyrosine phosphorylation in the cell surface translocation of AnxA2 was further confirmed by pretreating the cells with sodium orthovanadate, a tyrosine phosphatase inhibitor, and prior to stimulation with ionophore.

On recovery of cell surface proteins by biotinylation and avidin-based affinity purification, we observed an increase in the ionophore-induced cell surface levels of AnxA2 in cells pretreated with sodium orthovanadate, indicating that augmentation of tyrosine phosphorylation increases the association of AnxA2 to the cell surface (Fig. 1E). The blots were reprobed with Na,K-ATPase antibody for loading control. These results demonstrate that in addition to intracellular Ca^{2+}, phosphorylation at Tyr- 23 regulates the trafficking and association of AnxA2 with the plasma membrane.

Phosphorylation at Tyr-23 promotes the association of AnxA2 with the low density Triton-insoluble (TI) membrane fractions on ionophore stimulation

To investigate the role of Tyr-23 phosphorylation in the association of AnxA2 with the lipid raft domains of the plasma membrane, we separated the plasma membrane into raft and non-

Figure.1

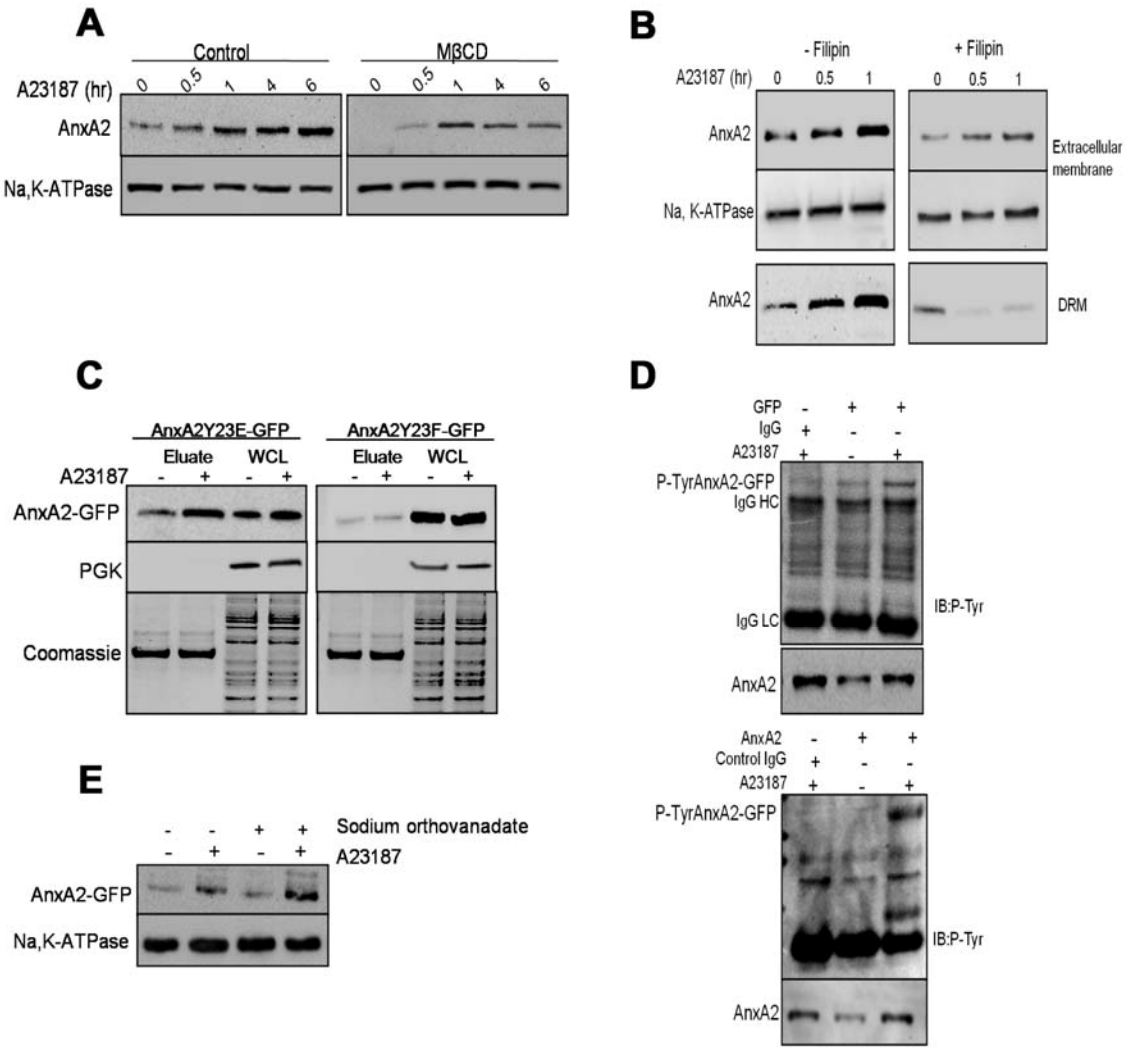
A
Control
MβCD
A23187 (hr)
0 0.5 1 4 6 0 0.5 1 4 6
AnxA2
Na,K-ATPase
B
- Filipin
+ Filipin
A23187 (hr) 0 0.5 1 0 0.5 1
AnxA2
Extracellular membrane
Na, K-ATPase
AnxA2
DRM
C
AnxA2Y23E-GFP
AnxA2Y23F-GFP
Eluate WCL Eluate WCL
A23187 - + - + - + - +
AnxA2-GFP
PGK
Coomassie
D
GFP - + +
IgG + - -
A23187 + - +
P-TyrAnxA2-GFP
IgG HC
IgG LC
IB:P-Tyr
AnxA2
AnxA2 - + +
Control IgG + - -
A23187 + - +
P-TyrAnxA2-GFP
IB:P-Tyr
AnxA2
E
- - + + Sodium orthovanadate
- + - + A23187
AnxA2-GFP
Na,K-ATPase

Figure 1. MβCD treatment decreases A23187 (ionophore)-induced cell surface translocation of AnxA2. NIH 3T3 cells were treated with 5 mM MβCD for 20 min, to deplete the cholesterol in the cellular membranes prior to treatment with 5 μM ionophore for the indicated periods of time. **(A)** The cell surface biotinylated extracts were subjected to immunoblot analysis for AnxA2 and the blots were reprobed for Na,K-ATPase for protein loading. **(B)** NIH 3T3 cells pretreated with filipin were untreated or treated with the ionophore for the indicated periods of time (30 min and 1 hr). Western immunoblotting of cell surface and detergent resistant membrane (DRM)-associated AnxA2 recovered by cell surface biotinylation followed by DRM extraction **(C)** GFP immunoblotting of EDTA eluates and whole cell lysates (WCL) isolated from cells expressing AnxA2Y23E-GFP and AnxA2Y23F-GFP in the presence and absence of ionophore. PGK and Coomassie staining was used as loading controls for WCL and EDTA eluates respectively. **(D)** EDTA eluates from AnxA2WT-GFP expressing cells were immunoprecipitated with anti-GFP and anti-AnxA2 antibodies and immunoblotted with phosphotyrosine antibody. The endogenous levels of AnxA2 are shown in the lower panels. **(E)** NIH 3T3 cells expressing AnxA2-GFP were stimulated with ionophore and treated with 100 μM sodium orthovanadate. The biotinylated extracts were immunoblotted with GFP antibody and the blots were reprobed with Na,K-ATPase antibody for loading control.

raft regions based on their solubility in Triton X-100. Immunoblotting with the non-raft marker, transferrin receptor (Tfr), raft marker caveloin-1 (Cav-1) and cytosolic PGK were performed to ascertain the purity of the Triton-soluble (TS) non-raft, low density Triton-insoluble (TI) raft and cytosolic fractions respectively. Ionophore treatment resulted in increased association of AnxA2Y23E-GFP with the TI raft fractions which is accompanied by a concomitant increase in the cell surface levels of AnxA2 (Fig. 2A, right panel) compared to the cells treated with the DMSO control (Fig. 2A, left panel). An increase in the association of AnxA2Y23E-GFP with the TS non-raft fractions was also observed upon ionophore treatment. The association of AnxA2Y23F-GFP with the TI and TS fractions was markedly reduced in ionophore-stimulated cells and a decrease in the cell surface expression of AnxA2 was also evident in both the ionophore and DMSO treated cells (Fig. 2B, right and left panels respectively).

To further demonstrate the importance of Tyr-23 phosphorylation in the raft-association of AnxA2, cells transfected with AnxA2Y23E-GFP or AnxA2Y23F-GFP were either unstimulated or stimulated with the ionophore. The lipid rafts were subsequently labeled with Alexa 594- conjugated CTXB which preferentially binds to GM1 gangliosides of the raft microdomains. Immunostaining for CTXB and GFP indicated a predominant co-localization of AnxA2Y23E- GFP with the GM1-rich raft microdomains which was markedly reduced in the cells expressing AnxA2Y23F-GFP on ionophore treatment (Fig. 2C, right panel). In cells not treated with the ionophore, the extent of lipid raft formation was moderate and both proteins, AnxA2Y23E-GFP and AnxA2Y23F-GFP were retained in the cytosol (Fig. 2C, left panel).

Zeiss Enhanced Co-localization Tool Software was used to measure the extent of co-

localization by calculating the weighted co-localization coefficients. The weighted co-localization coefficients for AnxA2Y23E-GFP, AnxA2Y23F-GFP and empty vector relative to CTXB were measured in the ionophore-treated cells to be 0.34 ± 0.15, 0.1 ± 0.02 and 0.02 ± 0.01 respectively. These results suggest a significant co-localization of Tyr-23 phosphorylated AnxA2 in the raft domains compared to the non-phosphorylated AnxA2. Immunoprecipitation of TS and TI fractions from cells expressing AnxA2Y23E-GFP, AnxA2Y23F-GFP and empty GFP vector indicated an increased recovery of AnxA2-GFP in the TI fractions of cells expressing AnxA2Y23E-GFP compared to the cells expressing AnxA2Y23F-GFP (Fig. 2D). Triton extraction of the cells expressing the empty GFP vector and immunoprecipitation of the TS and TI extracts from AnxA2Y23E-GFP transfected cells with control IgG was used as negative controls.

We further tested if tyrosine-phosphorylated AnxA2 could be immunoprecipitated from the raft microdomains on ionophore treatment. For this purpose, immunoprecipitation with GFP antibody was performed on TI extracts collected from ionophore stimulated and unstimulated cells. Tyrosine phosphorylated AnxA2 was observed in the TI fractions of cells stimulated with the ionophore (Fig. 2E). The endogenous levels of AnxA2 in the input fractions are shown in the lower panel. These results show that the association of AnxA2 with the detergent-resistant domains of the plasma membrane is dependent on the phosphorylation status of AnxA2 at Tyr-23.

Tyrosine 23 phosphorylation imparts on AnxA2 the ability to associate with low buoyant density lipid rafts isolated on sucrose floatation gradients

In order to confirm the importance of Tyr-23 phosphorylation in the raft association of

AnxA2, we separated the raft microdomains based on their density on sucrose flotation

Figure.2

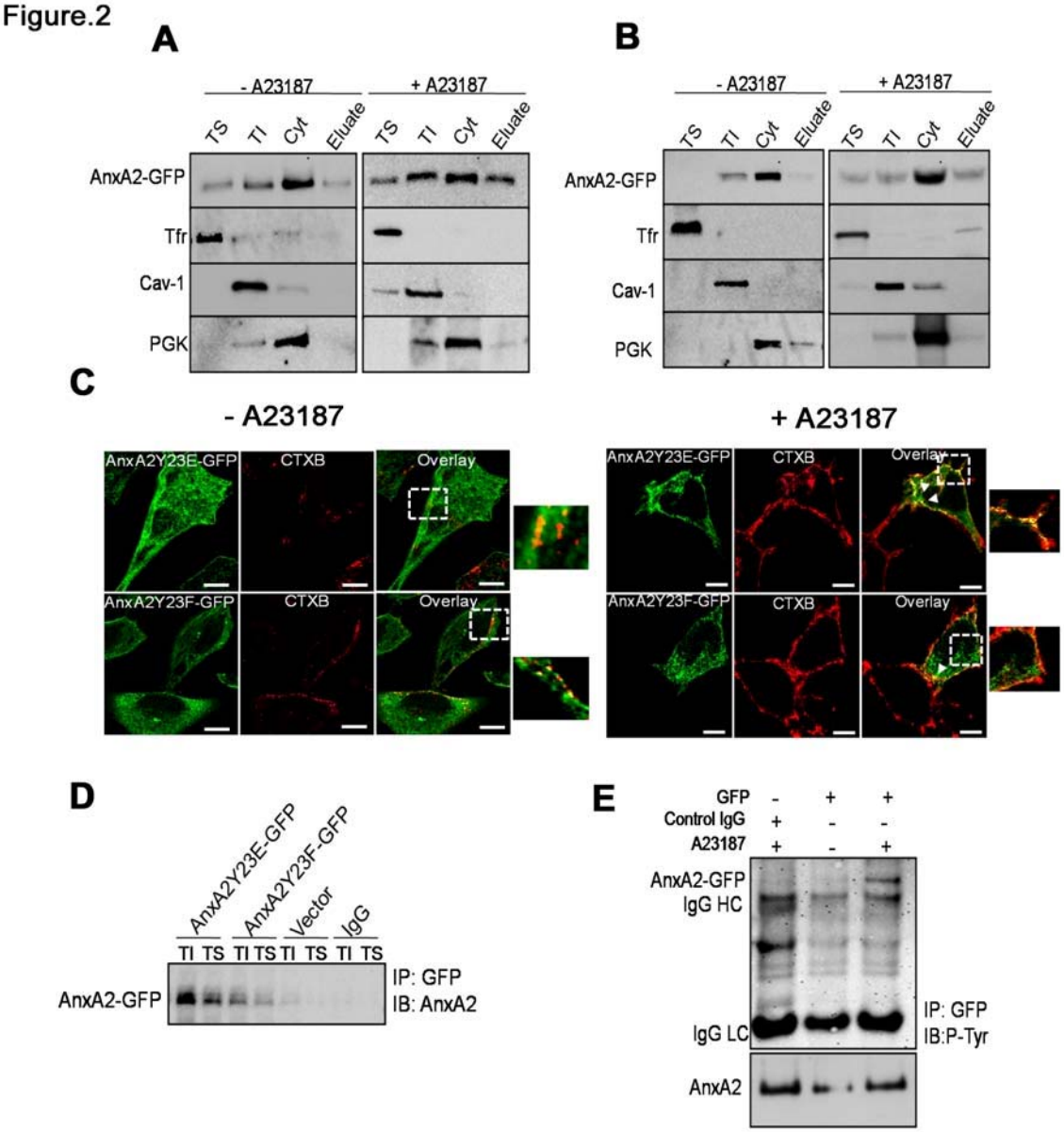
A
- A23187
+ A23187
TS
TI
Cyt
Eluate
AnxA2-GFP
Tfr
Cav-1
PGK
B
C
- A23187
+ A23187
AnxA2Y23E-GFP
AnxA2Y23F-GFP
CTXB
Overlay
D
AnxA2Y23E-GFP
AnxA2Y23F-GFP
Vector
IgG
TI TS TI TS TI TS TI TS
AnxA2-GFP
IP: GFP
IB: AnxA2
E
GFP
Control IgG
A23187
AnxA2-GFP
IgG HC
IgG LC
AnxA2
IP: GFP
IB:P-Tyr

Figure 2. Analysis of the localization of AnxA2 to the low-density triton insoluble fractions on ionophore stimulation AnxA2 is localized to the Triton-insoluble fractions on ionophore treatment **(A,B)** Cells transfected with AnxA2Y23E-GFP and AnxA2Y23F-GFP were treated with either with the ionophore or DMSO control. The vehicle control and ionophore-treated cells were incubated in EDTA and PBS buffer to collect the EDTA eluates and after lysis, the cytosolic fraction (cyt) was separated and the plasma membrane is subjected to fractionation with Triton-X-100 into Triton-soluble (TS) and Triton-insoluble (TI) fractions. The purity of the fractions was determined by immunoblotting with caveolin (Cav-1), transferrin (Tfr) and PGK antibodies. The distribution of AnxA2 in each of the fractions was analyzed by immunoblotting with AnxA2 antibody. **(C)** Ionophore-stimulated cells (right panel) and vehicle control treated cells (left panel), expressing AnxA2Y23E-GFP and AnxA2Y23F-GFP were incubated with CTXB (red) and subjected to immunocytochemistry with GFP antibody (green). The superimposed images revealed the co-localization of AnxA2Y23E-GFP and AnxA2Y23F-GFP proteins with CTXB-binding sites in the plasma membrane. The weighted co-localization coefficients were measured to be 0.34 ± 0.15, 0. 1 ± 0.05 and 0.02 ± 0.01 (SEM ±, n =9) for AnxA2Y23E-GFP, AnxA2Y23F-GFP and vector control respectively, Bars 20 μm **(D)** Immunoprecipitation of TI fractions from ionophore-stimulated cells expressing AnxA2Y23E-GFP, AnxA2Y23F-GFP and empty GFP vector with GFP antibody and immunoblotting with AnxA2 antibody. For negative control, immunoprecipitation with a non-specific antibody was used. **(E)** Immunoprecipitation of the TI fractions from unstimulated and ionophore-stimulated cells expressing AnxA2WT-GFP and immunoblotting with phosphotyrosine antibody.

gradients. The cholesterol-rich light membrane fractions 4-6 were distributed at the interface between 5 and 35% and contain an enrichment of raft marker Caveolin-1 (Cav-1); the heavier membrane fractions 7-9 showed a predominant expression of the non-raft marker transferrin receptor (Tfr); most cellular cytosolic protein was localized to the bottom of the gradient to fractions 10-12. In ionophore unstimulated cells, AnxA2 was found to be predominantly localized to the heavier fractions with very little distribution in the high and low density fractions of the membrane reflecting the principal distribution of the protein in the cytosol (Fig. 3A, 3B and 3C, left panels). On ionophore stimulation however, we observed a significant flotation of AnxA2 to the lighter sucrose fractions in cells expressing AnxA2-WTGFP and AnxA2Y23E-GFP (Fig. 3A and 3B, right panels). In cells expressing AnxA2Y23F-GFP however, the association of the protein to the lighter fractions was significantly compromised and the protein is predominantly localized to the heavier fractions (Fig. 3C, right panel). Cells transfected with empty GFP vector showed the localization of GFP to the cytosolic fractions in both unstimulated and ionophore stimulated cells (Fig. 3D, left and right panels). In the above experiments endogenous levels of AnxA2 showed a similar pattern of distribution with increased association with the raft fractions in ionophore-stimulated cells compared to the unstimulated controls (Fig. 3A, 3B, 3C and 3D). Densitometry analysis of the western immunoblots revealed that ~30-40% of the total cellular protein was localized to the low density rafts in ionophore-stimulated cells transfected with AnxA2WT-GFP and AnxA2Y23E-GFP respectively as opposed to 5% association in cells transfected with AnxA2Y23F-GFP. These results also provide compelling evidence that phosphorylation of AnxA2 at Tyr-23 is critical for the Ca^{2+}-dependent raft association of AnxA2.

Figure. 3

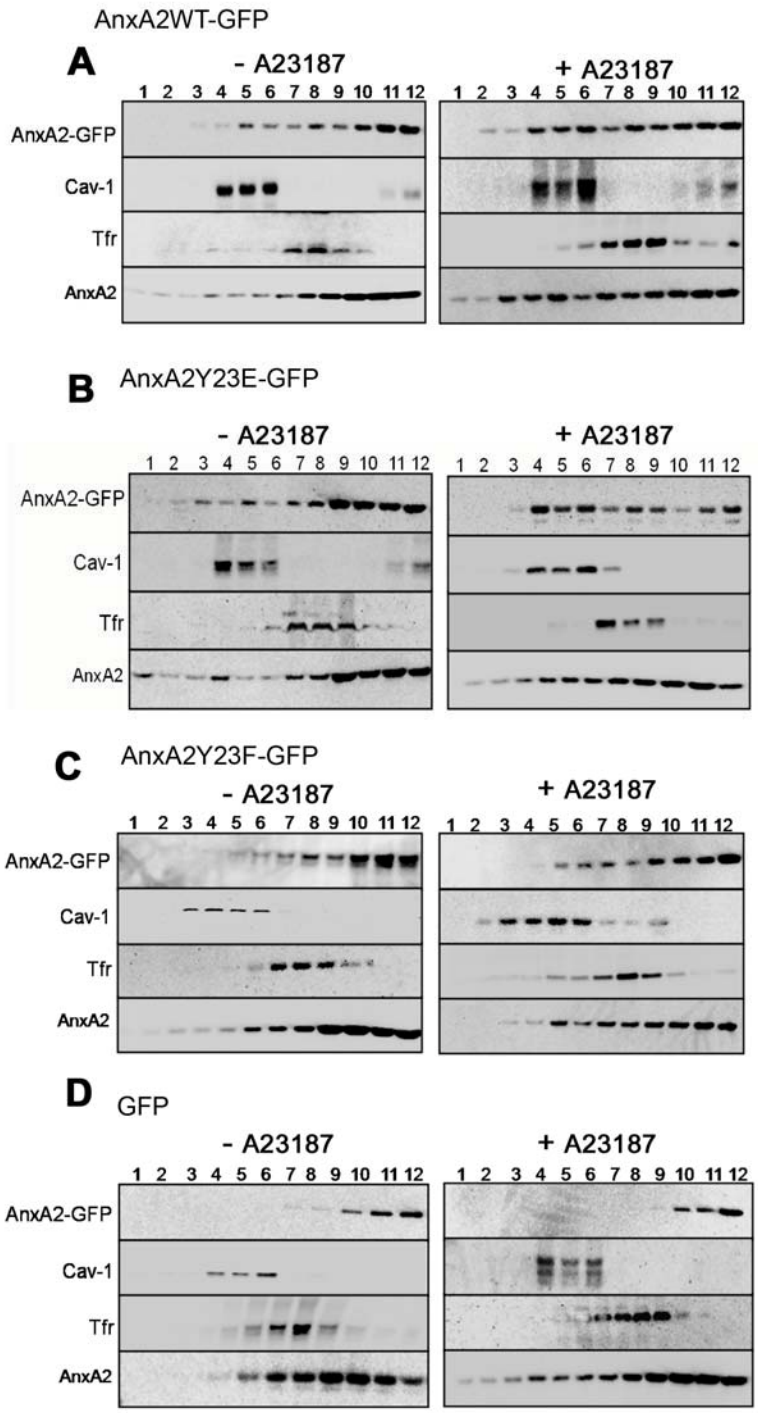
AnxA2WT-GFP
A
- A23187
+ A23187
1 2 3 4 5 6 7 8 9 10 11 12
AnxA2-GFP
Cav-1
Tfr
AnxA2
B
AnxA2Y23E-GFP
C
AnxA2Y23F-GFP
D
GFP

Figure 3. AnxA2 is recruited to the low density sucrose flotation gradients on ionophore stimulation **(A)** Resting and stimulated NIH 3T3 cells transfected with AnxA2WT-GFP were lysed in Na_2CO_3 buffer and subjected to (45-5%) discontinuous sucrose-density gradients. 12 fractions were collected and after TCA precipitation, they were subjected to western immunoblot analysis with AnxA2 antibody to determine the distribution of AnxA2 in each of the fractions. Fractions were immunoblotted for Cav-1 and Tfr to identify the lighter raft and heavier non-raft regions of the membrane respectively. Fraction 1 represents the top of the gradient. Fractions 4-6 represent the lighter and fractions 7-12 represent the heavier fractions **(B, C)** The distribution of AnxA2 in the raft, non-raft and the cytosolic fractions was determined in cells transfected with AnxA2Y23E-GFP and AnxA2Y23F-GFP and either stimulated or unstimulated with the ionophore. **(D)** Ionophore-treated and untreated cells transfected with the empty vector were fractionated on sucrose gradients. The amount of AnxA2 in each fraction was quantified by scanning three independent gels using the Alpha Imager software.

Ionophore treatment results in the trafficking of AnxA2 from the plasma membrane rafts to intracellular endocytic vesicles

We examined if the lipid raft-associated AnxA2 could be transported to other cellular destinations. Previous studies have shown that in addition to the plasma membrane, several intracellular vesicles of the endocytic pathway are known to contain raft-like domains (11, 27). Endosomes are known to be involved in the sorting of proteins to different cellular destinations and they are also known to invaginate from the lipid raft regions of the plasma membrane (28, 29). In an effort to understand the lipid raft and endocytic trafficking of AnxA2, we have assayed the distribution of AnxA2 in the endocytic vesicles using a previously well established procedure for the preparation of early and late endosomal fractions by flotation on 8-40% continuous sucrose gradients (30). Western immunoblotting of the 20 fractions revealed that early endosomal makers were recovered in fractions at the 35-25% interface whereas the late endosomal fractions were recovered in fractions at the 25-8% interface. As shown in Fig. 4A, AnxA2 was found to be enriched in both the early endosomal and late endosomal fractions. To ascertain the purity of the fractions, we used EEA1 and LAMP-1 which are markers for early endosomes and late endosomes respectively. In addition, we studied whether the distribution of AnxA2 in the endosomes is influenced by the cellular levels of cholesterol or Ca^{2+}. The post-nuclear supernatants (PNS) were mixed with 40% sucrose and overlaid on a step wise gradient as described above. Western immunoblotting of equal amounts of each fraction indicated that in

ionophore-treated cells, the distribution of AnxA2 in both the early endosomal and late endosomal fractions was significantly compromised when the cells were pretreated with MβCD. AnxA2 was also observed to be elevated in the PNS indicative of the increase in plasma

membrane levels of AnxA2 (Fig. 4B). These results suggest that AnxA2 is associated with early and late endosomal membrane domains rich in cholesterol.

Late endosomes are also characterized to possess a heterogeneous distribution of lipids and proteins in its limiting and intralumenal membranes with characteristics identical to the plasma membrane rafts (29). The raft-like domains could occur in the endocytic pathway as a result of *de novo* assembly or due to the pinching off of the plasma membrane rafts into the endocytic vesicles (15). Since endocytosis of the plasma membrane rafts is previously known to result in the formation of raft-like domains in the late endosomes (29, 31); we wanted to test if AnxA2 associated with the plasma membrane rafts could be internalized into the intracellular endosomes. We observed the co-internalization of AnxA2WT-GFP with Cav-1, which is known to be endocytosed by the clathrin-independent pathway (32). AnxA2WT-GFP co-localized with Cav-1 in discrete compartments in the cytosol (Fig. 4C, panel 3) and the extent of co-localization was markedly reduced in ionophore untreated cells (Fig. 4C, panel 1). In addition a marked reduction in the Cav-1 and AnxA2-GFP co-localization in both the plasma membrane and internalized vesicles was observed when cells were pretreated with MβCD in the absence and presence of the ionophore (Fig. 4C, panel 2 and panel 4 respectively). These results suggest that these vesicles contain membrane domains which possess raft-like characteristics. We also observed that a significant number of Cav-1 positive vesicles also contained LAMP-1 (Fig. 4C, panel 5). Lack of co-localization of AnxA2WT-GFP with calnexin, an endoplasmic reticulum marker further confirmed that these vesicles belong to the endosomal system (Fig. 4C, panel 6).

Higher magnification images in Fig. 4D, illustrate the co-internalization of AnxA2 and Cav-1 positive endosomes. In cells untreated with the ionophore the extent of co-localization of AnxA2 and Cav-1 was only 8% (Fig. 4D, panel 2) and the co-localization of Cav-1 with Rab5,

an early endosomal marker was only 3% (Fig. 4D, panel 3). In contrast, when the cells were treated with the ionophore, about 57% of the Cav-1 internalized vesicles were positively stained for AnxA2 (Fig. 4D, panel 5). 61% of the Cav-1 positive internalized vesicles were positive for Rab5. The increased co-localization of AnxA2 and Cav-1 in the presence of the ionophore suggests that AnxA2 in transited as a cargo by the Cav-1 positive vesicles and delivered to the early components of the endosomal pathway. BODIPY™-tagged lactosylceramide (LacCer) analog was used as a marker to label the vesicles internalized via the caveolar pathway.The internalization of AnxA2 and Cav-1 positive vesicles suggested that AnxA2 could be pinched off from the plasma membrane rafts into the endocytic vesicles. Since Cav-1 specifically binds to the detergent resistant regions of the plasma membrane, we wanted to test if AnxA2 could be recovered from the detergent resistant membranes (DRMs) of endosomes. For this purpose, DRMs were isolated from the late endosomes followed by purification by layering on continuous sucrose gradients. Ten fractions were collected and analyzed for the distribution of raft and non raft proteins. Upon ionophore treatment, significant levels of AnxA2 co-fractionated with GM1 and Cav-1 in fractions 2, 3 and 4 compared to ionophore untreated cells (Fig. 4D, right and left panels respectively). AnxA2 was also observed to cofractionate with LAMP1 suggesting that AnxA2 is also localized to a lesser degree to the non-raft regions of the endosomal membrane.

Previous studies have suggested that proteins which are trafficked to the intracellular lipid raft- containing vesicles are routed to the MVB pathway and lysosomes (8). Hence, we examined if AnxA2 is recruited form the late endosomal DRMs to the intralumenal components of the MVBs. We also wanted to determine if AnxA2 is a secretory component of the exosomes, which are extracellular derivatives of MVBs. For this purpose, we first investigated ionophore-

Figure. 4

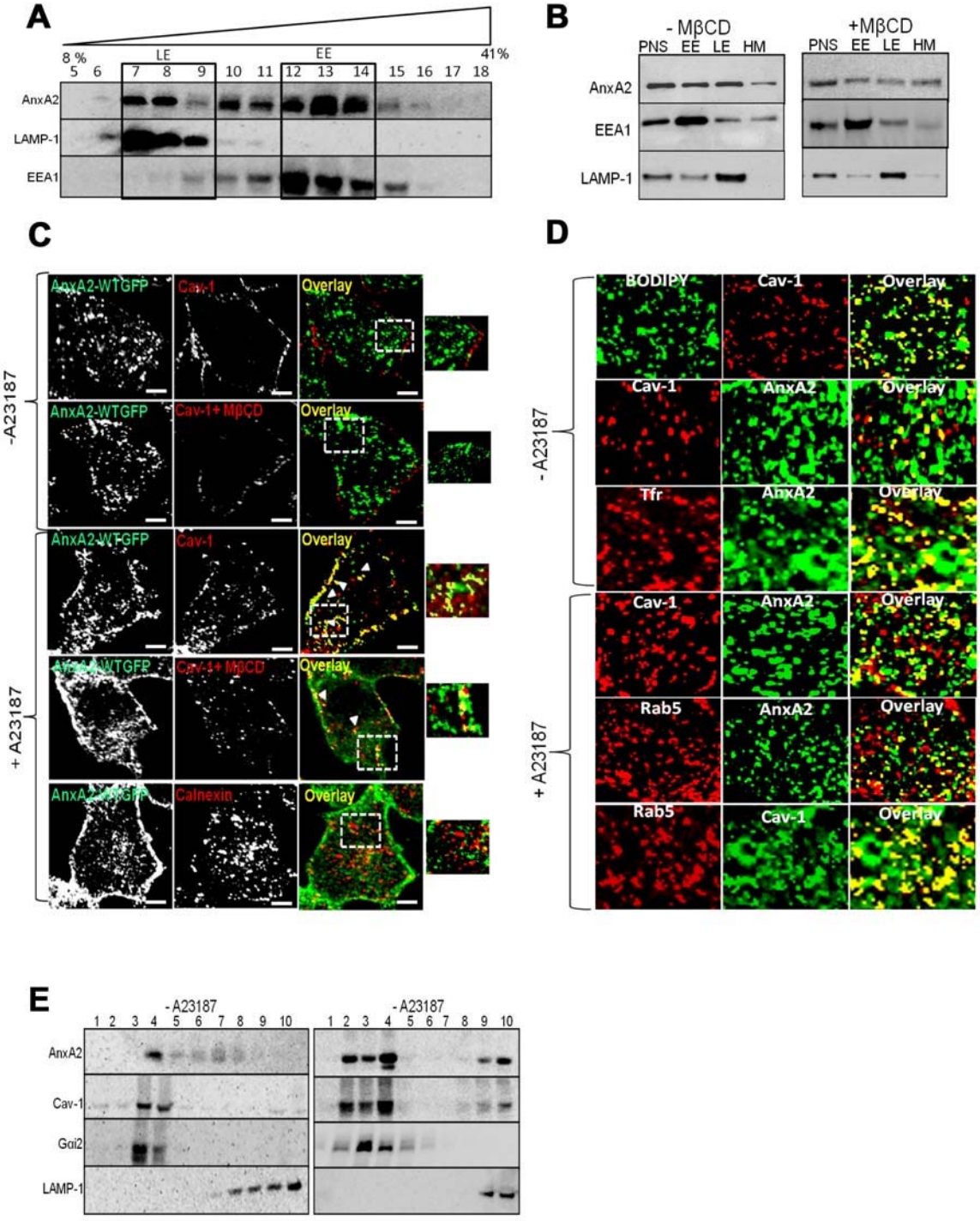
A
8 %
41%
LE
EE
5 6 7 8 9 10 11 12 13 14 15 16 17 18
AnxA2
LAMP-1
EEA1
B
- MβCD
+MβCD
PNS EE LE HM
PNS EE LE HM
AnxA2
EEA1
LAMP-1
C
-A23187
+ A23187
AnxA2-WTGFP
Cav-1
Overlay
AnxA2-WTGFP
Cav-1+ MβCD
Overlay
AnxA2-WTGFP
Cav-1
Overlay
AnxA2-WTGFP
Cav-1+ MβCD
Overlay
AnxA2-WTGFP
Calnexin
Overlay
D
- A23187
+ A23187
BODIPY
Cav-1
Overlay
Cav-1
AnxA2
Overlay
Tfr
AnxA2
Overlay
Cav-1
AnxA2
Overlay
Rab5
AnxA2
Overlay
Rab5
Cav-1
Overlay
E
- A23187
- A23187
1 2 3 4 5 6 7 8 9 10
1 2 3 4 5 6 7 8 9 10
AnxA2
Cav-1
Gαi2
LAMP-1

Figure 4. Endosomal recruitment of AnxA2. **(A)**. Post nuclear supernatants (PNS) were laid on the bottom of a centrifuge tube and mixed with 40.6% sucrose and overlaid with three steps of sucrose gradients (35%, 35% and 8.6%). Western immunoblotting of the sucrose gradient fractions with EEA1 and LAMP-1 which are markers for early endosomal and late endosomal fractions respectively. The fractions were also immunoblotted with AnxA2. **(B)** PNS were adjusted to the sucrose gradients as described above and subjected to centrifugation. Three interfaces were collected, the heavy membranes (HM) at the 40.6%-35% interface, early endosome (EE) at the 35%-25% interface and the late endosomes (LE) at the 25%-8.6% interface, Western immunoblotting of equal amounts of the three fractions with makers for EE, LE (EEA1 and LAMP-1 respectively) and AnxA2. **(C)** Confocal microscopy of NIH 3T3 fibroblasts expressing AnxA2WT-GFP, untreated (Panels 1 and 2) and treated with the ionophore (Panels 3-5). Co-localization of AnxA2WT-GFP with Cav-1 in the presence or absence of MβCD (Panels 3 and 4 respectively) and Calnexin (Panel 5). Bars 20 μm. **(D)** Higher magnification confocal microscopy images of cells untreated or treated with the ionophore for 20 min at 37°C. Prior to treatment with the ionophore the cells were loaded with BODIPY-Laccer and Alexa-conjugated transferrin. The cells were permeabilized and incubated in the corresponding primary and secondary antibodies for AnxA2, Cav-1 and Rab5. The overlay images illustrate the overlay of AnxA2 with Cav-1 and of Cav-1 with Rab5. **(E)** Late endosomes were subjected to suborgenellar fractionation followed by separation of late endosomal membranes on sucrose gradients. Ten fractions were collected from the top and analyzed by immunoblotting for the presence of the DRM markers caveolin-1 and GM1 in the low density fractions and LAMP-1 in high density fractions. The expression of AnxA2 was analyzed in the gradient fractions.

induced formation of MVBs in NIH 3T3 cells. In order to visualize the ionophore-induced formation of intracellular MVBs, NIH 3T3 cells, preloaded with a fluorescent lipid analog N-(lissamine rhodamine B sulfonyl)-phosphatidylethanolamine (N-Rh-PE) were simulated with ionophore. A significant increase in the number of N-Rh-PE stained intracellular MVBs was observed in a time-dependent manner upon ionophore treatment (Fig. 5A). Intracellular MVBs typically enclose a number of small 30-100 nm intralumenal vesicles characterized as exosomes. In order to establish that ionophore-induced MVB formation is associated with increased secretion of exosomes, the cells were treated with monensin, a drug that stimulates MVB exocytosis and enhances the secretion of exosomes, and wortmannin, a drug that inhibits the formation of MVBs. Quantification of secreted exosomes revealed a marked increase in the number of secreted exosomes in monensin and ionophore treated cells compared to the wortmannin and untreated control cells (Fig. 5B). To provide further proof to the role of Ca^{2+} in influencing the secretion of exosomes, the cells were treated with either ionophore alone or ionophore in combination with either EDTA or BAPTA-AM. A significant increase in the number of secreted exosomes was observed in cells stimulated with ionophore alone compared to the cells stimulated with ionophore in combination with either EDTA or BAPTA-AM (Fig. 5C). We also observed that ionophore stimulation induced a marked increase in the number of secreted exosomes in a time-dependent manner in comparison to the unstimulated cells (Fig. 5D).

In order to visualize the secretion of exosomes in a Ca^{2+}-dependent manner, cells were preloaded with Fluo-3 AM followed by labeling of the MVBs with a fluorescent lipid analog N-Rh-PE. The formation of MVBs containing luminal Ca^{2+} was observed in ionophore-stimulated cells which were markedly reduced in unstimulated cells (Fig. 5E). Taken together, these results

further support that ionophore treatment induces the release of secreted exosomes.

Figure. 5

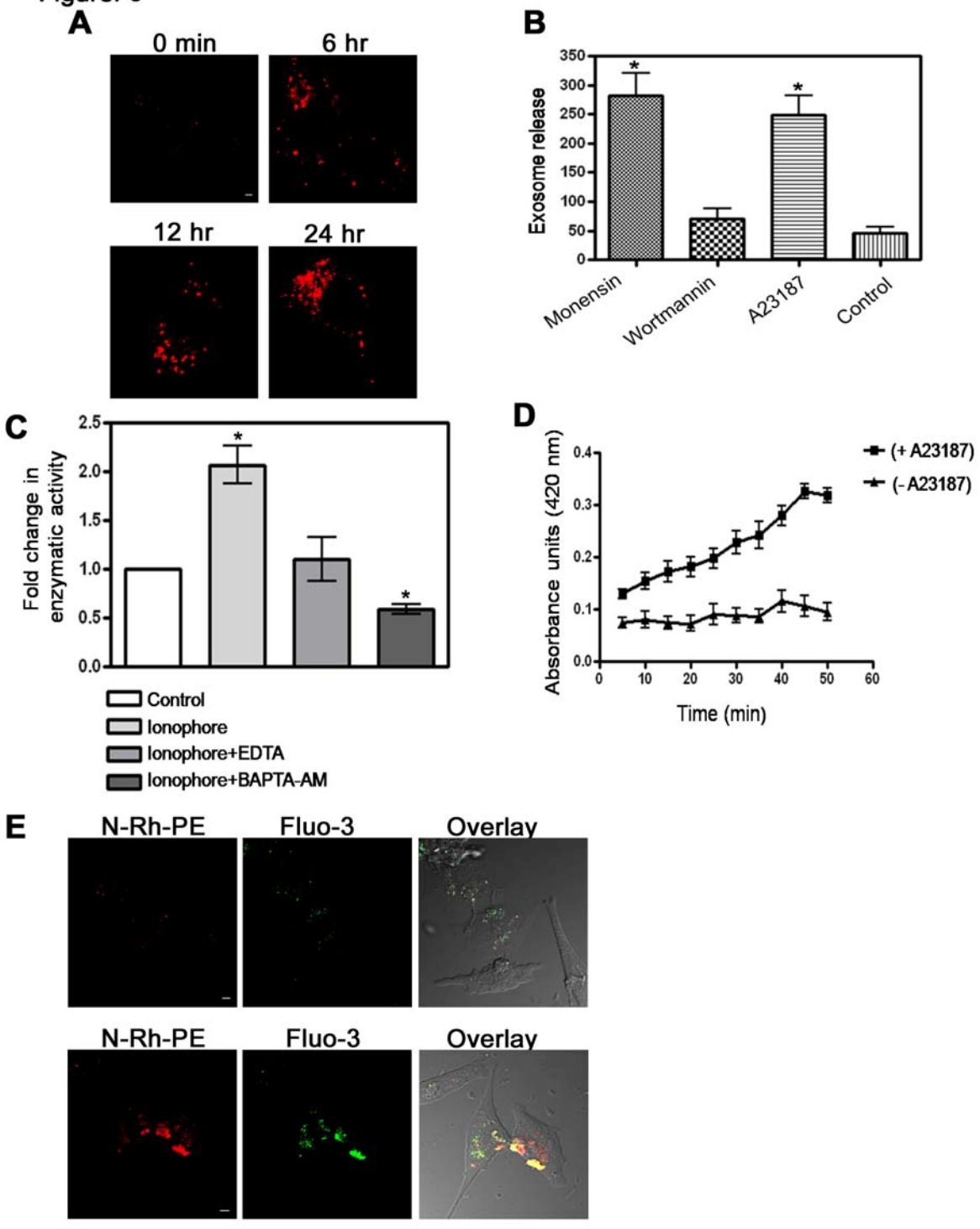

Figure 5. Ionophore treatment induces the secretion of exosomes in NIH 3T3 cells

(A) Confocal microscopy of NIH 3T3 cells preloaded with the fluorescent lipid analog N-Rh-PE and stimulated with the ionophore for the indicated periods of time. Bars 20 μm. **(B)** Quantification of secreted exosomes over 24 hrs in untreated cells and cells treated with monensin (1 μM), wortmannin (50 nM) and A23187 (5 μM) **(C)** Exosomes collected from the culture medium of cells stimulated with ionophore in combination with 1.5 mM EDTA and 20 μM BATA were quantitated by measuring the activity of AChE. The fold change in the enzymatic activity was plotted by normalizing the activity of the control to 1. * represents the significance at $p \leq 0.5$. **(D)** Quantification of the time-dependent secretion of the exosomes in the absence and presence of the ionophore by measuring the activity of AChE. The data are plotted as mean absorbance units ± SEM vs time in min. **(E)** NIH 3T3 cells were preloaded for 1 hr at 37°C with 15 μM Fluo-3 AM, the cells were later loaded with N-Rh-PE for 3 hr at 37°C and treated with the ionophore. The co-localization of Fluo-3 AM and N-Rh-PE at dense areas closer to the plasma membrane indicates the presence of intracellular Ca^{2+} in the MVEs, Bars 20 μm.

AnxA2 associates with intralumenal vesicles of the MVB in a Ca^{2+}-dependent manner

Based upon our observations that ionophore stimulation results in increased secretion of exosomes, we next determined whether AnxA2 is associated with secretory exosomes in a Ca^{2+}-dependent manner. Exosomes were extracted from the culture medium by serial centrifugation and the recovered high speed pellet was further purified by layering on sucrose gradients. Exosomes are known to migrate to a density ranging from 1.06-1.15 g/ml in a linear sucrose gradient (33). Consistent with these observations, upon ionophore treatment, NIH 3T3 secreted exosomes migrated to fractions with a density of 1.08-1.16 g/ml and co-fractionated with HSP70 and Tfr (Fig. 6A). The purity of the exosomal fraction was further confirmed by immunoblotting the exosome collected from the pooled sucrose gradient fractions and the cell lysate with antibodies against exosomal resident proteins and markers of the endoplasmic reticulum (Calnexin) and mitochondrion (Cytochrome C). As shown in Fig. 6B, the expression of AnxA2 was observed in the exosomal pellet along with the expression of exosomal makers (CD81, LAMP-1, CD63 and HSP70). Absence of calnexin and cytochrome C, which are markers for the endoplasmic reticulum and mitochondria, further confirmed the purity of the exosomal pellet (Fig 6B left panel). In order to confirm the association of AnxA2 with the MVB intralumenal vesicles, we immunostained MVBs with N-RH-PE, LBPA and CD81. Co-localization of AnxA2WT-GFP was observed with all the three MVB markers whereas co-localization was not observed with cytochrome C further confirming that AnxA2 is a component of MVBs (Fig. 6B, right panel). Next, we wanted to demonstrate the Ca^{2+}-dependent association of AnxA2 with the exosomes. We observed that ionophore treatment resulted in increased exosomal levels of both AnxA2 and HSP70 (Fig. 6C, upper panel) suggesting the ionophore-induced secretion of the exosomes. Furthermore, we quantitated the extent of exosomal secretion following ionophore treatment. Exosomes collected from the ionophore treated cells for the indicated periods of time

showed increased levels of AnxA2 which is accompanied by a concomitant increase in the levels of a exosomal resident protein, HSP70. (Fig. 6C, lower panel).

To determine if AnxA2 secreted from the exosomes can exogenously transferred from one cell type to another cell type, we made use of LNCaP-C1 cells stably expressing GFP and exosomes derived from MDA-MB231 cells. Cancer cells are known to secrete abundant levels of exosomes (34) and hence we made use of a breast cancer cell line, MDA-MB231 for exogenous exosomal transfer. LNCaP-C1 cells were incubated with exosomes derived from MDA-MB231 cells for a period of 30 min to 4 hr and subjected to immunostaining with AnxA2 antibody. AnxA2-specific immunostaining was observed as punctuate spots on the surface of LNCaP-C1 cells (Fig. 6D). Furthermore, incubation of LNCaP-C1 cells with MDA-MB231 derived exosomes for prolonged periods of time (4 hr) resulted in the internalization of AnxA2 as visualized by the intracellular localization of AnxA2-specific immunostaining.

To further analyze incorporation of AnxA2 in LNCaP-C1 cells delivered from exogenous MDA-MB231 derived exosomes, we performed TIRF microscopy to detect AnxA2 specific immunostaining in the subplasmalemmal regions and on the cell surface. TIRF microscopy showed an accumulation of AnxA2 positive exosomes on the cell periphery which was detectable as early as 15 min after incubation with exosomes. Incubation of exosomes for 4 hr resulted in their subsequent internalization in the intracellular endosomal compartments. LNCaP-C1 cells incubated with exosomes for 6 hr and treated with EDTA to chelate off peripheral AnxA2 showed the presence of only the internalized exosomes around the perinuclear regions. We observed that exosome internalization is an active process as cross linking the proteins with parafromaldehyde before addition of exosomes prevented both exosome accumulation and intracellular entry (Fig. 6E).

Figure. 6

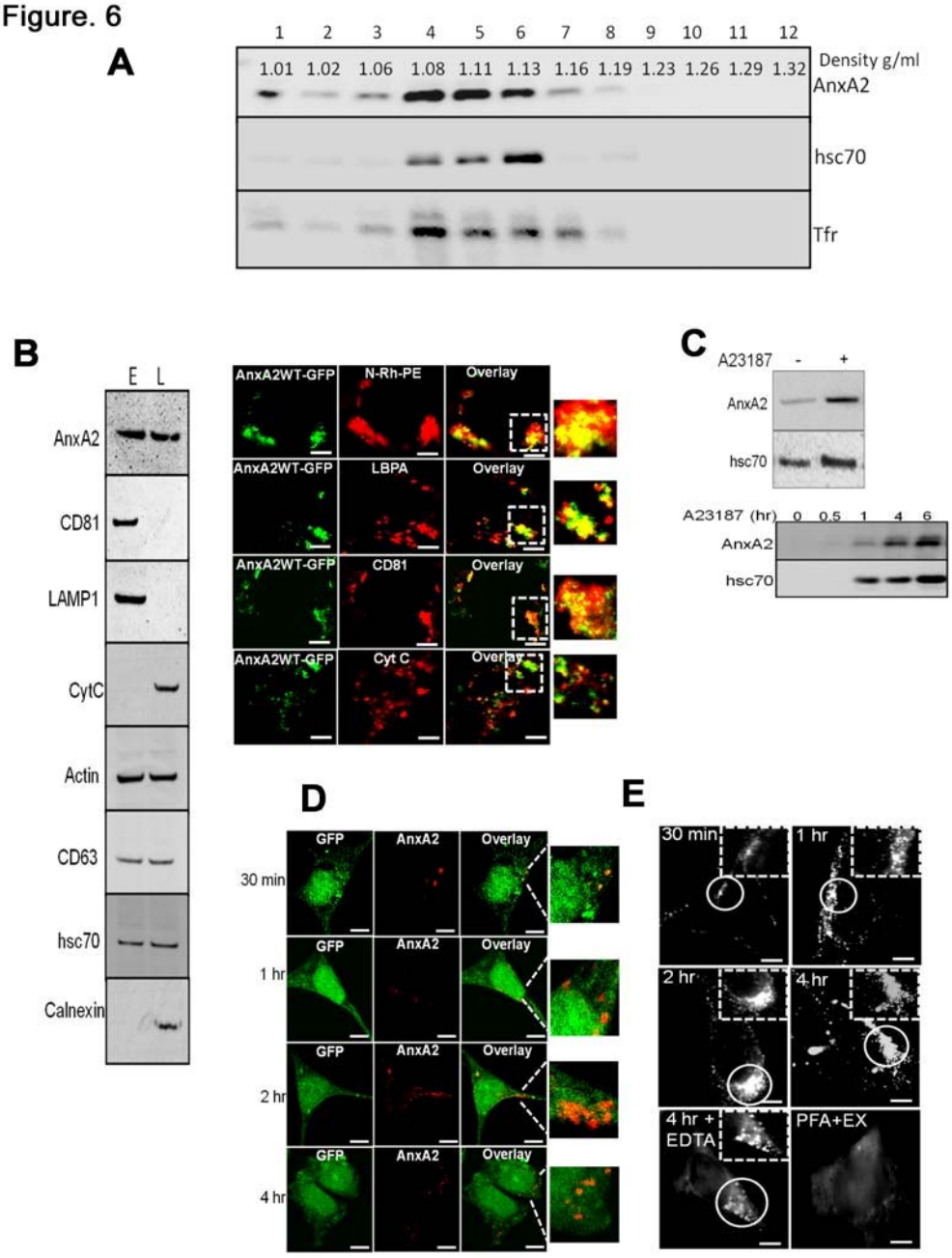
A
1 2 3 4 5 6 7 8 9 10 11 12
1.01 1.02 1.06 1.08 1.11 1.13 1.16 1.19 1.23 1.26 1.29 1.32
Density g/ml
AnxA2
hsc70
Tfr
B
E L
AnxA2
CD81
LAMP1
CytC
Actin
CD63
hsc70
Calnexin
AnxA2WT-GFP
N-Rh-PE
Overlay
LBPA
CD81
Cyt C
C
A23187 - +
AnxA2
hsc70
A23187 (hr) 0 0.5 1 4 6
D
GFP
AnxA2
30 min
1 hr
2 hr
4 hr
E
30 min
1 hr
2 hr
4 hr
4 hr + EDTA
PFA+EX

Figure 6. Exosomal association of AnxA2 on ionophore-stimulation.

(A) Pelleted exosomes were subjected to flotation on linear sucrose gradients (0.5-2 M sucrose) and subjected to ultracentrifugation. The fractions were collected and analyzed for expression of AnxA2 and exosome markers hsc70 and Tfr. Exosomes are shown to migrate to their characteristic density on the sucrose gradient. **(B)** Western immunoblotting of the exosomal pellet and whole cell lysate with exosomal protein markers (CD81, CD63, hsc70 and LAMP-1), endoplasmic reticulum (ER) and mitochondrial (Cytochrome C) markers (left panel). Co-localization of intracellular MVEs expressing AnxA2WT-GFP with the fluorescent lipid analog (N-RH-PE), LBPA, CD81 and Cytochrome C (right panel). Bars 20 μm. **(C)** Exosomes collected from ionophore treated cells were subjected to western immunoblot analysis to detect the expression of AnxA2 and hsc70 (upper panel) Exosomes were collected from cells stimulated with ionophore for the indicated periods of time and probed for AnxA2 and hsc70 (lower panel). **(D)** LNCaP-C1 cells stably expressing empty GFP (green) were incubated with exosomes derived from MDA-MB231cells for 30 min-4 hr. The overlay images indicate AnxA2-specific immunostaining on the surface of LNCaP-C1 cells (left panel). **(E)** LNCaP-C1 incubated with MDA-MB231-derived exosomes for the incubated periods of time and subjected to TIRF microscopy. As a control, cells were treated with 2% paraformaldehyde (PFA) after incubation with exosomes and analyzed by TIRF microscopy (right panel).Bars 20 μm.

AnxA2 is localized to the low density raft microdomains of the exosomes

Next, we examined the distribution of AnxA2 in the exosomes on ionophore stimulation. Triton-permeated exosomal fractions from ionophore-stimulated cells were subjected to detergent extraction in the presence of 1% CHAPS (Fig. 7A respectively) and overlaid on sucrose gradients. The gradient fractions were immunoblotted for CD81 (exosomal raft-associated protein) and AnxA2. In order to address the role of Tyr-23 phosphorylation in the association of AnxA2 with exosomes on ionophore treatment, we collected the whole cell lysate (L), plasma membrane (M) and exosomal membrane (E) fractions from cells expressing AnxA2WT-GFP, AnxA2 Y23E-GFP and AnxA2Y23F-GFP. SDS PAGE and immunoblotting with AnxA2 antibody revealed the distribution of AnxA2 in these fractions. As shown in Figure 7B, ionophore treatment resulted in an increased association of both AnxA2WT-GFP and AnxA2Y23E-GFP with the plasma membrane and exosomal membrane as opposed to the markedly diminished distribution of AnxA2Y23F-GFP. Further, we wanted to demonstrate the association of AnxA2 with the TI fractions of the exosomal membrane, the exosomal membranes from ionophore-stimulated cells were permeated with Triton X-100 and incubated in the presence of 1% CHAPS and layered on sucrose flotation gradients. Increased association of AnxA2-GFP fusion protein with the low density exosomal raft-like domains was observed in cells expressing AnxA2WT-GFP and AnxA2Y23E-GFP (Fig. 7C and 7D respectively). In contrast, cells expressing AnxA2Y23F-GFP showed a markedly diminished association of AnxA2 with the exosomal raft-like domains (Fig. 7E).

Figure. 7

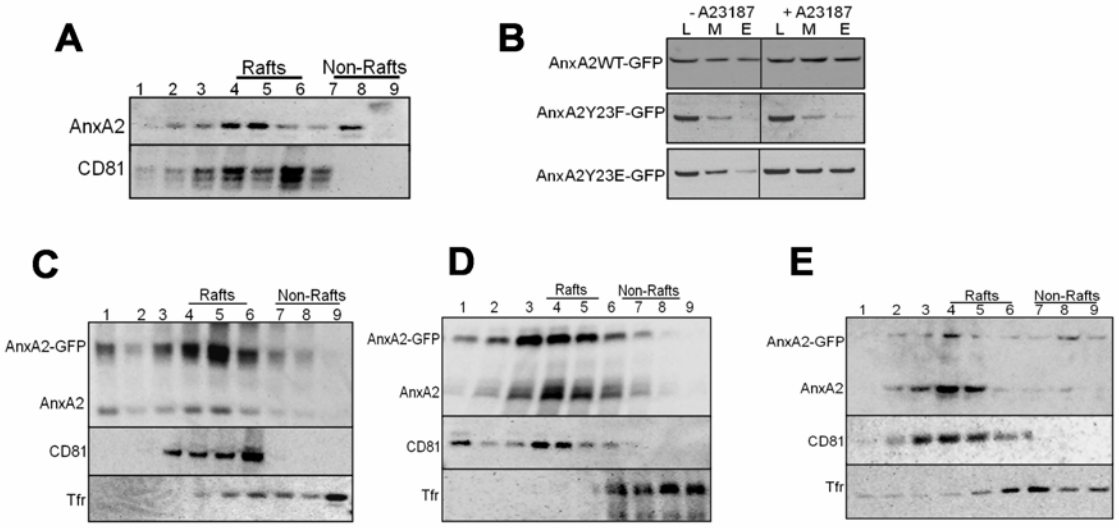
A
Rafts
Non-Rafts
1 2 3 4 5 6 7 8 9
AnxA2
CD81
B
- A23187
+ A23187
L M E L M E
AnxA2WT-GFP
AnxA2Y23F-GFP
AnxA2Y23E-GFP
C
Rafts
Non-Rafts
1 2 3 4 5 6 7 8 9
AnxA2-GFP
AnxA2
CD81
Tfr
D
Rafts
Non-Rafts
1 2 3 4 5 6 7 8 9
AnxA2-GFP
AnxA2
CD81
Tfr
E
Rafts
Non-Rafts
1 2 3 4 5 6 7 8 9
AnxA2-GFP
AnxA2
CD81
Tfr

Figure 7. Separation of exosomal membranes on sucrose flotation gradients.

(A) The exosomal pellet from pooled sucrose flotation gradients were incubated in the presence of 1% CHAPS and 1% Triton X-100 respectively and layered on sucrose gradients. The fractions were collected from the top and subjected to western immunoblotting with anti-CD81 and anti-AnxA2 antibodies. **(B)** Equal amounts of protein from the whole cell lysate (L), plasma membrane (M) and exosomal (E) fractions collected from the ionophore-stimulated cells expressing AnxA2WT-GFP, AnxA2Y23E-GFP and AnxA2Y23F-GFP were analyzed by western immunoblot for the expression of AnxA2. (C, D and E) Exosomal pellet from the above fractions recovered from cells expressing AnxA2WT-GFP, AnxA2Y23E-GFP and AnxA2Y23F-GFP respectively were separated by differential centrifugation on sucrose gradients after incubation with 1% CHAPS. Fractions were immunoblotted with AnxA2 and probed for raft (CD81) and non-raft (Tfr) marker proteins

To further demonstrate the association of wild-type AnxA2 and Tyr-23 phosphorylation mutants with the secreted exosomes, we performed flow cytometry analysis of exosomes. As shown in the Fig. 8, the exosomes contained a strong expression of surface CD81 and CD63 compared to the isotype controls. In contrast, the expression of CD40 and Na, K-ATPase which are plasma membrane markers was not observed on the exosomes confirming that the exosomal preparation was not contaminated by fragments of the plasma membrane. Moreover the exosomes showed a strong expression of AnxA2WT-GFP and AnxA2Y23E-GFP in ionophore- stimulated cells. However, the expression of AnxA2Y23F-GFP was significantly compromised. When exosomes were depleted of cholesterol by treating with EDTA, a marked reduction in the levels of AnxA2WT-GFP was observed, suggesting that AnxA2 is bound to the surface of exosomes in a Ca^{2+}-dependent manner.

Figure. 8

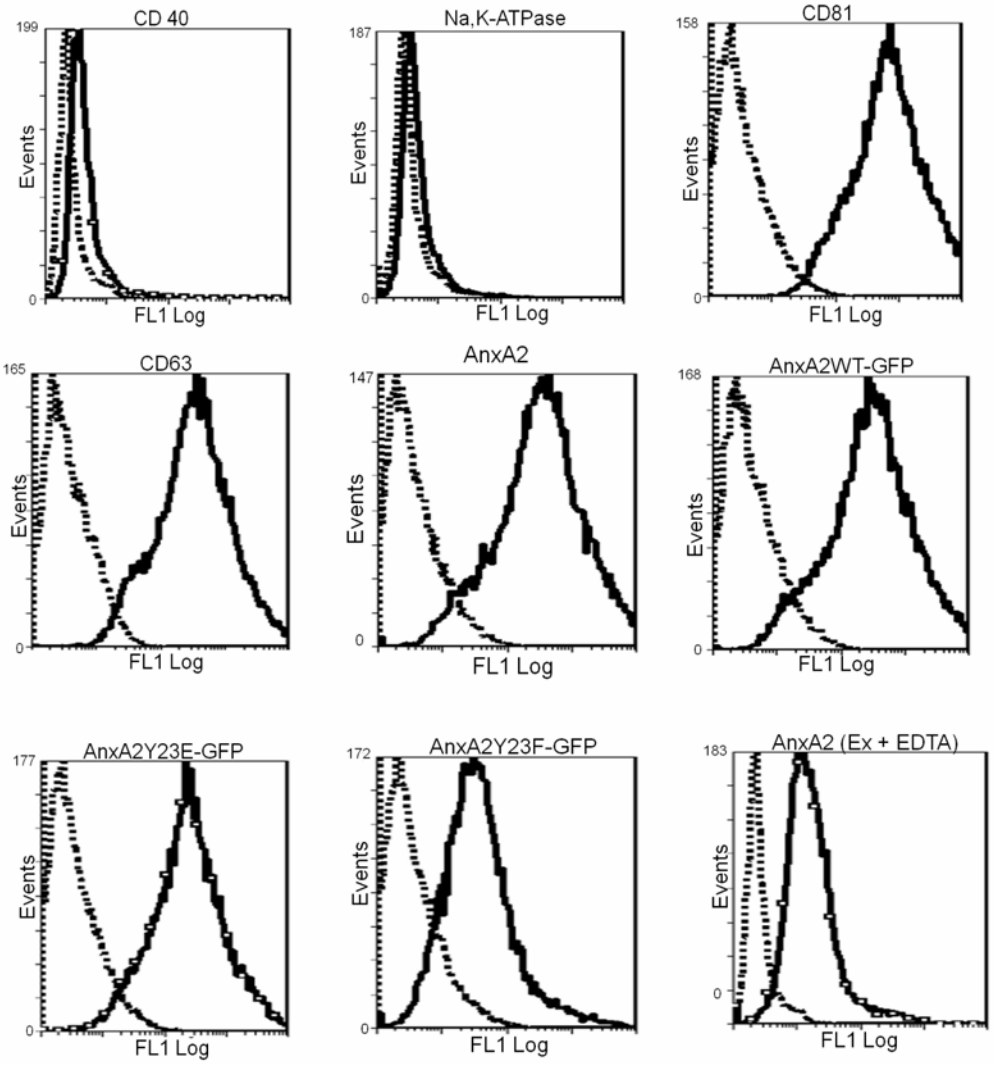
CD 40
199
Events
0
FL1 Log
Na,K-ATPase
187
Events
0
FL1 Log
CD81
158
Events
0
FL1 Log
CD63
165
Events
0
FL1 Log
AnxA2
147
Events
0
FL1 Log
AnxA2WT-GFP
168
Events
0
FL1 Log
AnxA2Y23E-GFP
177
Events
0
FL1 Log
AnxA2Y23F-GFP
172
Events
0
FL1 Log
AnxA2 (Ex + EDTA)
183
Events
0
FL1 Log

Figure 8. Exosomal expression of Wild-type AnxA2 and Tyr-23 phosphorylation mutants.

(A-J) Exosomes produced by ionophore-stimulated cells for 4 hr were coated on latex beads, labeled with the indicated antibody and subjected to flow cytometry analysis. Isotype controls are represented by broken lines and the continuous lines indicate staining by specific antibodies.

DISCUSSION

Our studies demonstrate that cell surface trafficking of AnxA2 is a multistep process mediated by a highly co-ordinated sequence of events in the intracellular endocytotic pathway. Elevated levels of Ca^{2+} moblilize cytosolic AnxA2 to the cholesterol-enriched domains of the plasma membrane called lipid rafts. Phosphorylation at Tyr-23 imparts on AnxA2 its ability to bind and stabilize with the lipid raft microdomains. After recruitment to the plasma membrane lipid rafts, AnxA2 is internalized from the lipid rafts by caveolae-mediated endocytosis. The internalized AnxA2 is delivered to the raft-like regions of the intracellular endocytic compartments which are believed to have originated as a result of plasma membrane endocytosis by clathrin-dependent and independent pathways. We observed the Ca^{2+}-dependent association of AnxA2 in the raft-like regions of the late endosomes and also in the MVB intralumenal vesicles. Furthermore, AnxA2 associated with the MVB intralumenal vesicles is released into the extracellular space upon fusion of the MVBs with the plasma membrane. We also observed the association of AnxA2 in the raft-like regions of the secretory exosomes which are originally the intralumenal vesicles of the MVB. Finally, our results indicate that the association of AnxA2 with the raft-like regions of the plasma membrane and the organellar membranes is largely dependent on the phosphorylation at Tyr-23.

One of the unresolved issues in AnxA2 biology is how the protein is translocated to the cell surface subsequent to stimuli that induce an increase in the intracellular levels of Ca^{2+} (2, 3). In an effort to identify the membrane dynamics that result in Ca^{2+}-dependent cell surface

translocation of AnxA2, we used an ionophore-stimulated model in NIH 3T3 cells. Ionophore-induced elevation of intracellular Ca^{2+} has been a particularly valuable model to study Ca^{2+}-dependent relocation of AnxA2 to cellular membranes (36). Relocation to the plasma membrane is related to several functions of AnxA2 including membrane trafficking, signaling events associated with Ca^{2+} handling and membrane-cytoskeletal interactions (37, 38).

Previous studies have indicated that AnxA2 is asymmetrically distributed in the plasma membrane as a result of its preferential localization to distinct membrane domains rich in PtdIns(4,5)P_2 (39, 40). Since PtdIns(4,5)P_2- rich regions comprise the detergent-insoluble regions of the membrane, AnxA2 has been identified as a raft-associated protein (41). Although the importance of Ca^{2+} in the localization of AnxA2 to the raft microdomains has been established, it is not known whether localization of AnxA2 to the lipid rafts is influenced by prior signaling events at the membrane.

Tyr-23 phosphorylation and lipid raft association of AnxA2: Previous studies have indicated the importance of Ca^{2+} as an indispensable stimulus for the relocation of AnxA2 to the membrane microdomains concentrated in the inner leaflet of the plasma membrane (38, 41-43). Although N-terminal phosphorylation of AnxA2 has been implicated in the regulation of several membrane activities of AnxA2, its involvement in the lipid raft association of AnxA2 has not been previously explored. The present study addressed the role of N-terminal phosphorylation events in the Ca^{2+}-dependent lipid raft localization of AnxA2. Here, we demonstrated that the distribution of AnxA2 to the lipid rafts and also the raft aggregation is markedly influenced by intracellular levels of Ca^{2+}. This translocation is also accompanied by a concomitant increase in the levels of AnxA2 associated with the non-raft regions suggesting the possibility that AnxA2 binds non-specifically to the non-raft regions of the membrane because of its affinity to the acidic phospholipids and is later recruited to the raft microdomains. Our studies involving both

the detergent and non-detergent based extraction of lipid rafts indicated that only the phosphomimetic mutant at Tyr-23 could be recovered from the lipid rafts. It is well established that proteins recruited to the lipid rafts are phosphorylated in the raft microenvironment by the raft-resident kinases (44). Since the Src kinase Lyn which is known to phosphorylate AnxA2 at Tyr-23 is localized to the rafts, it is possible that phosphorylation of AnxA2 at Tyr-23 occurs in the kinase-enriched lipid rafts (45). We suggest that phosphorylation at Tyr-23 may impart on AnxA2 the stability of association with the lipid rafts whereas the non-phosphorylated AnxA2 is destabilized from the raft microdomains.

Lipid rafts and protein sorting: Having demonstrated the involvement of Tyr-23 phosphorylation in the raft recruitment of AnxA2, one of the central questions that would arise subsequently is the role of raft-associated AnxA2. Rafts are originally identified as submicroscopic freely floating assemblies of liquid ordered domains of proteins and lipids (46). The dynamic nature of the rafts enables the movement of both proteins and lipids into and out of the rafts, and rafts are involved in the potentiation of intracellular signaling events (47). Lipid rafts are also known to contribute to membrane trafficking by the formation of transport carriers that form as a result of domain-induced budding from the lipid rafts at the cell surface and the sorting of proteins into a distinct class of endocytic vesicles (28, 48).

Vesicular sorting of lipid raft-associated AnxA2: The internalization of plasma membrane lipid rafts by the intracellular endocytic system has been extensively studied for the transport of GPI-anchored proteins (31). Endocytosis of protein and lipid raft components can occur via clathrin dependent and independent pathways (15). Recent evidence suggests that a majority of the proteins sorted into the lipid raft internalized vesicles are targeted to early and recycling endosomes via a clathrin-independent pathway (11, 49). In our studies, we observed the presence

of AnxA2 and Cav-1 positive internalized vesicles in the cytosol on ionophore treatment suggesting that AnxA2 follows similar pathways of lipid raft internalization. Although the mechanisms of caveolar endocytosis are not known, studies have suggested that proteins and lipids endocytosed via the caveolar pathway are integrated into the classical endosomal system. The budded caveolae referred to as endocytic caveolar carriers has different cellular destinations (50, 51). These vesicles can form a specialized organelle called caveosome in a Rab5-independent manner or can fuse with the endosomes in a RAB5-independent manner (52) . In our studies, we observed that AnxA2 and caveolae positive vesicles co-localize with Rab5 positive endosomes in a Ca^{2+}-dependent manner suggesting that the caveolar endocytosis is a mechanism by which the raft-like components are incorporated into the endosomal membranes. Our studies also suggest that AnxA2 is a component of the raft-like microdomains on the late endosomes. Although previous studies have suggested that the endosomal rafts are delivered from the plasma membrane by endocytosis via caveolae (53), further studies are essential to establish a direct relation between plasma membrane and endosomal rafts.

Proteins targeted to late endosmes have highly complex sorting systems because of the presence of distinct membrane domains in the late endosomal membranes (54). Sorting of proteins to the late endosomes is a common mechanism for the targeting of proteins to the ER and Golgi and transport of certain proteins from the plasma membrane by association with the intralumenal vesicles of the MVBs called exosomes (29). During the process of MVB formation proteins in the limiting membrane of the early endosomes are targeted to the internal vesicles of the MVB (54).

AnxA2 is known to associate with the endosomal membrane in a Ca^{2+}-independent manner in a manner which is different from its Ca^{2+}-dependent interaction with the negatively

charged phospholipids (55, 56). The Ca^{2+}-independent interaction of AnxA2 with the vesicular membranes is because of the presence of two copies of the YXXφ (X is any other amino acid and φ is a hydrophobic amino acid) motif in the N-terminus of AnxA2 (57). This motif is known to be essential in the interaction of AnxA2 with the clathrin adapter proteins that are involved in the sorting of the cargo to the clathrin coated vesicles (58). Phosphorylation of AnxA2 at Tyr-23 hinders the interaction of AnxA2 with the clathrin complexes and thereby preventing the endocytosis via clathrin coated vesicles (58). In the present study, we have identified the Ca^{2+}-dependent interaction of AnxA2 with the lipid rafts and its subsequent association with the endosomal system. Our results also indicate that AnxA2 is phosphorylated at Tyr-23 in response to ionophore-induced elevation in intracellular Ca^{2+}. Hence, we suggest that phosphorylation at Tyr-23 hinders the clathrin-dependent endocytosis and AnxA2 is endocytosed from the lipid rafts by clathrin-independent endocytosis mediated by caveolae.

The presence of AnxA2 in the DRMs of the late endosomes has lead us to examine the association of AnxA2 with the intralumenal vesicles of the MVBs. Exosomes are internal bilayer vesicles of the MVBs that originate when a limiting membrane of a late endosome is spontaneously invaginated (59). Maturing MVBs that contain several of these internally pinched off vesicles have three distinct destinations: 1) further maturation to from lysosomes, 2) serve as temporary storage for cellular proteins to avoid a degradation, or 3) secreted as exosomes by the fusion of the MVB limiting membrane with the plasma membrane (60). Biochemical analysis of the secreted exosomal membranes are similar in lipid composition to the rafts and several raft markers such as GM1, GM3, flotilin, Src kinase, Lyn, and the GPI anchored proteins CD55, CD58 and CD59 are known to be associated and secreted by the exosomes (21). These studies suggest that raft-like domains in the late endosomes and MVBs originate as a result of the pinching off of the plasma membrane into intracellular vesicles.

Sorting of AnxA2 from the plasma membrane lipid rafts to the exosomes: We demonstrate that ionophore stimulation induces the secretion of exosomes and exosomal AnxA2 can be exogenously transferred from one cell to another, suggesting the physiological role of exosomes in intercellular communication. The observation that elevated levels of intracellular Ca^{2+} promotes the secretion of exosomes is also supported by previous findings that Ca^{2+} influences multiple membrane fusion events in the trafficking of proteins across the endocytic pathway (61, 62). Furthermore, the isolation of raft-like microdomains from the exosomes has enabled us to determine that AnxA2 is a raft-associated component of the secretory exosomes. We have also studied the exosomal association of AnxA2 Tyr-23 phosphorylation mutants and our observations demonstrated that while the Tyr-23 phosphomimetic mutant of AnxA2 possessed the ability to associate with the secretory exosomes, the non-phosphomimetic mutant failed to do so. These observations, in addition to our previous findings that prevention of Tyr-23 phosphorylation inhibits the plasma membrane raft-association of AnxA2, suggested to us that the raft association of AnxA2 is critical for its entry into the exosomes.

In summary, our data provide insights into several unresolved issues concerning the Ca^{2+}-dependent cell surface translocation of AnxA2. The data presented here suggest several mechanistic approaches that facilitate the sorting of AnxA2 from the raft microdomains of the plasma membrane to the cell surface via its association with the DRMs of the endosomal system. These results outline the importance of secretory exosomes as functional carriers of AnxA2. A diagrammatic representation of the steps involved in the translocation of AnxA2 to the cell surface is presented in figure 9. In conclusion, these observations may suggest an alternate mechanism of non-classical protein secretion.

Figure.9

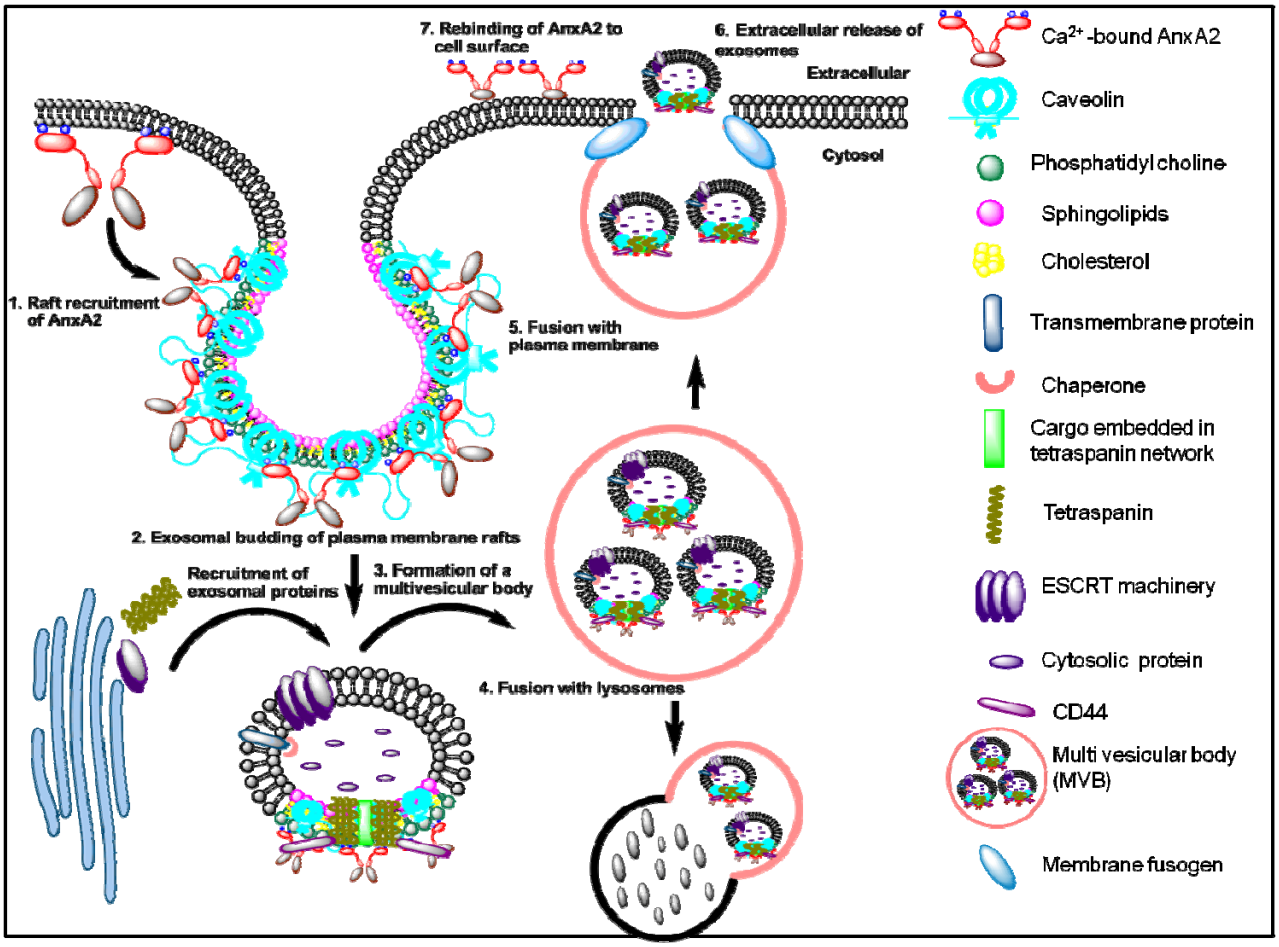
7. Rebinding of AnxA2 to cell surface
6. Extracellular release of exosomes
Extracellular
Cytosol
1. Raft recruitment of AnxA2
5. Fusion with plasma membrane
2. Exosomal budding of plasma membrane rafts
Recruitment of exosomal proteins
3. Formation of a multivesicular body
4. Fusion with lysosomes
Ca2+ -bound AnxA2
Caveolin
Phosphatidyl choline
Sphingolipids
Cholesterol
Transmembrane protein
Chaperone
Cargo embedded in tetraspanin network
Tetraspanin
ESCRT machinery
Cytosolic protein
CD44
Multi vesicular body (MVB)
Membrane fusogen

Figure. 9 Extracellular secretion of AnxA2 via the exosomal pathway.

A diagrammatic representation of several steps involved in the extracellular trafficking of AnxA2. 1. Recruitment of AnxA2 to the cholesterol and sphingolipid rich lipid rafts. 2. Budding of the plasma membrane rafts into the exosomal membrane. 3. Maturation of the exosomes into a MVB by deposition of inner limiting membrane. 4. Targeting of the MVBs either for lysosomal degradation or 5. Fusion with the plasma membrane. 6. Extracellular release of the exosomes and shedding of the exosomal contents. 7. Release of exosomal AnxA2 and binding to the cell surface.

REFERENCES

1. Gerke, V., Creutz, C. E., and Moss, S. E. (2005) *Nat. Rev. Mol. Cell Biol.* **6**, 449-461

2. Rescher, U., and Gerke, V. (2004) *J. Cell. Sci.* **117**, 2631-2639

3. Gerke, V., and Moss, S. E. (2002) *Physiol. Rev.* **82**, 331-371

4. Lambert, O., Cavusoglu, N., Gallay, J., Vincent, M., Rigaud, J. L., Henry, J. P., and Ayala-Sanmartin, J. (2004) *J. Biol. Chem.* **279**, 10872-10882

5. Danielsen, E. M., van Deurs, B., and Hansen, G. H. (2003) *Biochemistry* **42**, 14670-14676

6. Ayala-Sanmartin, J., Zibouche, M., Illien, F., Vincent, M., and Gallay, J. (2008) *Biochim. Biophys. Acta* **1778**, 472-482

7. Rescher, U., Ruhe, D., Ludwig, C., Zobiack, N., and Gerke, V. (2004) *J. Cell. Sci.* **117**, 3473-3480

8. Helms, J. B., and Zurzolo, C. (2004) *Traffic* **5**, 247-254

9. Nelson, W. J., and Rodriguez-Boulan, E. (2004) *Nat. Cell Biol.* **6**, 282-284

10. Fullekrug, J., and Simons, K. (2004) *Ann. N. Y. Acad. Sci.* **1014**, 164-169

11. Gagescu, R., Demaurex, N., Parton, R. G., Hunziker, W., Huber, L. A., and Gruenberg, J. (2000) *Mol. Biol. Cell* **11**, 2775-2791

12. Pelkmans, L., Kartenbeck, J., and Helenius, A. (2001) *Nat. Cell Biol.* **3**, 473-483

13. Benlimame, N., Le, P. U., and Nabi, I. R. (1998) *Mol. Biol. Cell* **9**, 1773-1786

14. Nichols, B. J., Kenworthy, A. K., Polishchuk, R. S., Lodge, R., Roberts, T. H., Hirschberg, K., Phair, R. D., and Lippincott-Schwartz, J. (2001) *J. Cell Biol.* **153**, 529-541

15. Sharma, P., Sabharanjak, S., and Mayor, S. (2002) *Semin. Cell Dev. Biol.* **13**, 205-214

16. Hurley, J. H., and Emr, S. D. (2006) *Annu. Rev. Biophys. Biomol. Struct.* **35**, 277-298

17. Wollert, T., and Hurley, J. H. (2010) *Nature* **464**, 864-869

18. Thery, C., Zitvogel, L., and Amigorena, S. (2002) *Nat. Rev. Immunol.* **2**, 569-579

19. Stoorvogel, W., Kleijmeer, M. J., Geuze, H. J., and Raposo, G. (2002) *Traffic* **3**, 321-330

20. Wubbolts, R., Leckie, R. S., Veenhuizen, P. T., Schwarzmann, G., Mobius, W., Hoernschemeyer, J., Slot, J. W., Geuze, H. J., and Stoorvogel, W. (2003) *J. Biol. Chem.* **278**, 10963-10972

21. de Gassart, A., Geminard, C., Fevrier, B., Raposo, G., and Vidal, M. (2003) *Blood* **102**, 4336-4344

22. Abrami, L., Liu, S., Cosson, P., Leppla, S. H., and van der Goot, F. G. (2003) *J. Cell Biol.* **160**, 321-328

23. Bagnat, M., Keranen, S., Shevchenko, A., Shevchenko, A., and Simons, K. (2000) *Proc. Natl. Acad. Sci. U. S. A.* **97**, 3254-3259

24. Beer, C., Andersen, D. S., Rojek, A., and Pedersen, L. (2005) *J. Virol.* **79**, 10776-10787

25. Mayran, N., Parton, R. G., and Gruenberg, J. (2003) *EMBO J.* **22**, 3242-3253

26. Brown, M. T., and Cooper, J. A. (1996) *Biochim. Biophys. Acta* **1287**, 121-149

27. Brown, D. A., and London, E. (1998) *Annu. Rev. Cell Dev. Biol.* **14**, 111-136

28. Nichols, B. (2003) *J. Cell. Sci.* **116**, 4707-4714

29. Sobo, K., Chevallier, J., Parton, R. G., Gruenberg, J., and van der Goot, F. G. (2007) *PLoS One* **2**, e391

30. de Araujo, M. E., Huber, L. A., and Stasyk, T. (2008) *Methods Mol. Biol.* **424**, 317-331

31. Parton, R. G., and Richards, A. A. (2003) *Traffic* **4**, 724-738

32. Mayor, S., and Pagano, R. E. (2007) *Nat. Rev. Mol. Cell Biol.* **8**, 603-612

33. Silverman, J. M., Clos, J., de'Oliveira, C. C., Shirvani, O., Fang, Y., Wang, C., Foster, L. J., and Reiner, N. E. (2010) *J. Cell. Sci.* **123**, 842-852

34. Koga, K., Matsumoto, K., Akiyoshi, T. *et al.* (2005) *Anticancer Res.* **25**, 3703-3707

35. Smalheiser, N. R. (2007) *Biol. Direct* **2**, 35

36. Barwise, J. L., and Walker, J. H. (1996) *J. Cell. Sci.* **109 (Pt 1)**, 247-255

37. de Graauw, M., Tijdens, I., Smeets, M. B., Hensbergen, P. J., Deelder, A. M., and van de Water, B. (2008) *Mol. Cell. Biol.* **28**, 1029-1040

38. Rescher, U., Ludwig, C., Konietzko, V., Kharitonenkov, A., and Gerke, V. (2008) *J. Cell.*

Sci. **121**, 2177-2185

39. Hayes, M. J., Shao, D. M., Grieve, A., Levine, T., Bailly, M., and Moss, S. E. (2009) *Biochim. Biophys. Acta* **1793**, 1086-1095

40. Oliferenko, S., Paiha, K., Harder, T., Gerke, V., Schwarzler, C., Schwarz, H., Beug, H., Gunthert, U., and Huber, L. A. (1999) *J. Cell Biol.* **146**, 843-854

41. Chasserot-Golaz, S., Vitale, N., Umbrecht-Jenck, E., Knight, D., Gerke, V., and Bader, M. F. (2005) *Mol. Biol. Cell* **16**, 1108-1119

42. Babiychuk, E. B., and Draeger, A. (2000) *J. Cell Biol.* **150**, 1113-1124

43. Deora, A. B., Kreitzer, G., Jacovina, A. T., and Hajjar, K. A. (2004) *J. Biol. Chem.* **279**, 43411-43418

44. Simons, K., and Toomre, D. (2000) *Nat. Rev. Mol. Cell Biol.* **1**, 31-39

45. Arcaro, A., Aubert, M., Espinosa del Hierro, M. E., Khanzada, U. K., Angelidou, S., Tetley, T. D., Bittermann, A. G., Frame, M. C., and Seckl, M. J. (2007) *Cell. Signal.* **19**, 1081-1092

46. Foster, L. J., and Chan, Q. W. (2007) *Subcell. Biochem.* **43**, 35-47

47. Rajendran, L., and Simons, K. (2005) *J. Cell. Sci.* **118**, 1099-1102

48. Schuck, S., and Simons, K. (2004) *J. Cell. Sci.* **117**, 5955-5964

49. Le Roy, C., and Wrana, J. L. (2005) *Nat. Rev. Mol. Cell Biol.* **6**, 112-126

50. Pfeffer, S. R. (2001) *Nat. Cell Biol.* **3**, E108-10

51. Pelkmans, L., Burli, T., Zerial, M., and Helenius, A. (2004) *Cell* **118**, 767-780

52. Parton, R. G. (2004) *Dev. Cell.* **7**, 458-460

53. Simons, K., and Gruenberg, J. (2000) *Trends Cell Biol.* **10**, 459-462

54. Gruenberg, J., and Stenmark, H. (2004) *Nat. Rev. Mol. Cell Biol.* **5**, 317-323

55. Morel, E., Parton, R. G., and Gruenberg, J. (2009) *Dev. Cell.* **16**, 445-457

56. Zeuschner, D., Stoorvogel, W., and Gerke, V. (2001) *Eur. J. Cell Biol.* **80**, 499-507

57. Turpin, E., Russo-Marie, F., Dubois, T., de Paillerets, C., Alfsen, A., and Bomsel, M. (1998) *Biochim. Biophys. Acta* **1402**, 115-130

58. Creutz, C. E., and Snyder, S. L. (2005) *Biochemistry* **44**, 13795-13806

59. Booth, A. M., Fang, Y., Fallon, J. K., Yang, J. M., Hildreth, J. E., and Gould, S. J. (2006) *J. Cell Biol.* **172**, 923-935

60. Simons, M., and Raposo, G. (2009) *Curr. Opin. Cell Biol.*

61. MacDonald, P. E., Eliasson, L., and Rorsman, P. (2005) *J. Cell. Sci.* **118**, 5911-5920

62. Mayorga, L. S., Beron, W., Sarrouf, M. N., Colombo, M. I., Creutz, C., and Stahl, P. D. (1994) *J. Biol. Chem.* **269**, 30927-30934

63. Rubin, D., and Ismail-Beigi, F. (2003) *Am. J. Physiol. Cell. Physiol.* **285**, C377-83

64. Savina, A., Furlan, M., Vidal, M., and Colombo, M. I. (2003) *J. Biol. Chem.* **278**, 20083-20090

65. Zhuang, L., Lin, J., Lu, M. L., Solomon, K. R., and Freeman, M. R. (2002) *Cancer Res.* **62**, 2227-2231

66. Brown, D. A. (2002) *Curr. Protoc. Immunol.* **Chapter 11**, Unit 11.10

67. Savina, A., Vidal, M., and Colombo, M. I. (2002) *J. Cell. Sci.* **115**, 2505-2515

68. Merendino, A. M., Bucchieri, F., Campanella, C. *et al.* (2010) *PLoS One* **5**, e9247

CHAPTER IV

A competitive hexapeptide inhibitor of Annexin A2 prevents hypoxia-induced angiogenic events

ABSTRACT

Extracellular proteolysis is an indispensable requirement for the formation of new blood vessels during neovascularization and is implicated in the generation of several angiogenic regulatory molecules. Anti-proteolytic agents have become attractive therapeutic strategies in diseases associated with excessive neovascularization. Annexin A2 (AnxA2) is an endothelial cell surface receptor for the generation of active proteolytic factors like plasmin. Here, we show that AnxA2 is abundantly expressed in the neovascular tufts in a murine model of proliferative retinopathy. Exposure to hypoxic conditions results in elevation of the AnxA2 and tPA in human retinal microvascular endothelial cells (RMVECs). We show that a hexapeptide competitive inhibitor LCKLSL targeting the N-terminal tPA-binding site of AnxA2 binds efficiently to cell surface AnxA2 compared to the control peptide, LGKLSL. Treatment with the competitive peptide inhibits the generation of plasmin and suppresses the VEGF-induced activity of tPA under hypoxic conditions. Application of the competitive peptide in the chicken chorioallantoic membrane (CAM) assay results in suppression of the neo angiogenic response which is also associated with significant changes in the vascular sprouting. These results suggest that AnxA2-mediated plasmin generation is an important event in angiogenesis and this process is inhibited by a specific competitive hexapeptide inhibitor of tPA binding to AnxA2

INTRODUCTION

Neovascularization, the sprouting of new blood capillaries from preexisting blood vessels is a multistep process that occurs in a series of co-ordinated steps (1). One of the earliest mechanisms in neovascularization is the degradation of extracellular matrix (ECM) surrounding the basement membrane, formation of a lesion in the basement membrane, migration of the endothelial cells to form a new capillary sprout and further migration and proliferation of endothelial cells to elongate the sprout (1). Proteolysis of the ECM is an important prerequisite for the endothelial cells to migrate, proliferate and form a new blood vessel and this process requires an array of extracellular proteolytic events (2, 3). The extracellular proteolytic system comprises serine proteases and their activators including tissue plasminogen activator (tPA), urokinase plasminogen activator (uPA), their physiological inhibitor, plasminogen activator inhibitor-1 (PAI-1) and PAI-2 (23) (4). Plasmin, a central component of this system, is a broad spectrum trypsin-like serine protease degrading several components of the ECM like laminin and fibrin, activates inactive pro-matrix metalloproteinases (MMPs) and also increases the bio-availability of $VEGF_{165}$ and $VEGF_{189}$ (4-6). The generation of plasmin-induced angiogenic response is regulated by a balance of plasminogen activators, tPA and uPA (7, 8). Recent evidence indicates a correlation between elevated levels of VEGF, tPA and PAI-1 in patients with proliferative diabetic retinopathy (9) . Also, elevated levels of plasminogen activators have been observed in type 1 diabetic patients with retinopathy (10-12). An understanding the molecular mediators that potentiate the endogenous activity of plasminogen activators can have potential implications in the inhibition of ECM degradation and subsequent ocular

neovascularization. Spatial restriction of proteolysis is identified as a common mechanism for not only limiting the proteolysis to the pericellular environment but also amplifying the extracellular proteolytic cascade (13). Annexin A2 (AnxA2), a member of a family of Ca^{2+}-dependent phospholipid binding proteins is a cell surface co-receptor for tPA and plasminogen (14). By binding to both plasminogen and tPA, AnxA2 brings the two enzymes in close proximity and increases the catalytic efficiency of plasmin generation by ~60 fold (15). The result is a highly efficient plasmin-mediated proteolytic cascade which promotes neovascularization by increasing the efficiency of endothelial cell invasion across the ECM (16).

tPA binds to the N-terminus of AnxA2 corresponding to the site LCKLSL encompassing the 7-12 residues of AnxA2 (17, 18). The presence of a cysteine residue is crucial for tPA binding and the interaction is inhibited in the presence of homocysteine (19). Sequential mutations in the N-terminus of AnxA2 have indicated that cysteine at position 8 is critical for the tPA binding activity and the mutation of this residue significantly reduces the binding efficiency of tPA to AnxA2 (18). An array of synthetic peptides containing cysteine residues and spanning the N-terminus of AnxA2 were generated and tested for their ability to bind to the tPA binding site of AnxA2 (18). Among these peptides, a hexapeptide with the sequence LCKLSL that is identical to the tPA-binding site of AnxA2 and containing a cysteine residue at position 8 was shown to be more than 95% efficient in competitively inhibiting tPA binding to AnxA2 (18).

In this report, we identify the anti-angiogenic activity of the N-terminal LCKLSL hexapeptide competitive peptide inhibitor of tPA binding to AnxA2. We show that hypoxia-induced angiogenic responses result in an increase in the endothelial cell surface binding of tPA and AnxA2 which is followed by a concomitant increase in the generation of plasmin. Furthermore, we demonstrate that treatment of hypoxic-RMVECs with the hexapeptide

competitive peptide inhibitor prevents the formation of AnxA2-tPA cell surface complex and also reduces the plasmin-generating activity of tPA. Furthermore, in a chicken chorioallantoic membrane (CAM) assay, the hexapeptide was also able to specifically inhibit VEGF-induced neovascularization suggesting its potential involvement in the VEGF pathway. Taken together, this study elucidates the mechanisms by which excessive extracellular proteolysis can be inhibited by modulating the ability of tPA to bind to its cell surface receptor, AnxA2.

MATERIALS AND METHODS

Isolation and culture of human retinal microvascular endothelial cells

Human retinas were procured from the Lions Eye Institute for Transplant & Research (LEITR, Tampa, FL) within 24 hours postmortem (20). The eyes were enucleated, hemisected and the lenses and vitreous were removed. The retinas were removed and placed in HBSS buffer containing 1% penicillin-streptomycin (Gibco). The retinas were digested with 0.5% collagenase (Worthington Biochemical) in Ca^{2+} and Mg^{2+}-free PBS at 37°C for 35-40 minutes. Following digestion, the retinal digests were incubated in endothelial growth medium (EGM-2) (Lonza) with 10% FBS (Gibco) and the digests were dissociated by trituration and centrifuged. The cells were passed through a double layer of sterile 40 μm sterile nylon mesh (Falcon) and pelleted by centrifugation at 400X g for 10 minutes. After washing the cells twice with EGM-2, the cell suspension was incubated with 200 μl of anti-PECAM coated magnetic dyanabeads (Invitrogen). The RMVECs bound to the magnetic beads were recovered using a magnetic particle collector and resuspended in EGM-2. The cells were seeded on fibronectin (Sigma) coated flasks and grown in EGM-2 supplemented with growth factors. The cells were passaged for 6-8 passages and tested for the expression of von Willebrand's factor (VWF) (Sigma) and also for their ability to from capillary tubes on matrigel basement membrane (Invitrogen).

Peptide synthesis

The LCKLSL and control LGKLSL peptides were synthesized using solid phase methods (Genscript). The peptides were purified (≥94%) by preparative reverse phase HPLC. The hexapeptide sequence was analyzed by MALDI-TOF mass spectrometry. Biotinylated peptides

were prepared by adding biotin groups to the C-terminal lysine residue of the peptides by an amide bond. The positive charge on the lysine residue was later removed.

Generation of hypoxic culture conditions

For the generation of hypoxic conditions, cells from P2-P4 were incubated in the presence of 95% N_2 and 5% CO_2 gas mixture in a hypoxic chamber (Proox C21; BioSperix) under the control of the Proox controller (model 110; BioSpherix) set to 3% O_2 at 37°C and 100% relative humidity. Cells incubated under standard normoxic conditions (95% air and 5% CO_2) from the same batch and passage were used as normoxic controls.

Antibodies and reagents

Antibodies and reagents were purchased from the following sources: Anti-AnxA2 (BD Pharmingen), anti-tPA (American Diagnostica), Glu-plasminogen (American Diagnostica), recombinant human tPA (American Diagnostica), anti-VWF (Sigma). Matrigel (Invitrogen), Sulfo-NHS-LC-biotin (Pierce), sepharose-conjugated streptavidin (Sigma), D-Val-Leu-Lys-7-Amino-4(Trifluoromethyl)-coumaride (Sigma), recombinant human tPA, Glu-plasminogen (American Diagnostica), tPA concentration and activity ELISA kits (Innovative Research).

EDTA elution and cell surface biotinylation

Confluent cultures of RMVECs were washed with 0.5 mM EDTA and PBS buffer (Gibco) for 20 minutes at 37^0C. The EDTA eluates were collected as described (21), concentrated using NANOSEP omega 10K filters (Pall Corporation) and subjected to SDS-PAGE and western immunoblot analysis. In this report, the EDTA washes will be referred to as EDTA eluates. Cell surface proteins were subjected to biotinylation with 0.5 mg/ml of EZ-link-sulfo-NHS biotin (Pierce) and recovered with avidin-conjugated sepharose (Sigma) as previously described (22).

Confocal microscopy and Total Internal Reflection (TIRF) microscopy.

Double immunostaining for AnxA2 and tPA followed by confocal microscopy was performed as described (23). TIRF microscopy was preformed to reveal the cell surface expression of AnxA2 (24). Cells were grown on 22 mm glass coverslips (VWR International), fixed in 4% ice cold paraformaldehyde in PBS for 10 minutes at 4°C. The cells were processed for AnxA2 immunostaining with a mouse monoclonal anti-AnxA2 antibody (Transduction Laboratories, 1:500 dilution) and observed under the Olympus IX71 microscope equipped with a commercial TIRF attachment using Olympus 60x NA=1.45 PlanApo oil objective and Hamamatsu C4742-95 high-resolution digital camera utilizing a progressive scan interline transfer CCD chip with no mechanical shutter and Peltier cooling. Images were acquired with identical image acquisition parameters.

Plasmin generation assay

The assay was performed according to the previously established protocols (25). RMVECs were treated with 5 μM LCKLSL peptide and 5 μM LGKLSL control peptides and exposed to hypoxic conditions. After a few washes, the cells were incubated with 100 nM Glu-plasminogen (American Diagnostica) for 1 hour and subsequently treated with the fluorogenic plasmin substrate D-VLK-AMC (D-Val-Leu-Lys 7-amido-4-methylcoumarin) (Sigma). Substrate hydrolysis was measured at 4 minute intervals as relative fluorescence units (RFUs) in a fluorescence spectrophotometer at 380 nm excitation and 460 nm emission wavelengths. The readings were collected in replicates of 4 and the rate of plasmin generation was determined using linear regression analysis of the plots of RFUs versus time^2 as described previously (25).

ELISA detection for total tPA and active tPA

The levels of total tPA and active tPA in the EDTA eluates and conditioned medium

were measured using the commercially available enzyme linked immunosorbent assay (ELISA) kits (Innovative Research) following the manufacturer's instructions. Conditioned medium and EDTA eluates from normoxic and hypoxic RMVECs were added to the wells of a 96 well microtiter plate along with the tPA standards. The primary anti-human tPA antibody was later added followed by the addition of a HRP-conjugated secondary antibody and the reaction was read by the addition of the TMB substrate at 450 nm. Data are expressed as means ± SD and the sampled were plated in triplicate wells for each experiment, and every experiment was repeated at least three times.

Chicken chorioallantoic membrane (CAM) assay

Nine-day old fertilized white leghorn chicken embryos (Charles River SPAFAS Inc.) were maintained in at 37°C and 60% relative humidity conditions. The extent of vascularization in the eggs was examined with the aid of an egg lamp and a small hole was made in the air sack at the area where prominent blood vessels are located. A window was cut with the aid of a scapel blade and the air sack was gently displaced. Collagen filter discs saturated with 1 μg/ml of VEGF were placed on the CAMs of nine-day old chicken embryos followed by the daily topical application of 20 μg/ml of LCKLSL and LGKLSL peptides. Filter discs saturated with VEGF and PBS served as positive and negative controls respectively. Each group consisted of 6-9 eggs were treated for daily for 3 days and on the 4^{th} day, the CAMs underlying the filter discs were isolated and analyzed. Angiogenesis was assessed in the CAMs by counting the number of visible blood vessel branch points in each field and the images were taken using a Nikon Diaphot camera. CAMs were later fixed, embedded in paraffin, sectioned and stained with hematoxylin and eosin (H&E). The number of vessels was later counted.

Shell-less chicken embryo culture

Three day old fertilized white leghorn chicken eggs were rinsed with 70% ethanol and opened into 100 mm glass petri dishes. The embryos were incubated under aseptic conditions at 37 °C for 7-9 additional days. The LCKLSL and LGKLSL control peptides (20 µg) and VEGF (100 ng/ µl) were added to collagen filter discs (4 mm X 4 mm squares). The filter discs were later placed onto the CAM of a 12-day old embryo in the area devoid of major blood vessels. The embryos were returned to a humidified incubator at 37°C with 3% CO_2 for 48 hours. After the incubation period, the CAMs were visualized under an inverted light microscope and the images were taken using a Nikon Diaphot camera.

Quantitation of angiogenesis

Quantitative assessment of angiogenesis in the CAM images was performed using the computer assisted CAM image analysis. Changes in the vascular length, branch, junction, end, triple and quadruple points was quantified by creating the binary images after application of a common threshold value. The binary images were converted into skeletonized images using NIH imageJ software (http://rsbweb.nih.gov/ij/) and later quantified using analyze skeleton plugin (http://imagejdocu.tudor.lu/doku.php?id=plugin:analysis:analyzeskeleton:start) of imageJ.

Mouse-model of oxygen-induced retinopathy

Hypoxia-normoxia induced proliferative retinopathy was induced in a mouse model as previously published. Briefly, postnatal day 7 (P7), littermates along with their nursing mothers were exposed to 75% oxygen for 5 days, and returned to room air (21% oxygen) for 5 days. The control littermates were placed in room air for the entire period. At the end of the experimental period, the animals were euthanized and the eye globes were enucleated, fixed in 4% paraformaldehyde and embedded in paraffin. Serial sections (5 µm) of the retina were subjected to immunostaning with AnxA2 antibody as described previously (26).

Statistical Analysis

Statistical analysis was performed using GraphPad 5.0 software (GraphPad Software Inc., La Jolla, CA). Mann-Whitney test was used when comparing two groups and the Kruskal-Wallis test with Dunn's post-test for three or more multiple comparisons. Significance was defined as $P < 0.05$. Results are presented as mean ± the standard error of the mean (SEM)

RESULTS

Isolation of a homogenous population of RMVECs and characterization for the expression of AnxA2

Since endothelial cells are known to abundantly express AnxA2, we used RMVECs as a model to study the involvement of AnxA2 in hypoxia-induced angiogenic events. A homogenous population of RMVECs was isolated using magnetic beads coated with an antibody against the endothelial cell specific marker, PECAM-1. After immunoaffinity purification with PECAM-1-coated magnetic beads, the cells were attached to fibronectin coated plates within 24 hours. The cells grew to confluence in 8-9 days forming contact-inhibited monolayers and demonstrated endothelial cell specific cobblestone morphology (Supplementary Fig. 1A). We also tested the cells for their ability to form capillary tubes on matrigel basement membrane. Shown in the supplementary Fig. 1B is a phase contrast image of the capillary tubes formed within 3 hours after seeding on matrigel basement membrane. In order to confirm that the isolated cells are indeed RMVECs, we immunostained these cells with VWF followed by confocal microscopy which indicated that nearly all of the cells are positive for VWF (Supplementary Fig. 1C). The cells can be cultured for 6-8 passages, retain their ability to form tubes and are positive for the endothelial cell markers. If any other cell types begin to appear during subsequent passaging, reselection was employed by enrichment with PECAM-1 coated magnetic beads.

The isolated RMVECs were tested for the intracellular and cell surface expression of AnxA2. Immunostaining with AnxA2 followed by confocal microscopy revealed the intracellular expression of AnxA2 (Supplementary Fig. 1C) and the merge indicated no co-localization of VWF and AnxA2. TIRF microscopy was performed to detect the presence of

AnxA2 on the cell surface and AnxA2 was observed as dense and punctuate spots on the cell surface. The cells were also immunostained with a cytosolic protein, tubulin followed by TIRF microscopy to serve as a negative control (Supplementary Fig. 1D).

Induction and evaluation of hypoxia-induced angiogenic events in cultured RMVECs

For the generation of hypoxic conditions, cells were incubated in the presence of 95% N_2 and 5% CO_2 gas mixture in a hypoxic chamber which generates 3% O_2 levels at 37°C and 100% relative humidity. Our preliminary findings have indicated that RMVECs exposed to hypoxic conditions (3% O_2) for 3-7 hours were morphologically distinguishable from normoxic RMVECs and these cells were able to form capillary tubes when seeded on matrigel basement membrane. When the cells were incubated under hypoxic conditions (3% O_2) for the indicated periods of time, an increase in the length of the capillary tubes was observed in the presence of growth factors like VEGF and FGF-2 as visualized in the phase contrast images. On quantification of the capillary tubes using NIH ImageJ software, tube length following 7 hours of hypoxic exposure was measured to be ~80 μm compared to the tube length of ~25 μm measured in cells exposed to normoxic conditions for the identical period of time (Fig. 1C).

Hypoxia induces an upregulation in the expression of AnxA2 in cultured RMVECs and in the vascular tufts of oxygen-induced retinopathy mouse sections

To test whether the levels of AnxA2 were influenced by hypoxic exposure, RMVECs were incubated for 3 and 7 hours under hypoxic conditions. In order to recover the cell surface AnxA2, we made use of its Ca^{2+}-binding property to chelate AnxA2 and its cell surface interactors with EDTA and PBS buffer. The cell surface eluates are henceforth referred to as EDTA eluates. Western immunoblot analysis of the whole cell lysates (Fig. 1B, left panel) and EDTA eluates (Fig. 1B, right panel) demonstrated that exposure to hypoxic conditions for 3

hours and 7 hours resulted in the upregulation of the intracellular (50% increase on hypoxic exposure for 7 hours compared to the normoxic control) and surface levels of AnxA2 (30% increase on hypoxic exposure for 7 hours compared to the normoxic control). Confocal microscopy of RMVECs exposed to hypoxic conditions for the indicated periods of time (30 minutes-7 hours) and immunostained with AnxA2 antibody showed an increased intracellular expression of AnxA2 localized predominantly to the capillary extensions in cells incubated under hypoxic conditions compared to cells incubated under normoxic conditions (Fig. 1C). In order to prove the involvement of AnxA2 in the hypoxia-induced neovascular responses of the retina, we used the mouse oxygen-induced retinopathy (OIR) model. OIR model progresses in two phases to retinopathy, in the first phase the mouse retinal vasculature is subjected to hyperoxia-induced damage by exposing the animal to 75% O_2 from p7 to p12 (27). Vascular obliteration results during hyperoxia which downregulates the expression of VEGF and thereby effecting the survival of endothelial cells (28). In the second phase of the disease, retinopathy is initiated when the mice are returned to a normoxic environment (27). The vasculature responds to hypoxia by upregulating the secretion of angiogenic growth factors like VEGF leading to increased vascular sprouting, which is observed as neovascular tufts towards the vitreous (29). Immunostaining of the paraffin-embedded OIR mouse retinal sections with AnxA2 antibody revealed abundant expression of AnxA2 in the neovascular tufts of OIR sections at p17 (Fig. 1D). The nonvascular tufts were observed to be extending into the vitreous. Localization of AnxA2 in the neovascular tufts of the OIR sections suggests its involvement in the vaso-obliterative phase of oxygen-induced retinopathy.

Figure. 1

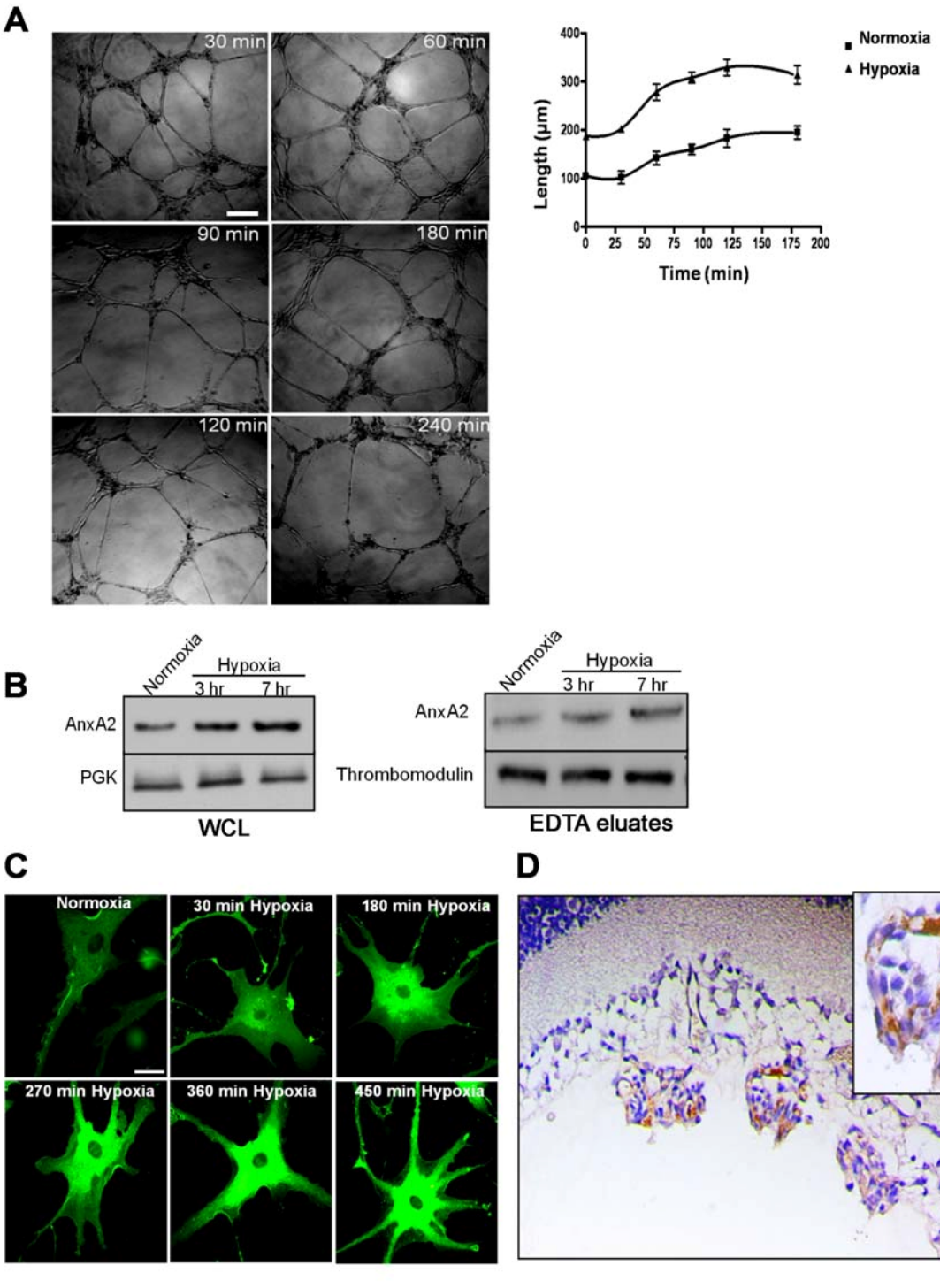
A
30 min
60 min
90 min
180 min
120 min
240 min
Length (μm)
Time (min)
Normoxia
Hypoxia
B
Normoxia
Hypoxia
3 hr
7 hr
AnxA2
PGK
WCL
Thrombomodulin
EDTA eluates
C
Normoxia
30 min Hypoxia
180 min Hypoxia
270 min Hypoxia
360 min Hypoxia
450 min Hypoxia
D

Figure 1. Enhancement of the length of the capillary tubes and hypoxia-induced expression of AnxA2 in RMVECs and mouse sections in a mouse model of OIR.

A. Phase contrast images of RMVECs seeded on matrigel and exposed to hypoxic conditions for the indicated periods of time. The length of the tubes was quantitated in three independent microscopic fields per experimental treatment using the NIH ImageJ soft ware. The data is represented as the mean length ± SE. Scale 200 μm. **B.** RMVECs were exposed to hypoxic conditions for the indicated periods of time. The cells were incubated in EDTA for 20 minutes and later subjected to lysis. The EDTA eluates and the whole cell lysates (WCL) were subjected to western immunoblot analysis with anti-AnxA2 antibody. PGK and thrombomodulin were used as loading controls for whole cell lysates and EDTA eluates respectively. ***C*** *RMVECs* exposed to hypoxic conditions for the indicated periods of time were fixed with 4% paraformaldehyde and immunostained with anti-AnxA2 antibody. Six representative images are shown indicating an increase in the expression of AnxA2 in response to hypoxia. Scale 50 μm

D. Immunohistochemistry of OIR retinal sections stained for AnxA2. Expression of AnxA2 in the vascular tufts penetrating from the inner limiting membrane of the OIR sections. Shown in the insight is a magnified image of the vascular tufts with intense staining for AnxA2. Scale 25 μm.

Hypoxia-induced upregulation of secreted and membrane-bound levels of AnxA2 and tPA in RMVECs

To determine if hypoxia induces an upregulation in the secretory levels of tPA, we performed a Enzyme Linked Immunosorbent Assay (ELISA) on the cell surface EDTA eluates and the conditioned medium. Our results indicate that RMVECs exposed to 3 hours and 7 hours of hypoxia secrete elevated levels of tPA in the conditioned medium compared to the normoxic RMVECs. The majority of secreted tPA was associated with the cell surface (2 fold increase in cells exposed to hypoxia for 7 hours compared to cells exposed to normoxia for 7 hours) and is recovered by incubating the cells with EDTA (Fig. 2A). Similarly, we also performed ELISA to detect the cell surface and secreted levels of AnxA2 under hypoxic conditions. We observed that under hypoxic conditions AnxA2 is predominantly associated with the cell surface with very little distribution in the conditioned medium (Fig. 2B). These results were also confirmed by immunoblot analysis of the EDTA eluates which showed an increase in the cell surface levels of AnxA2 and tPA under hypoxic conditions (Fig. 2C). Thrombomodulin, an EDTA-elutable endothelial cell surface protein was used as a control for loading. Immunoprecipitation of the RMVEC EDTA eluates also revealed an increase in the levels of the AnxA2-tPA complex in the cells exposed to hypoxic conditions compared to the basal levels under normoxic conditions (Fig. 2D). Furthermore, the increased presence AnxA2 and tPA complex on the surface of hypoxic RMVECs was demonstrated by immunostaining with anti-AnxA2 and anti-tPA antibodies followed by confocal microscopy. Hypoxic exposure for the indicated periods of time resulted in an increase in the expression of the AnxA2-tPA complex, found predominantly on the cell surface and in the extending protrusions of the capillary tubes. The extent of AnxA2-tPA co-localization was quantitated by measuring the colocalization coefficients using the Zeiss

Figure. 2

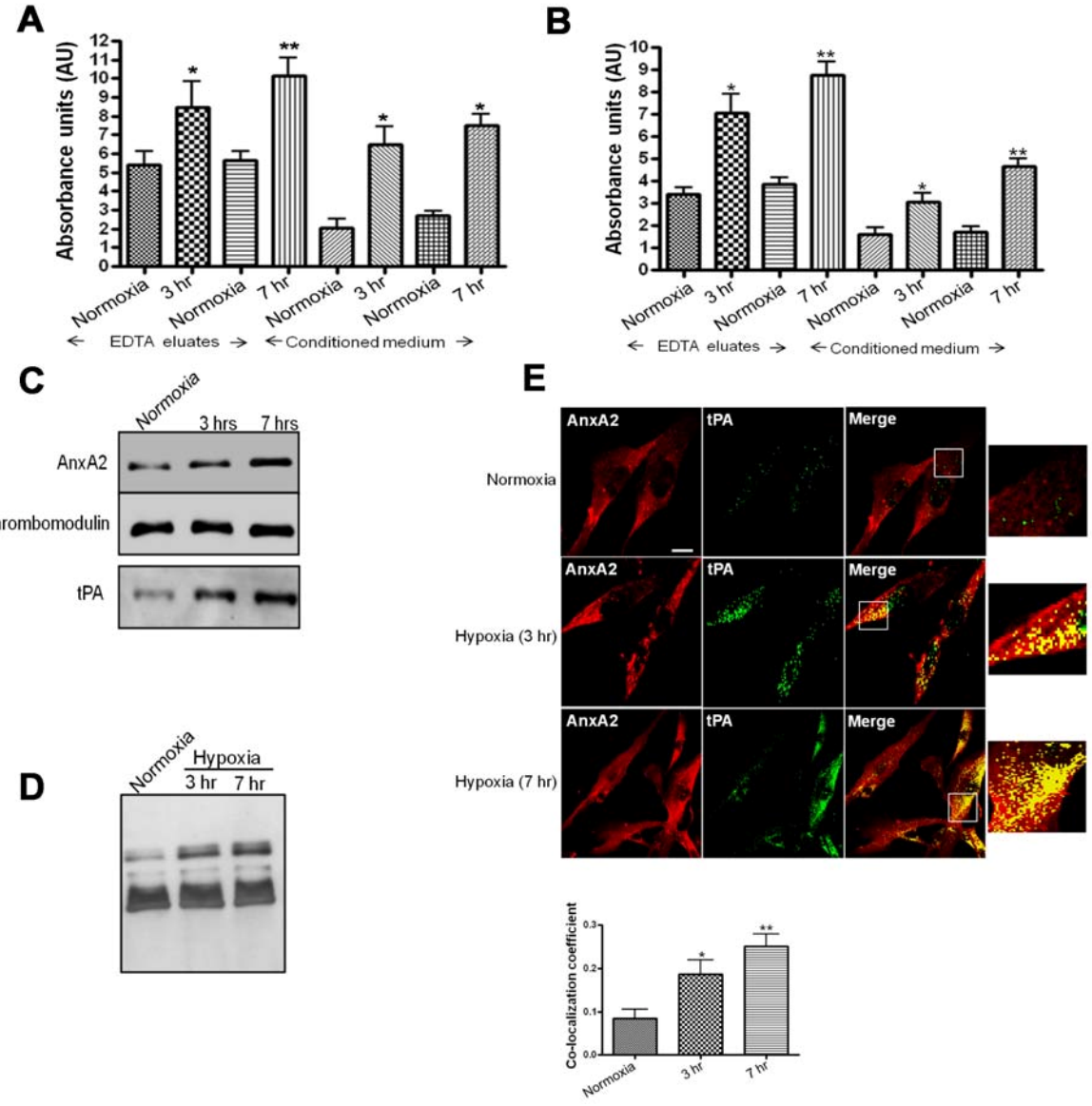
A
Absorbance units (AU)
Normoxia
3 hr
7 hr
← EDTA eluates →
← Conditioned medium →
B
C
3 hrs
AnxA2
Thrombomodulin
tPA
D
Hypoxia
E
AnxA2
tPA
Merge
Hypoxia (3 hr)
Hypoxia (7 hr)
Co-localization coefficient

Figure 2. Colocalization of the AnxA2-tPA complex in RMVECs exposed to hypoxic conditions

A. RMVECs were exposed to 3 and 7 hours of hypoxia. The conditioned medium and EDTA eluates were subjected to ELISA with tPA antibody. After the addition of TMB substrate, the reaction is measured spectrophotometrically at 450 nm. **B.** ELISA of the EDTA eluates and conditioned medium from RMVECs exposed to hypoxic (3 and 7 hours) and normoxic conditions with AnxA2 antibody. **C.** Western immunoblot analysis of the EDTA eluates from RMVECs exposed to hypoxic conditions with AnxA2 and tPA antibodies. Thrombomodulin was used as a loading control for the EDTA eluates. **D.** RMVEC lysates exposed to hypoxic conditions (3%) were subjected to immunoprecipitation with anti-AnxA2 antibody and immunoblotted with anti-tPA antibody. **E.** RMVECs grown to confluence on coverslips coated were exposed to hypoxic conditions (3%) for 7 hours. The cells were fixed and subjected to immunocytochemistry followed by confocal microscopy (Zeiss LSM 510, 40x water-immersion objective) with anti-AnxA2 (red) and anti-tPA (green) antibodies. Scale 20 μm. The extent of co-localization was measured using the Zeiss Enhanced Colocalization Tool software. Colocalization coefficients were calculated from 10 cells for each period of hypoxic exposure and the values are statistically processed using the GraphPad Prism software. The values of the weighted correlation coefficient ±SE are represented.

Enhanced Colocalization Tool software. The co-localization coefficients were measured to be 0.081 ± 0.05, 0.192 ± 0.04 and 0.257 ± 0.07 (mean ± SE) for RMVECS exposed to normoxia for 7 hours and hypoxic exposure for 3 hours and 7 hours respectively (Fig. 2E).

N-terminal hexapeptide LCKLSL inhibits the efficiency of tPA-mediated plasmin generation

To demonstrate the binding specificity of the synthetic hexapeptides LCKLSL and LGKLSL to AnxA2, hypoxic RMVECs (7 hours of hypoxia) were incubated in the presence of increasing concentrations of LCKLSL and LGKLSL peptides biotinylated at the C-terminus. The cell surface-bound biotinylated peptides were pulled down by incubating with sepharose-conjugated streptavidin and subjected to Western immunoblot analysis for AnxA2. The presence of AnxA2 in the streptavidin pull down extracts recovered from the cells treated with increasing concentrations of the biotinylated LCKLSL peptide suggests the specificity of its interaction with cell surface AnxA2 (Fig. 3A, upper panel). A modest recovery of AnxA2 on treatment with the LGKLSL biotinylated peptide suggests the lack of specificity (Fig. 3A, lower panel). The efficiency of the LCKLSL peptide in inhibiting the cell surface binding of tPA was also confirmed by performing a chromogenic plasmin generation assay in the presence of 100 nM plasminogen and a chromogenic plasmin substrate. Hypoxic exposure for 3 hours resulted in a ~2.0 fold increase in the levels of plasmin compared to the normoxic controls. The hexapeptide LCKLSL at a concentration of 10 μM resulted in a ~50% (S.E.; n=6) reduction in plasmin generation under hypoxic conditions compared to the control peptide, LGKLSL. The peptide seemed to have only moderate effects on the baseline levels of plasmin generation in cells exposed to normoxic conditions (Fig. 3B). The hexapeptide was also tested for its ability to inhibit the capillary tube formation. In the presence of LCKLSL the length of the capillary tubes

Figure. 3

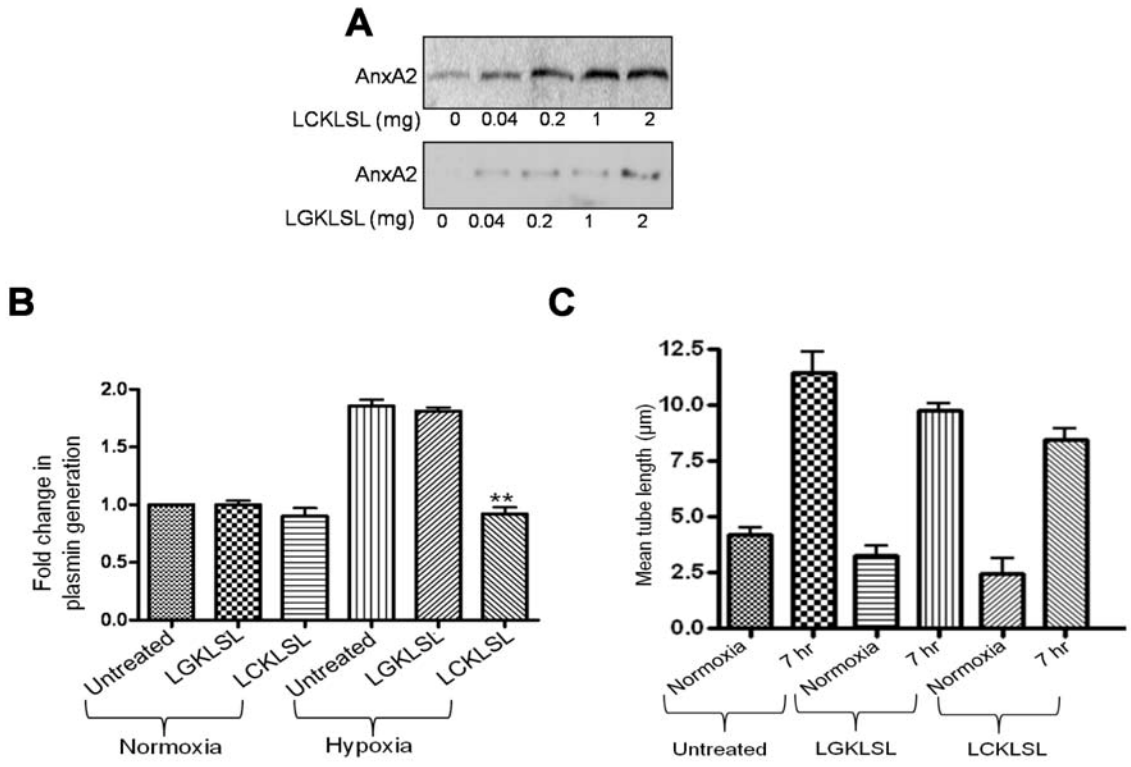
A
AnxA2
LCKLSL (mg) 0 0.04 0.2 1 2
AnxA2
LGKLSL (mg) 0 0.04 0.2 1 2
B
Fold change in plasmin generation
2.0
1.5
1.0
0.5
0.0
**
Untreated
LGKLSL
LCKLSL
Untreated
LGKLSL
LCKLSL
Normoxia
Hypoxia
C
Mean tube length (μm)
12.5
10.0
7.5
5.0
2.5
0.0
Normoxia
7 hr
Normoxia
7 hr
Normoxia
7 hr
Untreated
LGKLSL
LCKLSL

Figure 3. Effect of LCKLSL hexapeptide on hypoxia-induced plasmin generation

A. Confluent RMVECs exposed to hypoxia for 7 hours were incubated in the presence of biotinylated (LCKLSL) and control (LGKLSL) hexapeptides and the biotinylated proteins were isolated by conjugation with streptavidin. The pulled down extracts were subjected to immunoblotting with AnxA2 antibody. **B.** A chromogenic plasmin generation assay of RMVECs treated with the LCKLSL and LGKLSL peptides and exposed to hypoxic conditions for 7 hours in the presence of recombinant plasminogen and a plasmin substrate. The fold increase in plasmin generation was calculated by normalizing the initial rates of plasmin generation in untreated cells which was assigned a value of 1. Data shown here are mean ± SE (n=7 for untreated controls and n=5 for peptide treatments) **C.** Quantification of capillary tube formation of RMVECs seeded on matrigel basement membrane and incubated with the LCKLSL peptide and LGKLSL peptide in the presence of recombinant plasminogen. The cells exposed to normoxic conditions were used as controls to measure the baseline levels of tube formation. Images were acquired using a phase contrast microscope and quantified using the NIH ImageJ software. The data are represented as mean tube length ± SE and the tubes were quantified in five different microscope fields per sample. Each experiment was performed in triplicate and repeated at least twice.

in hypoxic RMVECs cultured on matrigel was reduced by ~60% compared to the ~15% reduction in the tube length in the presence of the scrambled peptide, LGKLSL (Fig. 3C).

AnxA2 N-terminal hexapeptide LCKLSL inhibits VEGF-induced tPA activity in RMVECs under hypoxic conditions

Vascular obliteration and ischemia are common features of microvascular angiopathies (30). Retinal hypoxia is suggested to be an important factor in the induction of vascular leakage followed by an upregulation in the secretion and activity of VEGF, a major angiogenic cytokine (31). VEGF is known to regulate many steps in the angiogenic process and is primarily involved in inducing extracellular proteolysis by upregulating the expression and activity of plasminogen activators (32). The effects of increasing concentrations of VEGF in modulating the levels of cell surface-associated tPA was tested in RMVECs under normoxic and hypoxic conditions. On exposure to hypoxic conditions for 7 hours, RMVECs exhibited a dose-dependent increase in the cell surface levels of tPA in response to VEGF (Fig. 4A).

Furthermore, we also measured the activity of cell surface tPA in the presence of VEGF. We observed a time and dose-dependent increase in the antigen activity of cells surface tPA in hypoxic RMVECs. The increase in the antigen activity of tPA was consistent with the observed increase in the cell surface levels of tPA under hypoxia (Fig. 4B).

Since our data indicated that VEGF acts as a potent inducer of tPA in hypoxic RMVECs, we investigated if inhibition of tPA binding to AnxA2 could dampen the VEGF-induced, tPA-mediated activation of plasminogen to plasmin. Previous studies have shown the involvement of AnxA2 in VEGF-induced neovascular responses and the role of AnxA2 as a cell surface catalytic center for the accelerated conversion of plasminogen to plasmin is directly implicated in these processes (33). Here, we wanted to demonstrate the efficacy of the LCKLSL hexapeptide in

Figure. 4

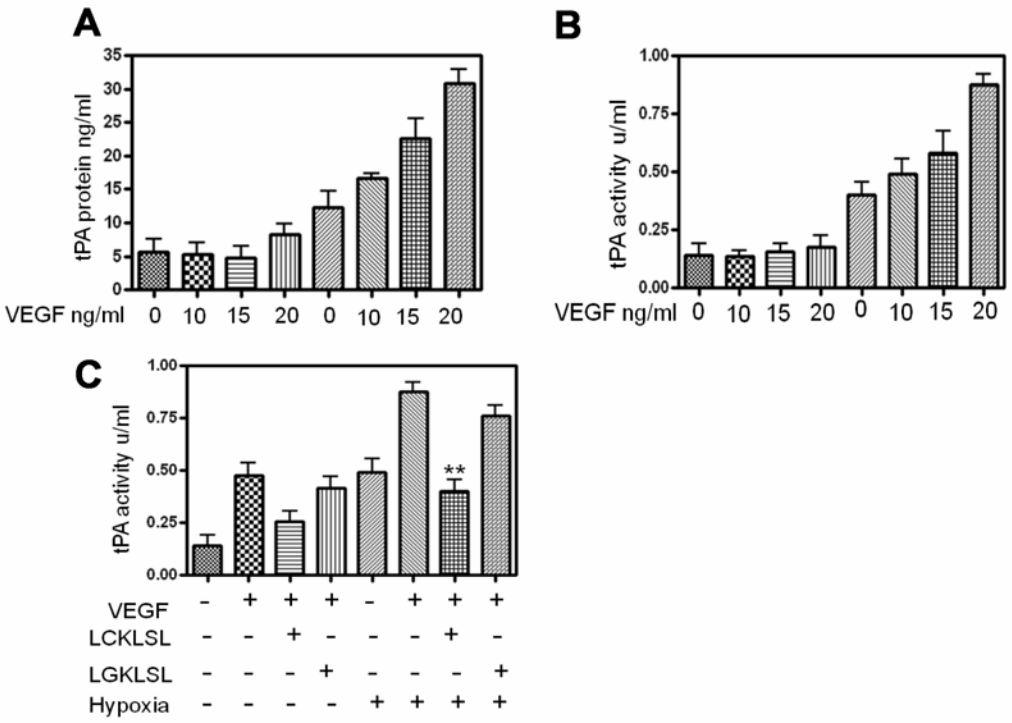
A
tPA protein ng/ml
35
30
25
20
15
10
5
0
VEGF ng/ml 0 10 15 20 0 10 15 20
B
tPA activity u/ml
1.00
0.75
0.50
0.25
0.00
VEGF ng/ml 0 10 15 20 0 10 15 20
C
tPA activity u/ml
1.00
0.75
0.50
0.25
0.00
**
VEGF - + + + - + + +
LCKLSL - - + - - - + -
LGKLSL - - - + - - - +
Hypoxia - - - - + + + +

Figure 4. Effect of the LCKLSL hexapeptide on VEGF-induced activity of tPA in RMVECs under hypoxic conditions

A. Effect of VEGF on the secreted and cell surface levels of tPA was determined by ELISA of the EDTA eluates in the presence of the indicated concentrations of VEGF. Exposure to VEGF resulted in a significantly increased production of secreted and cell surface levels of t-PA. Data are represented as the mean concentration of tPA in ng/ml. The experiments were performed at least in triplicate with triple values each. $*P < 0.05$; $**P < 0.01$ versus the control. **B.** VEGF-induced increase in the activity of tPA was measured in the EDTA eluates using an ELISA-based activity assay. Data are represented as mean tPA activity in U/ml. The experiments were performed at least in triplicate with triple values each. $*P < 0.05$; $**P < 0.01$ versus the control. **C.** RMVECs were exposed to hypoxia by co-incubating the cells with VEGF and the LCKLSL and LGKLSL peptides. The efficiency of the peptides in inhibiting VEGF-induced plasmin generation was measured by performing chromogenic plasmin generation assay. The data are represented as absorbance units (AUs). Cells exposed to normoxic conditions and treated with vehicle control were used as negative controls. The experiments were performed at least in triplicate with triple values each versus the control. $*P < 0.05$; $**P < 0.01$

inhibiting VEGF-induced activity of tPA. Our results demonstrate that VEGF at a concentration of 20 ng/ml significantly increased the plasmin-generating activity of tPA under hypoxic conditions, which can be substantially inhibited by treatment with the LCKLSL competitive peptide. In contrast, treatment with the LGKLSL control peptide was not efficient in inhibiting VEGF-induced activation of tPA suggesting the importance of the cysteine residue in the binding of tPA to AnxA2 (Fig. 4C). VEGF was also observed to moderately induce the secretion of tPA in cells exposed to normoxic culture conditions.

AnxA2 N-terminal hexapeptide abrogates the neovascular responses an *in vivo* model of angiogenesis

The role of AnxA2 in the neovascular responses was further demonstrated by performing a chicken chorioallantoic membrane assay (CAM) by implanting collagen sponges supplemented with 5 µg of the N-terminal competitive peptide, LCKLSL or the control peptide, LGKLSL on the allantoic membrane of fertilized chicken eggs. After 30 hours of incubation, the allantoic membrane was recovered and assayed for vascular response. A significant decrease in the number of vascular branch points and regression of angiogenesis was observed in the LCKLSL peptide treated embryos compared to the control peptide treated group. The embryos treated with VEGF showed abundant vessels and intense vascular proliferation which was absent in the PBS-treated CAMs (Fig. 5A). A quantitative assay of the H & E stained CAM sections revealed a large decrease in the number of erythrocyte-filled blood vessels in the LCKLSL peptide treated CAMs. CAMs treated with the LGKLSL peptide showed a marked reduction in the blood vessels in comparison with the VEGF-treated CAMs which showed a marked increase in both the number and size of the erythrocyte-filled vessels (Fig. 5B). The CAM images were initially binarized to back and white and were skeletonized. Shown in the Fig. 5C is a multicolor

representation of the skeletonized images with the primary vessels shown in yellow, the secondary vessels in pink and the tertiary vessles in green. In addition, we also performed a shell less CAM assay. At embryonic day 5 the embryo and its embryonic membranes were transferred to a glass petridish for further development. The yolk sac was divided into four sectors and the test substances were applied on collagen sponges on day 12. As a positive control collagen sponges dipped in VEGF was placed in two of the four sectors. Phase contrast images of the CAM indicated increased vasoobliteration in the LCKLSL peptide treated sector compared to the LGKLSL treatment (Fig. 5D).

The length of the vessels and other vascular parameters were quantitated by use of computer-assisted digital image analysis using imageJ. In order to compare between the treatment groups, the vessel width is normalized by skeletonizing the images and the total vessel length was calculated. We observed that treatment with the LCKLSL peptide significantly decreased the vascular length while the LGKLSL peptide did not result in significant changes in the vascular length (Fig. 5E). In addition, we analyzed the vascular architecture by counting the number of vascular branches, junctions and vessel ends per image. At a dose of 5 μg/ml, LCKLSL peptide significantly decreased the number of branches, junction and end points indicating that the peptide is efficient in inhibiting the microvascular sprouting from existing vessels (Fig. 5E). We also quantitated the total number of triple and quadruple points which correlate with the microvascular sprouting. The LCKLSL-treated CAMs showed a significant increase in the number of triple and quadruple points in comparison with the LGKLSL treated CAMs (Fig. 5E).

Figure. 5

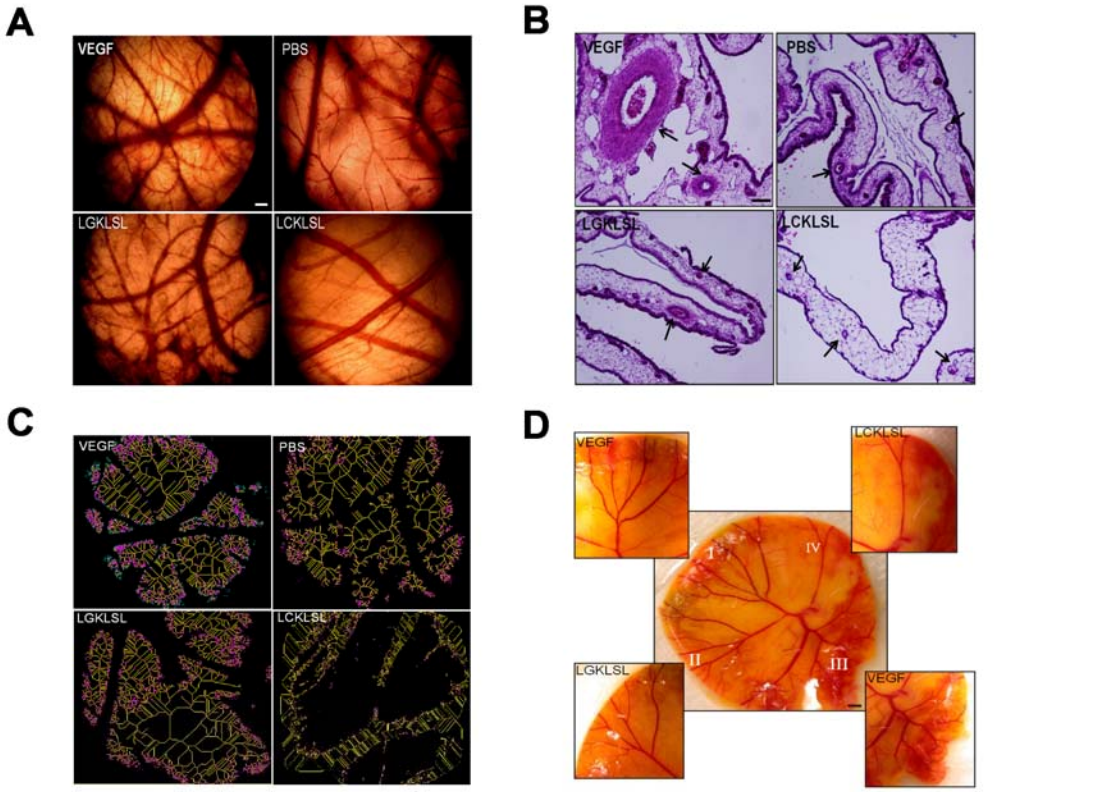
A
VEGF
PBS
LGKLSL
LCKLSL
B
VEGF
PBS
LGKLSL
LCKLSL
C
VEGF
PBS
LGKLSL
LCKLSL
D
VEGF
LCKLSL
I
IV
II
III
LGKLSL
VEGF

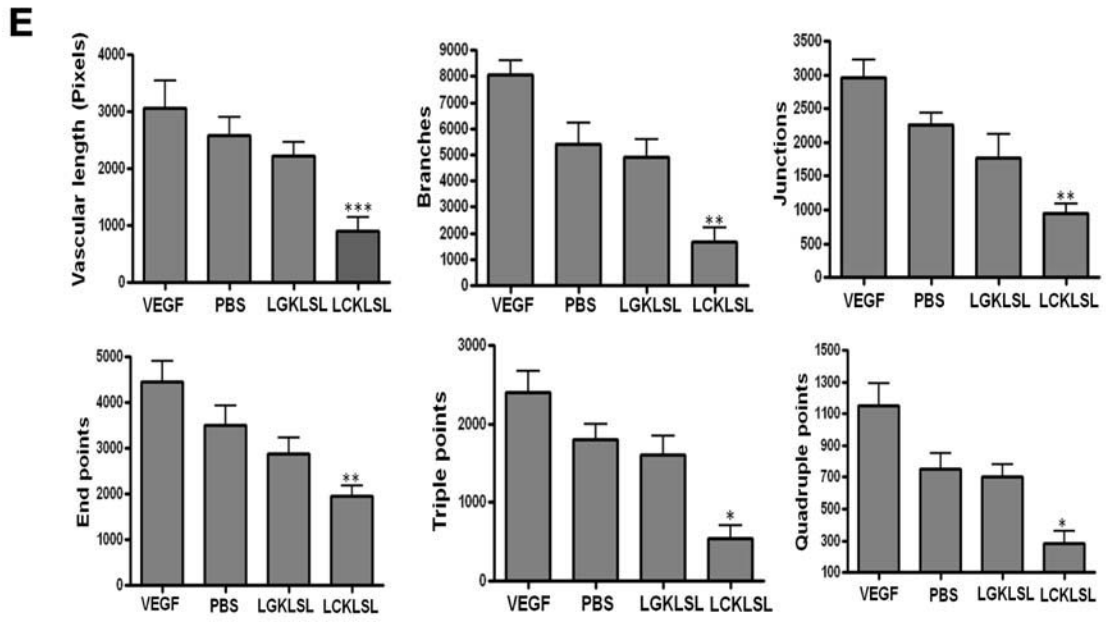
E
Vascular length (Pixels)
Branches
Junctions
End points
Triple points
Quadruple points
VEGF
PBS
LGKLSL
LCKLSL

Figure 5. Chorioallantoic membrane assay (CAM) assay to test the vascular responses to the (LCKLSL) and scrambled peptide (LGKLSL).

A. A 1cm opening was made on the top of the egg and incubated with collagen sponges supplemented with 5 μg/ml of the LCKLSL and LGKLSL peptides as well as VEGF and PBS. Scale 200 μm **B.** H&E staining of the paraffin embedded CAM sections showing the vascular obliteration in the presence of the peptide which was absent on treatment with scrambled peptide. The vehicle control had no effects and vascular hyperproliferation was observed in the presence of VEGF. Scale 100 μm **C.** A multicolor representation of the skeletonized images in different treatment groups. Primary, secondary and tertiary vessels are shown in yellow, pink and green respectively. **D.** A shell less egg assay segregated into 4 sectors treated with the experimental and control peptides along with VEGF that serves as positive control**.** Scale 200 μm **E.** Skeletonized CAM images were scored for total vascular length, number of braches, junctions, end points, triple and quadruple points. The results are represented as mean ±SE. *, $p<0.05$; **, p0.01 and ***, $p<0.005$.

DISCUSSION

Neovascular responses are initiated as a result of vascular occlusion of the retinal capillaries and the generation of hypoxic conditions in the retina (31, 34). The initial generation of hypoxia if followed by the increase in angiogenic growth factors primarily VEGF which upregulates the expression of several extracellular proteinases by microvascular endothelial cells (32). Recent evidence has suggested that vascular endothelial cells under hypoxia selectively upregulate the expression of tPA on stimulation with VEGF (32, 35). Hyperactivation of the plasmin-plasminogen system has been observed in type-1 diabetic patients with PDR compared to the patients with no microvascular complications (10).The disturbances in fibrinolytic homeostasis are caused primarily by the increased synthesis of plasminogen activators by retinal endothelial cells in response to a hypoxic angiogenic stimuli triggered by diabetes (11). In type-1 diabetic patients with retinopathy increased levels of tPA to plasminogen activator inhibitor (PAI-1) (a physiological inhibitor of tPA) and $VEGF_{165}$ were found in plasma (9). Thus, a complex interplay between the $VEGF_{165}$, plasmin-plasminogen system and MMPs mediate fibrin degradation and endothelial cell migration (35). These findings suggest that intervention in the molecular pathways associated with increased generation and activity of plasmin, which is the end product in the plasmin-plasminogen pathway, can have potential implications in the treatment of both PDR and ROP.

Extracellular proteolysis is an indispensable process in angiogenesis which is required for degradation of the ECM and the regulation of cytokine activity (36). This process is mediated by a cohort of extracellular proteases, protease inhibitors and their cell surface receptors produced

both by the endothelial and nonendothelial cells (37). The extracellular plasmin-plasminogen system is known to play an essential role in ECM remodeling (38). The plasmin-plasminogen system is a family of serine proteinases which are involved in divergent angiogenic processes like activation of matix metallo proteinases (MMPs) and liberation of ECM-bound growth factors (7). The most potent member of the plasmin-plasminogen family is plasmin, a trypsin-like protease that degrades several components of ECM thereby facilitating migration and invasion of the endothelial cells which are crucial biological processes in angiogenesis (7). Several studies report a direct correlation between disruption of the plasmin-plasminogen system and angiogenesis (7, 39, 40), yet the molecular mechanisms that control this process and their implications in retinal vascular diseases are poorly understood.

Cell surface receptors that regulate the activity of extracellular proteolysis play crucial roles in the angiogenic processes (4, 13). In the vascular endothelium, AnxA2 is one of the well characterized receptors for plasminogen activation (14). Cell surface AnxA2 acts as a catalytic center for plasmin generation by binding to both tPA and plasminogen and facilitating ~60 fold increase in the rate of plasmin generation (15). Additional support for the role of AnxA2 as a profibrinolytic receptor comes from the observation that AnxA2 knockout mice show a complete reduction in the generation of extracellular plasmin on the surface of endothelial cells (41). Plasminogen binds to the C-terminal domain of AnxA2 and the binding requires the presence of lysine residues in plasminogen (17). Binding of tPA to AnxA2 occurs via a high affinity binding site on tPA and binding to AnxA2 also confers protection on tPA from its physiological inhibitor, plasminogen activator inhibitor -1 (PAI-1) (42). Previous studies have indicated that tPA binds to AnxA2 at a specific hexapeptide LCKLSL motif in the N-terminal domain and binding to AnxA2 confers protection on tPA from its physiological inhibitor, plasminogen

activator inhibitor -1 (PAI-1) (18). The presence of a cysteine residue at position 8 in the N-terminus of AnxA2 has been shown to be essential for tPA binding and the interaction was inhibited in the presence of homocysteine through the formation of a disulfide bond with the thiol group of cysteine 8 (18). Of the many synthetic peptides that contained a cysteine residue, the LCKLSL competitive hexapeptide which is identical to the N-terminal tPA-binding site on AnxA2 is known to be highly efficient in preventing the binding of tPA (18, 42). The hexapeptide binds covalently to AnxA2 and the binding is lost in peptides with a replacement of cysteine with glycine or alanine (18) .

In the current study, we report the potential anti-angiogenic roles of a competitive LCKLSL hexapeptide inhibitor of tPA binding to AnxA2 in neovascularization. We used hypoxia-induced vascular induction as a model study the influence of the peptide on neovascularization. Here, we studied the expression of AnxA2 in the neovascular regions of a mouse model of OIR. Our results indicated overexpression of AnxA2 in the vascular tufts of OIR mice. In isolated human RMVECs exposed to hypoxic conditions, an upregulation in the cell surface and intracellular levels of AnxA2 and tPA was observed and increased levels of AnxA2-tPA complex could be isolated from hypoxic RMVECs. We also demonstrate that increase in the levels of AnxA2 and tPA in hypoxic RMVECs is accompanied by a concomitant upregulation in the generation of plasmin. Furthermore, the selectivity and specificity of the LCKLSL hexapeptide in the binding of AnxA2 was confirmed by a pulldown assay using C-terminally biotinylated peptides and affinity conjugation with streptavidin. Hypoxic RMVECs were also shown to upregulate the secretion and antigen activity of tPA on stimulation with VEGF. The LCKLSL peptide and LGKLSL peptide were tested for their efficiency in inhibiting the hypoxia-induced generation of plasmin. Our results demonstrate that the LCKLSL peptide significantly

inhibited the extent of plasmin generation in hypoxic RMVECs compared to the control LGKLSL peptide. Finally in an *in vivo* CAM angiogenesis assay, application of the LCKLSL hexapeptide on the CAM membrane inhibited both the vascular density and vascular sprouting. Taken together, the data presented here identifies the anti-angiogenic role of a competitive hexapeptide inhibitor in preventing AnxA2-mediated neovascular responses in the retina.

SUPPLEMENTARY METHODS

Tube formation assay on matrigel

Matrigel (BD Biosciences) was used to coat the 24- well plates. After polymerization at 37 °C for 30 min, the cells (40,000 cells/well) were added suspended in 0.5 ml of EGM-2 medium. After incubation for 3 hours, the images of the capillary tubes was taken under a phase-contrast microscope.

Confocal microscopy and Total Internal Reflection (TIRF) microscopy.

Double immunostaining for AnxA2 and VWF followed by confocal microscopy was performed as described in the methods section. TIRF microscopy was preformed to reveal the cell surface expression of AnxA2 (Ohara-Imaizumi M et al., 2004). Cells were grown on 22 mm glass coverslips (VWR International), fixed in 4% ice cold paraformaldehyde in PBS for 10 minutes at 4°C. The cells were processed for AnxA2 immunostaining with a mouse monoclonal anti-AnxA2 antibody (Transduction Laboratories, 1:500 dilution) and observed under the Olympus IX71 microscope equipped with a commercial TIRF attachment using Olympus 60x NA=1.45 PlanApo oil objective and Hamamatsu C4742-95 high-resolution digital camera utilizing a progressive scan interline transfer CCD chip with no mechanical shutter and Peltier cooling. Images were acquired with identical image acquisition parameters.

Supplementary Figure. 1

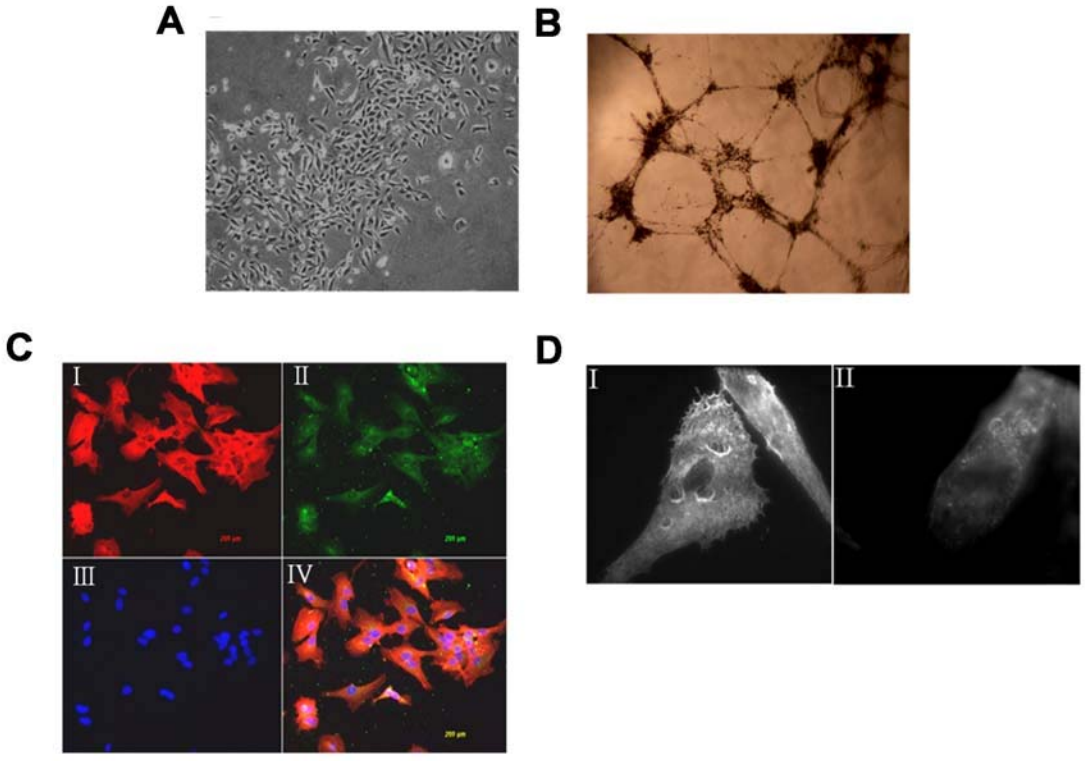

Supplementary Figure legend

Figure. 1. (A) RMVECs isolated from human donor eyes by immunoaffinity purification using magnetic beads coated with anti-PECAM antibody. A phase contrast image of the isolated primary RMVECs in culture. **(B)** Isolated RMVECs were seeded on matrigel coated plates and incubated at 37 ºC for 12 hours. A phase contrast image of tube formation by RMVECs on matrigel in vitro**. (C)** Immunocytochemistry of RMVECs stained for AnxA2 (I), VWF (II) and DAPI (III). The overlay image indicates no co-localization of AnxA2 and VWF **(D)** TIRF microscopy of RMVECs stained for AnxA2 (I). The cells were also stained for a cytosolic protein, tubulin to serve as negative control.

REFERENCES

1. Milkiewicz M, panovic E, Doyle JL, and Haas TL. (2006) , 333-57

2. Pepper, M. S., Montesano, R., Mandriota, S. J., Orci, L., and Vassalli, J. D. (1996) *Enzyme Protein* **49**, 138-162

3. van Hinsbergh VW, Engelse MA, and Quax PH. (2006) *Arterioscler Thromb Vasc Biol.* **26(4)**, 716-28

4. Lijnen, H. R. (2001) *Ann. N. Y. Acad. Sci.* **936**, 226-236

5. Hajjar KA, and Deora A. (2000) *Curr Atheroscler Rep.* **2(5)**, 417-21

6. Houck, K. A., Leung, D. W., Rowland, A. M., Winer, J., and Ferrara, N. (1992) *J. Biol. Chem.* **267**, 26031-26037

7. Castellino, F. J., and Ploplis, V. A. (2005) *Thromb. Haemost.* **93**, 647-654

8. Fukao, H., Ueshima, S., Okada, K., and Matsuo, O. (1997) *Jpn. J. Physiol.* **47**, 161-171

9. Simpson AJ, Booth NA, Moore NR, Lewis SJ, and Gray RS. (1999) *Acta Diabetol.* **36(3)**, 155-8

10. Almér LO, Pandolfi M, and Osterlin S. (1975) *Ophthalmologica.* **170(4)**, 353-61

11. Grant MB, and Guay C. (1991) *Invest Ophthalmol Vis Sci. 1991 Jan;32(1):53-64.* **32(1)**, 53-64

12. Hattenbach LO, Allers A, Gümbel HO, Scharrer I, and Koch FH. (1999) *Retina. 1999* **19(5**, 383-9

13. Pepper, M. S. (2001) *Thromb. Haemost.* **86**, 346-355

14. Kim J, and Hajjar KA. (2002) *Front Biosci.* **1(7)**, 341-8

15. Hajjar KA, and Menell JS. (1997) *Ann N Y Acad Sci.* **15**, 337-49

16. Hajjar KA, and Acharya SS. (2000) *Ann N Y Acad Sci. 2000 may;902:265-71.* **902**, 265-71

17. Hajjar KA, Jacovina AT, and Chacko J. (1994) *J Biol Chem.* **269(33)**, 21191-7

18. Roda O, Valero ML, Peiró S, Andreu D, Real FX, and Navarro P. (2003) *J Biol Chem.* **278(8)**, 5702-9

19. Hajjar KA, Mauri L, Jacovina AT, Zhong F, Mirza UA, Padovan JC, and Chait BT. (1998) *J Biol Chem.* **273(16)**, 9987-93

20. Su, X., Sorenson, C. M., and Sheibani, N. (2003) *Mol. Vis.* **9**, 171-178

21. Mai, J., Finley, R. L.,Jr, Waisman, D. M., and Sloane, B. F. (2000) *J. Biol. Chem.* **275**, 12806-12812

22. Peterson, E. A., Sutherland, M. R., Nesheim, M. E., and Pryzdial, E. L. (2003) *J. Cell. Sci.* **116**, 2399-2408

23. Liu, J., Rothermund, C. A., Ayala-Sanmartin, J., and Vishwanatha, J. K. (2003) *BMC Biochem.* **4**, 10

24. Ohara-Imaizumi M, Nishiwaki C, Kikuta T, Nagai S, Nakamichi Y, and Nagamatsu S. (2004) *Biochem J.* **381(pt1)**, 13-8

25. Jacovina, A. T., Zhong, F., Khazanova, E., Lev, E., Deora, A. B., and Hajjar, K. A. (2001) *J. Biol. Chem.* **276**, 49350-49358

26. Wilkinson-Berka, J. L., Alousis, N. S., Kelly, D. J., and Gilbert, R. E. (2003) *Invest. Ophthalmol. Vis. Sci.* **44**, 974-979

27. Scott, A., and Fruttiger, M. (2010) *Eye (Lond)* **24**, 416-421

28. Shweiki, D., Itin, A., Soffer, D., and Keshet, E. (1992) *Nature* **359**, 843-845

29. Sone, H., Kawakami, Y., Segawa, T., Okuda, Y., Sekine, Y., Honmura, S., Segawa, T., Suzuki, H., Yamashita, K., and Yamada, N. (1999) *Life Sci.* **65**, 2573-2580

30. Nguyen, T. T., and Wong, T. Y. (2009) *Curr. Diab Rep.* **9**, 277-283

31. Arjamaa, O., and Nikinmaa, M. (2006) *Exp. Eye Res.* **83**, 473-483

32. Pepper, M. S., Ferrara, N., Orci, L., and Montesano, R. (1991) *Biochem. Biophys. Res. Commun.* **181**, 902-906

33. Zhao, S. H., Pan, D. Y., Zhang, Y., Wu, J. H., Liu, X., and Xu, Y. (2010) *Chin. Med. J. (Engl)* **123**, 713-721

34. Zhang, S. X., and Ma, J. X. (2007) *Prog. Retin. Eye Res.* **26**, 1-37

35. Ratel D, Mihoubi S, Beaulieu E, Durocher Y, Rivard GE, Gingras D, and Béliveau R. (2007) *Thromb Res.*

36. Cheresh, D. A., and Stupack, D. G. (2008) *Oncogene* **27**, 6285-6298

37. Roy, R., Zhang, B., and Moses, M. A. (2006) *Exp. Cell Res.* **312**, 608-622

38. Parfyonova, Y. V., Plekhanova, O. S., and Tkachuk, V. A. (2002) *Biochemistry (Mosc)* **67**, 119-134

39. Rakic, J. M., Maillard, C., Jost, M., Bajou, K., Masson, V., Devy, L., Lambert, V., Foidart, J. M., and Noel, A. (2003) *Cell Mol. Life Sci.* **60**, 463-473

40. Parfyonova, Y. V., Plekhanova, O. S., and Tkachuk, V. A. (2002) *Biochemistry (Mosc)* **67**, 119-134

41. Ling Q, Jacovina AT, Deora A, Febbraio M, Simantov R, Silverstein RL, Hempstead B, Mark WH, and Hajjar KA. (2004) *J Clin Invest* **113(1)**, 38-48

42. Cesarman GM, Guevara CA, and Hajjar KA. (1994) *J Biol Chem.* **269(3)**, 21198-203

SUMMARY AND DISCUSSION

AnxA2, a member of the Ca^{2+}-binding proteins is one of the most widely studied members of the annexin family (1). Although, several extracellular functions have been proposed for AnxA2, the mechanisms of cell surface translocation of AnxA2 have remained obscure (2). The unique architecture imparts on AnxA2 several divergent functions in many different cell types (3). Because of the presence of C-terminal Ca^{2+}-binding domains, many of its cellular

functions depend on the cellular levels of Ca^{2+} (4). Unlike other members of the annexin family,

AnxA2 has a unique ability to undergo conformational changes in the C-terminus on binding to Ca^{2+} that increases its affinity to bind to the acidic phospholipids in the plasma membrane and intracellular membranes (4, 5). AnxA2 possesses a bipartite structure and the N-terminus of AnxA2 comprises the regulatory domain involved in several post translational modifications and interactions with other proteins (6). Although the C-terminus of AnxA2 is essential for the initial recruitment of AnxA2 to the plasma membrane, the regulatory events at the N-terminus are essential for its stability at the membrane (7).

In an effort to understand, the Ca^{2+}-dependent interactions of AnxA2 with the plasma membrane, we studied the functions of AnxA2 in a retinal neuronal cell line. We have utilized a retinal cell line as a model to study the functions of AnxA2 because the role of AnxA2 has not been clear. In our studies, we observed that the retinal neuronal cell line

(RGC-5) is responsive to glutamate-induced intracellular Ca^{2+} mobilization. Since the increase in intracellular Ca^{2+} is a potent stimulus for the binding of AnxA2 to the plasma membrane (4), we used the glutamate- induced Ca^{2+} influx as a model to study the AnxA2 plasma membrane dynamics. Our studies suggested that AnxA2 is translocated to the cell surface in response to glutamate treatment. Although, we observed an increase in the extracellular levels of AnxA2, we did not detect any changes in the intracellular levels of AnxA2 suggesting that the cell surface translocation of AnxA2 does not require a *de novo* protein synthesis. This observation is consistent with the previous results which suggest that in response to heat stress (8), AnxA2 translocation to the cell surface occurs in the presence of protein synthesis inhibitors. In our unreported results, we also observed that glutamate-induced extracellular translocation of AnxA2 is not inhibited in the presence of ER-Golgi disrupter, Befildin A suggesting that the extracellular translocation of AnxA2 is independent of the ER-Golgi secretory pathway.

In order to study the N-terminal regulatory events involved in the glutamate-induced cell surface translocation of AnxA2, we have carefully looked at the three potential phosphorylation sites in the N-terminus of AnxA2. We generated single and double phosphomimetic and non- phosphomimetic mutants at all the three phosphorylation sites (S11, S25 and Y23). Since intracellular Ca^{2+} signaling pathways often converge on the activation of protein kinase C (9), we speculated that S11 and S25 which are known to be phosphorylated by PKC influence glutamate- induced cell surface translocation of AnxA2. To our surprise, we observed that cell surface translocation of AnxA2 in the presence of glutamate is not influenced by the phosphorylation status at S11 or S25 but by phosphorylation at Y23. Since the phosphomimetic mutant at Y23 is

phosphorylated by pp60C-Src, which is a plasma membrane resident kinase, we predicted that phosphorylation at Y23 occurs at the plasma membrane and this event is essential for the stability of AnxA2 in the plasma membrane.

Previous studies have suggested that neuronal cells in the presence of glutamate-induced excitotoxicity secrete excessive levels of tPA (10, 11). The extracellular tPA activates and cleaves its substrate plasminogen to generate plasmin, a potent protease (10, 12). The effects of plasmin in the neuronal cells are to degrade the underlying ECM components to induce the substrate-detachment and anoikis of the neurons (12, 13). Since tPA and plasminogen are both secretory proteins, they require an anchor to bring together the two proteins in close proximity and facilitate increased proteolytic activity (14). AnxA2 is the only known cell surface receptor that binds to both the tPA and its substrate plasminogen to increase the catalytic activity of plasmin generation (15). In our studies, we observed that AnxA2-meidates the generation of plasmin in response to glutamate treatment. Our data also suggests that N-terminus of Anx2 is the catalytic domain is indispensable for the plasmin-generating activity of AnxA2.

These results have left us with several unanswered questions regarding the membrane dynamics of AnxA2. One of the most fundamental questions is the mechanism by which the leader-less protein, AnxA2 is translocated to the cell surface. Since AnxA2 does not possess a signal sequence it has to follow the non-classical pathways of protein secretion (16). The non- classical secretory pathways have been categorized to happen in several different mechanisms that bypass the classical ER-Golgi secretory pathways (17). Careful observation has enabled us to rule out the plasma membrane blebbing, transmembrane transporter and direct flipping as the mechanism of AnxA2 non-classical

secretion. We speculated that AnxA2 could be secreted into the extracellular surface by integrating into the vesicular pathway. This led us to the second most important question, the mechanistic details of the recruitment of AnxA2 to the vesicular pathway.

In order to answer these questions, we used NIH3T3 cells treated with the Ca^{2+} ionophore as a model to study the Ca^{2+} induced plasma membrane dynamics of AnxA2. Treatment of cells with mild concentrations of the Ca^{2+} ionophore has been used in several studies to study the cell surface translocation of AnxA2 (18, 19). In this model, we observed that AnxA2 is recruited to

specific microdomains in the plasma membrane rich in cholesterol and sphingolipids in response

to treatment with the Ca^{2+} ionophore. These cholesterol-rich microdomains in the plasma membrane called as lipid rafts which function as signaling platforms by recruiting and clustering proteins in specific sites of the membrane (20, 21). In addition, our observations that disrupting lipid rafts by a cholesterol-solubilizing drug MBCD, decreases the ionophore-induced cell surface pool of AnxA2 suggested that lipid rafts function in contributing to the extracellular levels of AnxA2. This observation leads us to believe that the function of lipid rafts is not only in the signaling events but also has a role in protein trafficking across cellular destinations. AnxA2 is phosphorylated by the raft-resident PP60C-Src and this event is essential for the stability of AnxA2 in the plasma membrane. We also believe that AnxA2 is capable of lateral mobility

across the plasma membrane, as the protein is initially localized in the non-raft regions and later is associated with the lipid rafts. This aspect of AnxA2 is probably due to its indiscrete binding to the acidic phospholipids .Lateral mobility is a characteristic feature of most of the lipid raft- associated proteins and AnxA2 is no exception. When AnxA2 is bound to the

membrane, its N- terminus is hangs out like a tail creating the spatial freedom of the kinases to phosphorylate the residues in the N-terminus.

One of the most intriguing aspects of our study is the transport of lipid raft-associated AnxA2. We observed that after recruitment to the lipid rafts, AnxA2 is internalized into distinct intracellular vesicles positive for caveolin. The caveolar endocytosis has previously been observed to be a mechanism of pathogen entry and it is surprising that similar mechanisms also contribute to non-classical protein secretion (22, 23). The internalized AnxA2 is trafficked to the intralumenal vesicles of the MVEs by bypassing the classical vesicular pathway and subsequently escaping the lysosomal degradation. Exosomes are the intralumenal vesicles of the MVEs which are secreted into the extracellular space upon fusion of the MVE with the plasma membrane (24). They originate by the inward budding of the limiting membrane of the endosomes during endosome maturation. Several membrane proteins and lipids destined for degradation are routed to these intraluminal veiscles to be fuse with the lysosomes (25). Some proteins however, escape the endosomal degradation and are recycled back to the plasma membrane (26). We postulated here, that exosomal secretion constitutes a non-classical pathway of secretion of leaderless proteins. These vesicles are not to be confused with the intracellular structures involved during RNA processing. Several leaderless proteins like galectin and Fibroblast growth factor (FGF) and heat sock proteins are known to be secreted by associating with the exosomes (27). The rate limiting step in the association of these proteins with the exosomes is their targeting to the plasma membrane, as it is known that these vesicles are byproducts of the classical vesicular pathway that originates from the plasma membrane (25, 28).

Although the mechanisms of exosomal transport of proteins are not well elucidated, the secretory exosomes are capable of releasing its content once it reaches the target cell plasma membrane (29). Hence exosomes are known to function as intercellular carries of molecular information. In our studies, we demonstrated that exosomal AnxA2 is transferred from one cell and delivered to the target cell (30). We also show that exosomal AnxA2 is also capable of internalization during longer periods of incubation. It has become apparent that sorting of AnxA2 into the exosomes results in the extracellular transport and exogenous recruitment of AnxA2 to the neighboring cell.

In this thesis, we also studied the potential functions of extracellular AnxA2. For these studies we used primary human RMVECs because AnxA2 Is abundantly expressed in the endothelial cells. The role of AnxA2 in facilitating the hypoxia-induced vascular changes is explored. We observed that hypoxia induces an upregulation in the intracellular and cell surface levels of AnxA2. Since AnxA2 does not possess a hypoxia response element (HRE) in its promoter, we believe that hypoxic changes influence the expression of AnxA2 at the post- transcriptional level; the details of this mechanism remain to be explored. Under hypoxic conditions, AnxA2 acts as a potent inducer of plasmin generation. The plasmin-generating ability of AnxA2 can be inhibited by a competitive peptide inhibitor targeted to the tPA-binding site of AnxA2. The use of this peptide in inhibiting retinal angiogenesis can have potential advantages over the currently used treatments like laser photocoagulation which can affect the post natal mitotic function and hamper visual function. Since angiogenesis is a multi-step pathway mediated by an array of growth factor proteins and ECM molecules, the process can be targeted in multiple ways. The use of small hexapeptide pharmacological inhibitors that attenuate the plasmin generation can have

tremendous implications in inhibiting the angiogenic responses.

REFERENCES

1. Moss, S. E., and Morgan, R. O. (2004) *Genome Biol.* **5**, 219

2. Siever, D. A., and Erickson, H. P. (1997) *Int. J. Biochem. Cell Biol.* **29**, 1219-1223

3. Raynal P, and Pollard HB. (1994) *Biochim. Biophys. Acta* **1197(1)**, 63-93

4. Gerke, V., Creutz, C. E., and Moss, S. E. (2005) *Nat. Rev. Mol. Cell Biol.* **6**, 449-461

5. Babiychuk, E. B., and Draeger, A. (2000) *J. Cell Biol.* **150**, 1113-1124

6. Gerke, V., and Moss, S. E. (2002) *Physiol. Rev.* **82**, 331-371

7. Ayala-Sanmartin, J., Zibouche, M., Illien, F., Vincent, M., and Gallay, J. (2008) *Biochim. Biophys. Acta* **1778**, 472-482

8. Deora, A. B., Kreitzer, G., Jacovina, A. T., and Hajjar, K. A. (2004) *J. Biol. Chem.* **279**, 43411-43418

9. Toke, J., Patocs, A., Gergics, P., Bertalan, R., Toth, M., Racz, K., and Tulassay, Z. (2009)

Orv. Hetil. **150**, 781-790

10. Nicole, O., Docagne, F., Ali, C., Margaill, I., Carmeliet, P., MacKenzie, E. T., Vivien, D., and Buisson, A. (2001) *Nat. Med.* **7**, 59-64

11. Kumada, M., Niwa, M., Hara, A., Matsuno, H., Mori, H., Ueshima, S., Matsuo, O., Yamamoto, T., and Kozawa, O. (2005) *Invest. Ophthalmol. Vis. Sci.* **46**, 1504-1507

12. Mali, R. S., Cheng, M., and Chintala, S. K. (2005) *FASEB J.* **19**, 1280-1289

13. Miles, L. A., Hawley, S. B., Baik, N., Andronicos, N. M., Castellino, F. J., and Parmer, R. J. (2005) *Front. Biosci.* **10**, 1754-1762

14. Herren, T., Swaisgood, C., and Plow, E. F. (2003) *Front. Biosci.* **8**, d1-8

15. Kim, J., and Hajjar, K. A. (2002) *Front. Biosci.* **7**, d341-8

16. Danielsen, E. M., van Deurs, B., and Hansen, G. H. (2003) *Biochemistry* **42**, 14670-14676

17. Nickel, W. (2003) *Eur. J. Biochem.* **270**, 2109-2119

18. Barwise, J. L., and Walker, J. H. (1996) *J. Cell. Sci.* **109 (Pt 1)**, 247-255

19. Blanchard, S., Barwise, J. L., Gerke, V., Goodall, A., Vaughan, P. F., and Walker, J. H. (1996) *J. Neurochem.* **67**, 805-813

20. Helms, J. B., and Zurzolo, C. (2004) *Traffic* **5**, 247-254

21. Simons, K., and Toomre, D. (2000) *Nat. Rev. Mol. Cell Biol.* **1**, 31-39

22. Pelkmans, L., Burli, T., Zerial, M., and Helenius, A. (2004) *Cell* **118**, 767-780

23. Pelkmans, L., Kartenbeck, J., and Helenius, A. (2001) *Nat. Cell Biol.* **3**, 473-483

24. Johnstone, R. M. (2006) *Blood Cells Mol. Dis.* **36**, 315-321

25. Thery, C., Zitvogel, L., and Amigorena, S. (2002) *Nat. Rev. Immunol.* **2**, 569-579

26. van Niel, G., Porto-Carreiro, I., Simoes, S., and Raposo, G. (2006) *J. Biochem.* **140**, 13-21

27. Zhang, N. N., Liu, X., Sun, J., Wu, Y., and Li, Q. W. (2009) *Yi Chuan* **31**, 29-35

28. Stoorvogel, W., Kleijmeer, M. J., Geuze, H. J., and Raposo, G. (2002) *Traffic* **3**, 321-330

29. Hegmans, J. P., Gerber, P. J., and Lambrecht, B. N. (2008) *Methods Mol. Biol.* **484**, 97-109

30. Simons, M., and Raposo, G. (2009) *Curr. Opin. Cell Biol.*